

AD-A036 210

DAYTON UNIV OHIO RESEARCH INST
STABILITY OF HIGHLY-COOLED COMPRESSIBLE LAMINAR BOUNDARY LAYERS--ETC(U)
OCT 76 L I BOEHMAN, M G MARISCALCO
UDRI-TR-76-70

F/G 20/4

F33615-74-C-3067

AFFDL-TR-76-148

NL

UNCLASSIFIED

1 OF 2

AD
A036210



ADA 036210

AFFDL-TR-76-148

12
B.S.

THE STABILITY OF HIGHLY COOLED COMPRESSIBLE LAMINAR BOUNDARY LAYERS

UNIVERSITY OF DAYTON RESEARCH INSTITUTE

DECEMBER 1976

TECHNICAL REPORT AFFDL-TR-76-148
FINAL REPORT FOR PERIOD APRIL 1974 - OCTOBER 1976



Approved for public release; distribution unlimited

COPY AVAILABLE TO DDC DOES NOT
PERMIT FULLY LEGIBLE PRODUCTION

AIR FORCE FLIGHT DYNAMICS LABORATORY
AIR FORCE WRIGHT AERONAUTICAL LABORATORIES
AIR FORCE SYSTEMS COMMAND
WRIGHT-PATTERSON AIR FORCE BASE, OHIO 45433

NOTICE

When Government drawings, specifications, or other data are used for any purpose other than in connection with a definitely related Government procurement operation, the United States Government thereby incurs no responsibility nor any obligation whatsoever; and the fact that the government may have formulated, furnished, or in any way supplied the said drawings, specifications, or other data, is not to be regarded by implication or otherwise as in any manner licensing the holder or any other person or corporation, or conveying any rights or permission to manufacture, use, or sell any patented invention that may in any way be related thereto.

This report has been reviewed by the Information Office (OI) and is releasable to the National Technical Information Service (NTIS). At NTIS, it will be available to the general public, including foreign nations.

This technical report has been reviewed and is approved for publication.

J. Christopher Boison

J. CHRISTOPHER BOISON
Project Engineer

FOR THE COMMANDER:

Donald J. Harney

DONALD J. HARNEY
Asst for Experimental Simulation
Aeromechanics Division

| | |
|--------------------------------|---|
| ADDITIONAL | |
| UTS | Write Section <input checked="" type="checkbox"/> |
| DOC | Defn Section <input type="checkbox"/> |
| UNANNOUNCED | <input type="checkbox"/> |
| JUSTIFICATION | |
| BY | |
| DISTRIBUTION/AVAILABILITY CODE | |
| SEC. | AVAIL. and/or SPECIAL |
| A | |

Copies of this report should not be returned unless return is required by security considerations, contractual obligations, or notice on a specific document.

Unclassified

SECURITY CLASSIFICATION OF THIS PAGE (When Data Entered)

| 19 REPORT DOCUMENTATION PAGE | | READ INSTRUCTIONS BEFORE COMPLETING FORM | |
|--|---|---|--|
| 1. REPORT NUMBER AFFDL-TR-76-148 | 2. GOVT ACCESSION NO. | 3. RECIPIENT'S CATALOG NUMBER | |
| 4. TITLE (and Subtitle) STABILITY OF HIGHLY COOLED COMPRESSIBLE LAMINAR BOUNDARY LAYERS. | 5. TYPE OF REPORT & PERIOD COVERED Final Report. 23 Apr 1974- 22 Oct 1976 | 6. PERFORMING ORG. REPORT NUMBER UDRI-TR-76-70 | |
| 7. AUTHOR(s) Louis I. Boehman, Ph. D. Michael G. Mariscalco | 8. CONTRACT OR GRANT NUMBER(s) F33615-74-C-3067 | 9. PROGRAM ELEMENT, PROJECT, TASK AREA & WORK UNIT NUMBERS Project Number 1929 Task Number 192904 Work Unit Number 19290411 | |
| 9. PERFORMING ORGANIZATION NAME AND ADDRESS University of Dayton Research Institute 300 College Park Avenue Dayton, Ohio 45469 | 10. CONTROLLING OFFICE NAME AND ADDRESS Air Force Flight Dynamics Laboratory Thermomechanics Branch, FXE Wright-Patterson Air Force Base, Ohio 45433 | 11. REPORT DATE 22 Oct 1976 | |
| 12. MONITORING AGENCY NAME & ADDRESS (if different from Controlling Office) | | 13. NUMBER OF PAGES 129 | |
| 14. DISTRIBUTION STATEMENT (of this Report) Approved for public release; distribution unlimited. | | 15. SECURITY CLASS. (of this report) Unclassified | |
| 16. DISTRIBUTION STATEMENT (of the abstract entered in Block 20, if different from Report) | | 17. DECLASSIFICATION/DOWNGRADING SCHEDULE | |
| 18. SUPPLEMENTARY NOTES | | | |
| 19. KEY WORDS (Continue on reverse side if necessary and identify by block number) Boundary Layer Stability Small Disturbances Shock-Induced Flow Laminar Boundary Layer Shock Tube Wall Cooling | | | |
| 20. ABSTRACT (Continue on reverse side if necessary and identify by block number) A distinguishing feature of shock induced boundary layers is that the wall temperature (T_w) is less than the temperature at the edge of the boundary layer (T_e) for all shock Mach numbers (M_s). Boundary layer cooling in this type of flow is such that the disturbances ordinarily considered in boundary layer stability theory are completely damped out. This prompted a search for other disturbances which might be unstable in highly cooled boundary layers, two new classes of which have been discovered. Both classes | | | |

DD FORM 1473 1 JAN 73 EDITION OF 1 NOV 65 IS OBSOLETE

Unclassified

SECURITY CLASSIFICATION OF THIS PAGE (When Data Entered)

105 400

Unclassified

SECURITY CLASSIFICATION OF THIS PAGE(When Data Entered)

originate in the free stream and carry energy into the boundary layer. One class corresponds to supersonic disturbances which travel slower than the free stream while the other corresponds to supersonic disturbances, which travel faster than the free stream. With the first class of disturbance, it is now possible to remove the paradox that exists between linear stability theory predictions, and measured transition Reynolds numbers. The paradox is that linear stability theory predictions of critical Reynolds numbers, for flows with $T_w/T_e < 1$, exceed measured transition Reynolds numbers. For flows with $T_w/T_e \geq 1$, however, the critical Reynolds numbers are less than measured transition Reynolds numbers, and generally show qualitative agreement with transition Reynolds number variations in wall cooling, pressure gradient, and Mach number. The critical Reynolds number-amplification rate characteristics of this class of disturbances agrees qualitatively with Boison's recent measurements of transition in shock tube boundary layer flows, in the range of shock Mach numbers of 3 to 4.5. The stability characteristics of these newly discovered unstable disturbances are presented for shock Mach numbers in the range of 1.5 to 5.0, which corresponds to a Mach number range for the flow behind the moving shock of 0.6 to 1.84.

The stability of highly cooled, wind tunnel type boundary layers was also investigated. Results indicate that moderate amounts of surface cooling significantly enhance the stability of the boundary layer to both two and three dimensional subsonic disturbances. This implies that it is feasible to delay the transition from laminar to turbulent flow on an aerodynamic surface by cooling for the purpose of decreased friction drag and hence a general increase in the fuel economy of subsonic free flight vehicles.

It is thus recommended that an experimental test program be developed to study the effects of surface cooling on transition in steady flow, subsonic wind tunnel type boundary layers. A positive correlation with the linear stability theory as applied to free flight application should be sought.

Unclassified

SECURITY CLASSIFICATION OF THIS PAGE(When Data Entered)

FOREWORD

This report was prepared by the Aerospace Mechanics Division of the University of Dayton Research Institute, University of Dayton, Dayton, Ohio. This work was conducted under Contract F33615-74-C-3067, Project number 1929, "Boundary Layer Research." The principal investigator was Dr. Louis I. Boehman, Associate Professor of Mechanical Engineering. The coauthor of the report M. G. Mariscalco, Assistant Mechanical Research Engineer of the Applied Physics Division of UDRI. Dr. J. Christopher Boison, Branch Chief, Air Force Flight Dynamics Laboratory, Thermomechanics Branch (AFFDL/FXE), Wright-Patterson Air Force Base, Ohio, was the contract monitor.

The authors wish to acknowledge the significant contributions of Dr. J. P. Barber and H. F. Swift, of UDRI who assisted in preparation of the final report.

This research effort was initiated in April 1974 and was completed in October 1976.

The technical report was released by the authors in October 1976.

TABLE OF CONTENTS

| SECTION | PAGE |
|--|------|
| I INTRODUCTION AND BACKGROUND | 1 |
| 1.1 Boundary Layer Stability Terminology | 3 |
| 1.2 Review of Cooled Laminar Boundary Layer Stability | 6 |
| 1.3 Report Outline | 10 |
| II PARALLEL STEADY FLOW ANALYSIS OF SHOCK INDUCED FLOWS | 12 |
| 2.1 Mean Flow Profiles | 12 |
| 2.2 Formulation of the Stability Equations for a Shock Induced Boundary Layer | 14 |
| 2.3 Range of Flows Analyzed | 18 |
| III RESULTS OF ANALYSIS OF SHOCK INDUCED FLOWS | 21 |
| 3.1 Subsonic, Sonic, and Supersonic Disturbances in Shock Induced Flows | 21 |
| 3.2 Incoming and Outgoing Disturbances | 23 |
| 3.3 Families of Solutions | 26 |
| 3.4 Results for Shock Induced Flows | 26 |
| 3.5 Forced Response Analysis | 39 |
| 3.6 Effect of Varying Wall Cooling on Neutral Stability of Supersonic Incoming Waves | 43 |
| IV APPLICATION OF ANALYSIS TO SUBSONIC WIND TUNNEL BOUNDARY LAYERS | 45 |
| 4.1 Formulation of the Problem | 45 |
| 4.2 Results | 46 |
| 4.3 Comparison to Shock Induced Flow Results | 56 |
| 4.4 Effect of Wall Cooling on Local Skin Friction Coefficient | 58 |
| V SUMMARY, CONCLUSIONS AND RECOMMENDATIONS | 60 |
| 5.1 Summary | 60 |
| 5.2 Conclusions | 62 |
| 5.3 Recommendations | 63 |

TABLE OF CONTENTS (Concluded)

SECTION

| | | |
|------------|---|-----|
| Appendix A | Critique of Ostrack-Thornton Analysis | 64 |
| Appendix B | Description of Boundary Layer Stability Computer Program | 73 |
| References | | 114 |

LIST OF FIGURES

| Figure | | Page |
|--------|---|------|
| 1 | Sketch Showing Definition of Incoming and Outgoing Waves.(a) $c_r < 1 - 1/M_\infty$, (b) $c_r > 1 + 1/M_\infty$ | 5 |
| 2 | Transition Reynolds Number Correlation for $Re/ft = 5 \times 10^5$ | 9 |
| 3 | Boundary Layer Mean Flow Velocity Profile | 13 |
| 4 | Representative Boundary Layer Mean Velocity Profiles | 15 |
| 5 | Representative Boundary Layer Mean Temperature Profiles | 15 |
| 6 | Phase Velocity Versus Shock Mach Number in Shock Tube Flows | 22 |
| 7 | Two Dimensional Disturbance Neutral Stability Curve at $M_s = 1.5$ for Shock Tube Boundary Layer | 27 |
| 8 | Effect of Wave Number (α) on Amplification (c_i) for Varying Reynolds Number (R). Wave Angle; $\psi = 80^\circ$, $M_s = 1.5$ | 28 |
| 9 | Effect of Wave Number (α) on Phase Velocity (c_r) for Varying Reynolds Number (R). Wave Angle; $\psi = 80^\circ$, $M_s = 1.5$. | 28 |
| 10 | Effect of Wave Angle (ψ) on Amplification (c_i). $M_s = 3.0$. | 30 |
| 11 | Effect of Wave Angle (ψ) on Phase Velocity (c_r). $M_s = 3.0$. | 30 |
| 12 | Phase Velocity (c_r) Versus Wave Number (α) for First and Second Mode Regular Subsonic Disturbances | 31 |
| 13 | Amplification (c_i) Versus Wave Number for Subsonic Regular Family of Solutions. $M_s = 1.5, 2.0, \text{ and } 4.0$ | 31 |

LIST OF FIGURES (Continued)

| Figure | | Page |
|--------|---|------|
| 14 | Effect of Streamwise Wave Number (α) on Amplification Factor (c_i) for Varying Reynolds Number ($R = \sqrt{R_x}$) (106 Integration Steps), $M_s = 3.0$ | 35 |
| 15 | Phase Velocity (c_r) versus Streamwise Wave Number (α) at Varying Reynolds Number ($R = \sqrt{R_x}$) (106 Integration Steps), $M_s = 3.0$ | 35 |
| 16 | Effect of Wave Number (α) on Amplification (c_i), $M_s = 3.25$ | 36 |
| 17 | Effect of Wave Number (α) on Phase Velocity (c_r) for Varying Reynolds Number ($R = \sqrt{R_x}$), $M_s = 3.25$ | 36 |
| 18 | Effect of Wave Number (α) on Amplification Factor (c_i), $M_s = 3.5$ | 37 |
| 19 | Effect of Wave Number (α) on Phase Velocity (c_r), $M_s = 3.5$ | 37 |
| 20 | Effect of Wave Number (α) on Amplification (c_i) for $M_s = 3.25$ for Varying Reynolds Number | 40 |
| 21 | Effect of Wave Number (α) on Phase Velocity (c_r) for $M_s = 3.25$ for Varying Reynolds Number | 40 |
| 22 | Effect of Shock Mach Number on "Changeover" Reynolds Number | 41 |
| 23 | Transition Reynolds Number Correlation Showing Results from Golobic's Measurements (15) | 43 |
| 24 | The Effect of Wall Cooling on Neutral Stability Conditions from 2-D Disturbances at $M_s = 2.5$; (a) Wave Number, (b) Phase Velocity | 44 |
| 25 | Effect of Wall Cooling on Neutral Stability Conditions for 2-D Disturbances at $M_\infty = 0.603$; (a) Wave Number, (b) Phase Velocity | 47 |

LIST OF FIGURES (Concluded)

| Figure | | Page |
|--------|---|------|
| 26 | Effect of Wall Cooling on Neutral Stability Conditions for 2-D Disturbances at $M = 0.90$; (a) Wave Number, (b) Phase Velocity | 48 |
| 27 | Effect of Wall Cooling on the Neutral Stability Frequency for 2-D Disturbances at $M_{\infty} = 0.9$ | 49 |
| 28 | Effect of Streamwise Wave Angle on Neutral Stability Conditions for 3-D Disturbances for Insulated Wall at $M_{\infty} = 0.9$; (a) Wave Number, (b) Phase Velocity | 51 |
| 29 | Effect of Streamwise Wave Angle on Neutral Stability Conditions for 3-D Disturbances at $M_{\infty} = 0.90$ and $T_w/T_e = 0.824$; (a) Wave Number, (b) Phase Velocity | 52 |
| 30 | Effect of Streamwise Wave Angle on Neutral Stability Conditions for 3-D Disturbances at $M_{\infty} = 0.90$ and $T_w/T_e = 0.759$; (a) Wave Number, (b) Phase Velocity | 53 |
| 31 | Effect of Streamwise Angle on Neutral Stability Conditions for 3-D Disturbances at $M_{\infty} = 0.90$ and $T_w/T_e = 0.620$; (a) Wave Number (b) Phase Velocity | 54 |
| 32 | Effect of Wave Angle on the Neutral Stability Frequency for Three Dimension Neutral Disturbances | 55 |
| 33 | Comparison of the Relative Stability of Shock Tube and Wind Tunnel Boundary Layers, as a Function of Critical Reynolds Number and Wall Cooling Ratio | 57 |
| 34 | Motion of a Test Particle in Stationary and Moving Coordinate Systems | 70 |

LIST OF TABLES

| Table | | Page |
|-------|--|------|
| 1 | Moving Shock Waves - Mean Flow Results | 20 |
| 2 | Local Skin Friction Coefficient Comparison for Laminar and Turbulent Flow | 59 |

LIST OF SYMBOLS

| <u>Symbol</u> | <u>Definition</u> | <u>Characteristic Measure**</u> |
|---------------|--|---------------------------------|
| a | - Speed of sound | |
| c | - Complex phase velocity of disturbance $= c_r + ic_i$ | U_∞^*, U_2^* |
| \bar{c} | - Phase velocity in lab-fixed coordinate system | U_2^* |
| C | - Constant of proportionality relating boundary layer thickness to $x^* / (R_x)^{1/2}$ | |
| f | - Velocity disturbance amplitude in x^* direction | U_∞^*, U_2^* |
| f^* | - Temporal frequency, Hz | |
| $\bar{f}(y)$ | - Function which relates mean flow velocity in direction normal to wall to R_x , ie. $V(x, y) = \bar{f}(y) [2 (R_x)^{1/2}]$ | |
| G | - Temperature gradient in mean flow (See Table 1) | |
| h_e^* | - Enthalpy of free stream flow downstream of shock wave in shock fixed coordinate system | |
| h_t^* | - Stagnation enthalpy in shock-fixed coordinate system | |
| i | - Unit imaginary number, $\sqrt{-1}$ | |
| l | - Characteristic length | |
| M | - Mach number | |
| M_e | - Mach number of flow behind a shock, wave-shock-fixed coordinate system | |
| M_2 | - Mach number of flow behind a shock wave-lab-fixed coordinate system | |

** The first symbol refers to characteristic measure for a steady mean flow boundary-layer; the second symbol refers to characteristic measure for a boundary layer induced by a moving shock wave.

LIST OF SYMBOLS (Continued)

| <u>Symbol</u> | <u>Definition</u> | <u>Characteristic Measure**</u> |
|---------------|---|---------------------------------|
| M_s | - Mach number of moving shock wave = U_s^*/a_1^* | p_∞^* |
| \hat{M} | - Local Mach number relative to phase velocity | |
| p | - Pressure | p_∞^*, p_e^* |
| r | - Amplitude of density fluctuation | ρ_∞^*, ρ_e^* |
| Re_1 | - Reynolds number appearing in Ostrach-Thornton stability equations, $Re_1 = (2 R_x)^{1/2} T_w/T_e$ | |
| R_x | - Reynolds number: based on distance from leading edge in steady boundary layer flows, $R_x = U_\infty^* x^*/\nu_\infty^*$; based on total distance particle has traveled relative to wall in shock-induced flows, $R_x = U_2^* x^*/\nu_2^*$ | |
| R_X | - Reynolds number defined by Ostrach-Thornton, $R_X = R_x$ for shock-induced flows | |
| R_δ | - Reynolds number based on boundary layer thickness δ , $R_\delta = U_\infty^* \delta / \nu_\infty^*$ | |
| R_{crit} | - Critical Reynolds number | |
| R | - $(R_x)^{1/2}$ | |
| t | - Time | $x/U_\infty^*, l/U_2^*$ |
| Δt | - Time interval after shock moves past a given point | |
| T | - Temperature based on absolute thermodynamic scale | T_∞^*, T_e^* |
| u | - Fluctuating component of velocity in x^* direction | U_∞^*, U_2^* |
| u_w | - Ratio of wall velocity to free-stream velocity, U_w^*/U_e^* | |

LIST OF SYMBOLS (Continued)

| <u>Symbol</u> | <u>Definition</u> | <u>Characteristic Measure</u> ** |
|----------------|---|----------------------------------|
| U | - Mean flow velocity component in x^* direction | U_{∞}^*, U_2^* |
| U_{∞}^* | - Free stream, mean flow velocity in steady boundary layer, x^* direction | |
| U_e^* | - Free stream, mean flow velocity downstream of shock wave, shock-fixed coordinate system | |
| U_s^* | - Shock wave velocity in lab-fixed coordinate system | |
| U_w^* | - Velocity of wall in shock-fixed coordinate system $ U_s^* = U_w^* $ | |
| U_2^* | - Velocity of mean flow in free-stream behind moving shock wave $U_2^* = U_s^* - U_e^* $ | |
| v | - Fluctuating component of velocity in y^* direction | U_{∞}^*, U_2^* |
| V | - Mean flow component of velocity in direction normal to wall (y^* direction) | U_{∞}^*, U_2^* |
| x^* | - Dimensional distance parallel to wall in direction of free stream flow | |
| x | - Non-dimensional distance = (x^* / l) | |
| X^* | - Dimensional distance behind shock wave in shock-fixed coordinate system | |
| y^* | - Dimensional distance perpendicular to wall | |
| y or η | - Blasius similarity variable = $(y^* R / x^*)$ | |
| z^* | - Dimensional distance parallel to wall in direction transverse to free stream flow | |
| z | - Non-dimensional distance = (z^* / l) | l |

LIST OF SYMBOLS (Continued)

| <u>Symbol</u> | <u>Definition</u> | <u>Characteristic Measure</u> |
|---------------|--|-------------------------------|
| <u>Greek</u> | | |
| α | - Disturbance wave number in streamwise direction | l^{-1} |
| α_1 | - Disturbance wave number in x^* direction | l^{-1} |
| α_3 | - Disturbance wave number in z^* direction | l^{-1} |
| β | - Angular timewise frequency | $U_\infty^*/l, U_2^*/l$ |
| r | - Ratio of specific heats | |
| δ | - Boundary layer thickness | |
| η | - Blasius similarity variable = $(y^* R/x^*)$ | |
| θ | - Amplitude of temperature fluctuation | T_∞^*, T_e^* |
| θ | - Also used to represent mean flow enthalpy profile in shock-fixed coordinate system (Table 1) | |
| μ | - Dynamic viscosity | μ_∞^*, μ_e^* |
| ν | - Kinematic viscosity, (μ^*/ρ^*) | ν_∞^*, ν_e^* |
| λ | - Eigenvalues of differential equation | |
| π | - Amplitude of pressure fluctuation | ρ_∞^*, ρ_e^* |
| ρ | - Fluid density | |
| σ | - Prandtl number | σ_∞, σ_e |
| τ | - Time after shock wave moves past a given point on shock tube wall | |
| Φ | - Amplitude of disturbance stream function | |

LIST OF SYMBOLS (Concluded)

| <u>Symbol</u> | <u>Definition</u> | <u>Characteristic Measure</u> |
|---------------|---|--|
| <u>Greek</u> | | |
| ψ | - Wave angle of a disturbance | |
| Ω | - Normalized velocity profile = $\frac{u - u_w}{1 - u_w}$ | |
| ω | - Nondimensional frequency | $\frac{v_\infty^*}{U_\infty^{*2}}, \frac{v_e^*}{U_2^{*2}}$ |

Superscripts

- ()' - Derivative with respect to y
- ()* - Dimensional quantity
- ($\bar{}$) - Amplitude of fluctuating quantity

Subscripts

- ∞ - Free stream value (steady boundary layer flow)
- e - Free stream value based on flow behind shock
- 1 - Undisturbed flow conditions in front of moving shock wave
- 2 - Flow conditions in free stream of mean flow behind moving shock wave, lab-fixed coordinate system
- r - Real part of a complex number
- i - Imaginary part of a complex number
- w - Wall conditions
- o - Stagnation values

SECTION I

INTRODUCTION AND BACKGROUND

This report addresses the problem of determining the conditions under which the flow in a cooled laminar boundary layer becomes unstable when excited by low amplitude disturbances. The flow is considered to be unstable when a low amplitude disturbance imbedded in a cooled laminar boundary layer flow grows in time and/or space. The physical significance of this problem is that such processes initiate the transition from laminar to turbulent flow conditions in the boundary layer. The skin friction and rate of heat transfer are typically an order-of-magnitude greater in turbulent boundary layers than in laminar boundary layers when compared at the same Reynolds number. Therefore, the ability to understand, predict, and possibly suppress, boundary layer transition is of great engineering importance in the design of flight vehicles.

The problem of predicting the conditions under which a laminar boundary layer will begin to undergo the transition process represents one of the great, and as yet unsolved, problems of fluid dynamics. The mathematical description of fluid dynamic phenomena is a system of non-linear partial differential equations. To the present time, this system has resisted all attempts to obtain solutions which are valid for boundary layer flows undergoing transition. Therefore, simplified versions of the general equations are used to study the transition process. The simplified equations used in the present study are called the small disturbance stability equations. They are a linearized version of the general (Navier-Stokes) equations. The linearized small disturbance equations are themselves not very amenable to direct solution because of the partial differential nature of the equations. Therefore, a further simplification is introduced. The boundary layer is considered to be locally parallel. That is, the growth of the boundary layer thickness over a wavelength of a disturbance is

neglected. This simplification allows one to reduce the partial differential equations to ordinary differential equations. Thus, the parallel flow boundary layer stability equations have been used in the work described in this report. This model was employed to study the conditions under which small disturbances will grow in space and/or time in a cooled laminar boundary layer flow.

The reasons why cooled laminar boundary layers are specifically addressed in this report are:

1. Previous experimental investigations of boundary layer transition have shown that cooling a boundary layer generally (but not always) increases the stability of the boundary layer. Thus, the potential exists for using boundary layer cooling as a means for delaying the onset of transition.
2. Recent advances in the field of parallel flow boundary layer stability theory have made it possible to further advance the use of this theory as a method for predicting the onset of transition.
3. Recently published measurements of transition in shock induced flows have shown an intricate variation of transition with wall cooling. These observations and other experimental results cannot be reasonably explained with existing theoretical results. New theoretical results using the most powerful methods currently available for solving the stability equations are necessary to understand these observations.
4. The present energy crisis has provided a new impetus for investigating both new and old techniques which could be used to reduce the aerodynamic drag of flight vehicles. Boundary layer control through wall cooling thus might be a useful means for reducing drag, conserving fuel resources, and extending the range and payload of aircraft.

1.1 BOUNDARY LAYER STABILITY TERMINOLOGY

In this paragraph a number of the more important terms which are used to classify the different types of disturbances which occur in compressible boundary layer flows are defined.

1.1.1 Sonic, Subsonic, and Supersonic Disturbances

A small disturbance having a velocity relative to the free-stream which is equal in magnitude to the speed of sound in the free-stream is called a sonic (acoustic) disturbance. The following definitions are introduced;

c_r^* = velocity of a disturbance (phase velocity),

a_∞^* = speed of sound in the free-stream,

U_∞^* = velocity of the free-stream,

M_∞ = Mach number of the free-stream.

The velocity of the free-stream, relative to an observer moving with the disturbance velocity, is $U_\infty^* - c_r^*$. The relative Mach number (\hat{M}) is;

$$\hat{M}_\infty = (U_\infty^* - c_r^*) / a_\infty^*, \quad (1)$$

which after multiplying and dividing by U_∞^* , becomes

$$\hat{M}_\infty = (1 - c_r^*) M_\infty, \quad (2)$$

where c_r is the nondimensional phase velocity c_r^* / U_∞^* . From the definitions of a sonic disturbance given at the beginning of Section 1.1.1, it follows that $\hat{M}_\infty = \pm 1$ for a sonic disturbance. Thus, if Equation (2) is solved for c_r corresponding to a sonic disturbance, the following two expressions for the phase velocity of sonic disturbances are obtained;

$$c_r = 1 + 1/M_\infty, \quad \hat{M} = -1, \quad (3)$$

$$c_r = 1 - 1/M_\infty, \quad \hat{M} = +1. \quad (4)$$

For a subsonic disturbance $|U_{\infty}^* - c_r^*|$ is less than a_{∞}^* and $-1 < \hat{M}_{\infty} < 1$.
Thus, for subsonic disturbances;

$$(1 - 1/M_{\infty}) < c_r < (1 + 1/M_{\infty}) \quad (5)$$

For supersonic disturbances $|\hat{M}_{\infty}| > 1$ and the phase velocity is;

$$c_r > 1 + 1/M_{\infty}, \quad \hat{M} < -1 \quad (6)$$

$$c_r < 1 - 1/M_{\infty}, \quad \hat{M} > +1 \quad (7)$$

1.1.2 Disturbances Having a Supersonic Relative Flow Region

Disturbances were classified in Section 1.1.1 as subsonic, sonic or supersonic based on the speed of sound in the free-stream. Because of the temperature gradient which exists in compressible boundary layers, it is possible to classify disturbances as subsonic, sonic, or supersonic with respect to the speed of sound at any point in the boundary layer. Thus, $\hat{M}(\eta)$ at any point η in the boundary layer can be defined as the velocity of the flow at η relative to the velocity of the disturbance divided by the local speed of sound, or;

$$\hat{M}(\eta) = (U^*(\eta) - c_r^*) / a^*(\eta). \quad (8)$$

For a perfect gas,

$$a^*(\eta) = a_{\infty}^* (T^*(\eta) / T_{\infty}^*)^{1/2} \quad (9)$$

after multiplying and dividing Equation (8) by U_{∞}^* and substituting Equation (9), the following expression for $\hat{M}(\eta)$ is obtained;

$$\hat{M}(\eta) = (U(\eta) - c_r) M_{\infty} / (T(\eta))^{1/2}. \quad (10)$$

A disturbance is considered to have a supersonic relative flow region in the boundary layer if $|\hat{M}| > 1$ over any region in the boundary layer.

1.1.3 Incoming and Outgoing Waves

A supersonic low amplitude disturbance produced in the free-stream will have an associated set of Mach waves as shown in Figure 1. If a boundary layer is present in the flow, Mach waves will impinge on it. Such a Mach wave impinging on a boundary layer is called an incoming wave. The wave produced by reflection of an incoming wave on the boundary is called an outgoing wave as illustrated in Figure 1. The reflected wave can be considered to have the properties of a Mach wave of opposite sense to the incoming Mach wave.

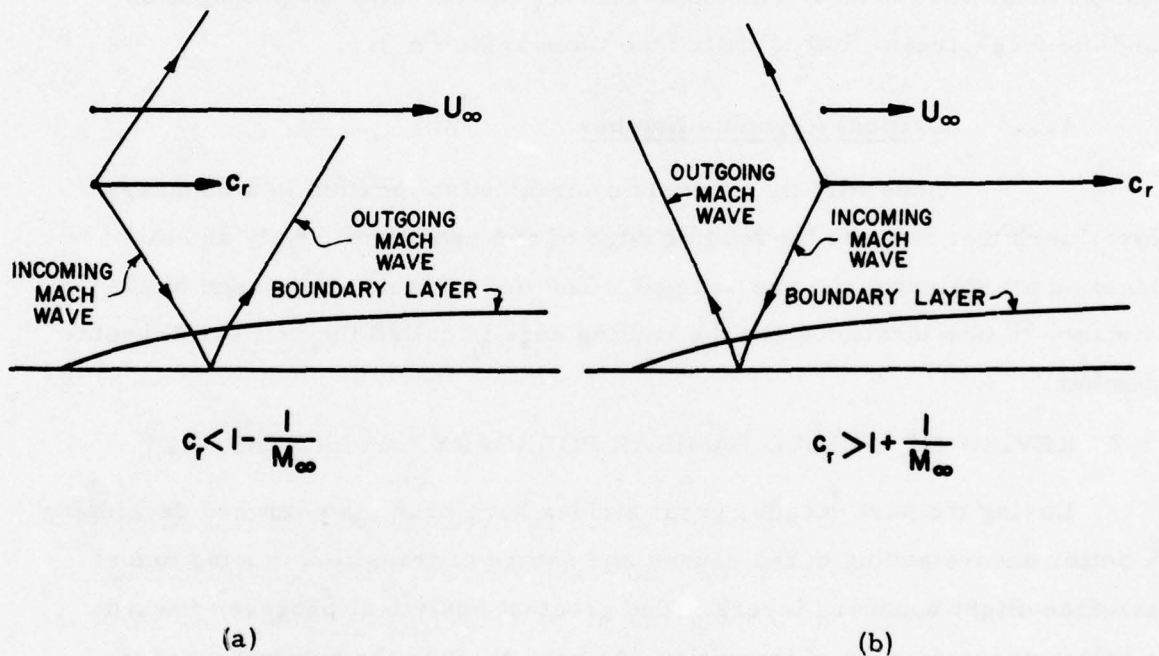


Figure 1. Sketch Showing Definition of Incoming and Outgoing Waves. (a) $c_r < 1 - 1/M_\infty$, (b) $c_r > 1 + 1/M_\infty$.

1.1.4 Two-Dimensional and Three-Dimensional Disturbances

In the parallel flow linear stability theory, the fluctuation of any disturbance parameter E is defined by a traveling wave of the form;

$$E(x, y, z, t) = \epsilon(y) e^{i(\alpha_1 x + \alpha_3 z - \omega t)} \quad (11)$$

If α_3 is zero, Equation (11) describes a plane wave which propagates in the direction of the free-stream flow. These waves are called two-dimensional waves (2-D). If α_3 is not zero, Equation (11) describes a wave which propagates obliquely to the free-stream flow. Such a wave is called a three-dimensional wave (3-D). The angle between the direction of propagation and the free-stream flow is called the wave angle (ψ).

1.1.5 Critical Reynolds Number

Generally there exists a streamwise location in a boundary layer such that between the leading edge of an aerodynamic body and this location all disturbances are damped. The Reynolds number based on the distance to this location from the leading edge is called the critical Reynolds number.

1.2 REVIEW OF COOLED LAMINAR BOUNDARY LAYER STABILITY

During the past decade, great strides have been made toward developing a better understanding of the causes and nature of transition in wind tunnel and free-flight boundary layers. The greatest analytical progress towards a better understanding of transition has been through the application of the linear stability theory of parallel flows.

Mack⁽¹⁾ made a major contribution in the application of the linear stability theory as a tool for understanding boundary layer transition by discovering multiple mode, multiple families of solutions to the compressible flow, small disturbance equations. He demonstrated the physical importance of these new types of solutions and formulated a quasi-theoretical model of transition for supersonic flows based on the linear stability theory of

parallel flows. Mack's quasi-theoretical model of transition includes two mechanisms for relating the influence of environmental disturbances to the response of the boundary layer. One mechanism is that of the forced oscillation of the boundary layer caused by a specific type of free stream pressure disturbance. The other mechanism is the response of the boundary layer to a spectrum of pressure disturbances. Within the context of these two mechanisms he was able to study the effect of Mach number, unit Reynolds number (Reynolds No. per foot of the free-stream), and wall cooling on transition in wind tunnel and free-flight boundary layers. He was basically successful in explaining how environmental disturbances can affect transition as Mach number, unit Reynolds number, and wall cooling change. The accuracy of Mack's transition model appears to be limited, for the most part, by the accuracy with which the nature of the environmental disturbances themselves are known. In order to apply Mack's model to the problem of predicting the location of the onset of transition in a flow situation, one must have available the basic results of a parallel flow, small disturbance stability analysis; namely, neutral stability curves and amplification rate versus frequency for a range of Reynolds numbers.

The considerable progress that has been made toward understanding transition in wind-tunnel and free-flight boundary layers has not been matched by progress in understanding transition in laminar boundary layers induced by a moving shock wave. This situation persists in spite of the fact that a considerable amount of experimental data on transition in shock-tube boundary layers has been generated during the past two decades. Morkovin⁽²⁾ has summarized the nuances and contradictory observations that have been made concerning transition in shock tube facilities and has also conducted an assessment of the level of understanding of wind-tunnel and free-flight boundary layer transition⁽³⁾.

Recently, Boison⁽⁴⁾ conducted a series of careful experiments which considered shock tube boundary layer transition. He examined the influence

on transition of environmental factors, such as wall vibration and free stream acoustic disturbances, in addition to the influence of wall cooling, unit Reynolds number, and Mach number. In these experiments, extraordinary precautions were taken to eliminate wall roughness as a possible cause of early transition. The transition is usually expressed in terms of the "transition" Reynolds number $(R_x)_T$ based on the length of the boundary layer at transition. Boison's data at a free stream Reynolds number per foot of 5×10^5 showed that, as wall cooling is increased, the transition Reynolds number first increased, then decreased (reversal), then increased again (re-reversal), then decreased, increased again, and so on; showing a number of transition reversals and re-reversals. The transition Reynolds number was found to be extremely sensitive to small changes in cooling especially at the larger cooling rates. Figure 2 shows Boison's transition results for $R_e/ft = 5 \times 10^5$ along with results of several other investigators. The wall cooling rate is expressed in terms of the wall temperature T_w and the boundary layer edge temperature T_e in this figure. The ratio T_w/T_e is inversely related to the magnitude of wall cooling (decreasing T_w/T_e corresponds to increasing wall cooling).

The first transition reversal loop ($0.17 < T_w/T_e < 0.36$) seems to be fairly well established although more results would be desirable to definitely show that only one loop, rather than perhaps two loops, exists in this wall cooling range. Also shown in Figure 2 is the calculation of Reshotko⁽⁵⁾ for the wall cooling required for complete stabilization of 2-D disturbances. It should be noted that this result is not based on a completely valid solution of the stability equations as determined by Mack (see page 14.1 of Reference 6). In particular, mean velocity and temperature profiles characteristic of shock tube boundary layers were not used.

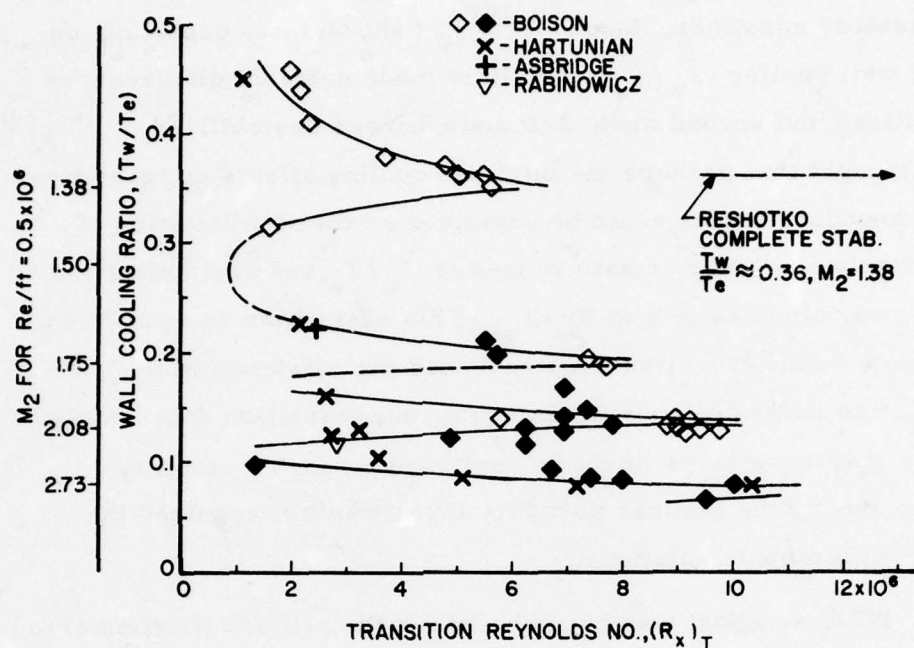


Figure 2. Transition Reynolds No. Correlation for $Re/ft = 5 \times 10^5$.

The description of only one stability analysis, using velocity and temperature profiles characteristic of compressible boundary layers behind a moving shock appears in the literature. That analysis, performed by Ostrach and Thornton⁽⁷⁾ in 1962, produced minimum critical Reynolds numbers that greatly exceeded the measured transition Reynolds numbers - the deviation increasing by orders of magnitude with increasing cooling, i.e., higher shock Mach numbers. Their analysis was based on the Dunn-Lin asymptotic approach⁽⁸⁾ and did not take into account 3-D disturbances. Ostrach and Thornton concluded that shock tube transition did not occur through amplification of low amplitude waves but rather was caused by large environmental disturbances which are present in shock tubes.

The existence of multiple mode, multiple family solutions to the parallel flow linear stability equations led to the suggestion by Morkovin⁽²⁾ that the Ostrach-Thornton analysis be redone using the full set of parallel

flow, linear stability equations. Mack^(9,10) had shown that, depending on the amount of wall cooling (T_w/T_e), 2-D first mode unstable disturbances could be stabilized and second mode 2-D disturbances destabilized. Morkovin⁽²⁾ thought that perhaps the intricate cooling effects on transition in shock tube boundary layers could be explained as the stabilization of first mode disturbances over certain ranges of T_w/T_e and destabilization of higher modes over other ranges of T_w/T_e . This suggestion was put forth prior to Boison's work. When Boison discovered the existence of the multiple transition reversal loops in his shock tube transition data he saw the possibility that these loops might be explained through a stability analysis of the shock tube laminar boundary layer which recognized the existence of multiple mode solutions.

In early 1972, an effort was begun by one of the authors (Boehman) to reconduct the Ostrach-Thornton analysis using the authors' computer programs which had been successfully applied to the steady flow supersonic boundary layer stability problem^(11,12). This initial effort was disappointing insofar as higher mode solutions for the shock tube laminar boundary layer could not be found. The first mode 2-D solutions only confirmed the results of Ostrach and Thornton. In this initial effort, it was found that the higher modes are associated with large values of the product of wave number (reciprocal of the spatial wavelength) and Reynolds number. This is characteristic of higher modes in low free-stream Mach number flows with high cooling rates. It was also found that larger numbers of very small integration steps were required to integrate the stability equations for shock-tube boundary layers. This report describes subsequent efforts to locate higher mode solutions to the parallel flow stability equations for highly cooled compressible boundary layers.

1.3 REPORT OUTLINE

Section II of this report describes the analysis of stability in shock induced boundary layer flows. The section begins with a description of the

calculation of the boundary layer mean flow profiles. This description is followed by a treatment of the formulation of the stability equations. Finally, some of the limits of applicability of the formulation are reviewed.

Section III presents the results of the analysis of boundary layer stability in shock induced flows. The results are preceded by a general description of the families of solutions identified by Mack. The specific results of this investigation are then presented and discussed.

Section IV describes the application of parallel boundary layer stability theory to another class of cooled boundary layer flows - steady flow boundary layers. A short description of the problem formulation is followed by a presentation and discussion of the results. The important similarities and differences with the results from shock induced flows are then discussed.

In Section V, the important conclusions of the study are presented for both shock induced and steady flow boundary layers and recommendations for further work are presented.

SECTION II

PARALLEL STEADY FLOW ANALYSIS OF SHOCK INDUCED FLOWS

The methods used to investigate the stability of the shock tube laminar boundary layers are presented in this section. In Section 2.1 the methods used to generate the mean flow velocity and temperature profiles are presented. In Section 2.2 it is shown that, when quasi-parallel, quasi-steady approximations are made for shock induced boundary layers, a set of stability equations are obtained which are identical to the stability equations for steady boundary layer flows.

A computer program, previously developed for steady flow boundary layer stability analysis, can then be applied to shock induced boundary layers. The equations and solution techniques of this program are described in detail elsewhere ^(11,12), but a brief description is included in Appendix B. Section 2.3 discusses the range of flow parameters that were considered in this investigation.

2.1 MEAN FLOW PROFILES

Mean flow velocity and temperature profiles are obtained by numerically integrating the laminar, compressible flow, boundary layer equations written in a shock fixed coordinate system. In this coordinate system described in Figure 3 the flow is steady and the boundary layer equations are formulated and solved according to the procedures developed by Mack ⁽¹³⁾ which served as the basis of the authors' computer program. Specifically, the program is set up to solve the steady laminar, compressible flow, boundary layer equations for flat plates with and without heat transfer at the wall. For the shock tube boundary layer calculation, the input quantities are as follows:

- Shock Mach number (M_s),
- Undisturbed flow temperature (T_1^*) and pressure (p_1^*),

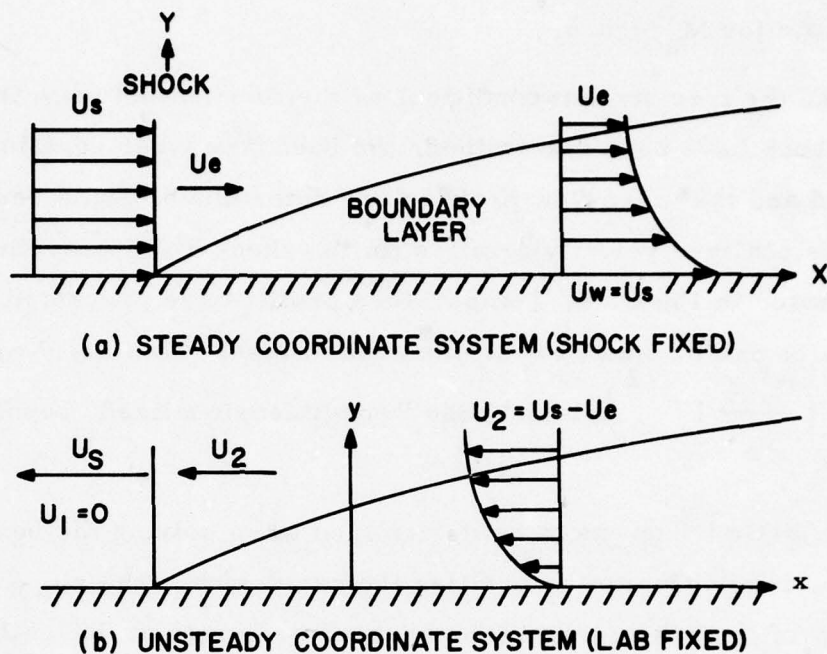


Figure 3. Boundary Layer Mean Flow Velocity Profile.

- Initial guesses for the slope of the velocity profile at the wall and the heat transfer rate at the wall.

The normal shock equations are solved to determine the free stream conditions of the flow downstream from the shock wave: M_e , U_e^* , T_e^* , p_e^* , h_e^* (enthalpy) and h_t^* (stagnation enthalpy of the free stream in the shock fixed coordinate system). These quantities are used to nondimensionalize the boundary layer equations. A basic assumption made in solving the boundary layer equations is that the initial temperature of the wall (T_w^*) is the same as T_1^* and that T_w^* remains constant. This assumption is reasonable because the time for heat transfer is very small (milliseconds or less) even though the heat transfer rate is high. The program is presently set up for air which is considered to be a gas that obeys the perfect gas law and has variable specific heats and transport properties.

Because dissociation and real gas effects are not considered, the program is only valid for $M_s < 6.5$.

Once the free stream conditions of the flow downstream from the normal shock have been determined, the boundary layer equations are integrated and the mean flow profiles are determined. Some representative nondimensionalized velocity profiles (in the shock-fixed coordinate system) are presented in Figure 4. Temperature profiles are presented in Figure 5. The profiles are presented in terms of the Blasius similarity variable $\left(\eta = \frac{Y}{X} \left(\frac{U_e^* X}{\nu_e} \right)^{1/2} \right)$ which is the "nondimensionalized" boundary layer thickness.

The basic unknowns to be determined when solving the boundary layer equations, in addition to the profiles themselves, are the slope of the velocity profile at the wall and the heat transfer rate at the wall. The Newton-Raphson technique is used to search for values of these two unknowns which will satisfy the proper boundary conditions at the edge of the boundary layer. After the solution converges, the velocity profile is transformed to the laboratory-fixed coordinate system and the velocity profiles in this coordinate system and the temperature profiles are then punched onto cards for use as a data deck for the Boundary Layer Stability computer program (BLSTAB).

2.2 FORMULATION OF THE STABILITY EQUATIONS FOR A SHOCK INDUCED BOUNDARY LAYER

The flow in a shock induced boundary layer is extremely difficult to analyze. Simplifying assumptions concerning the flow must be made in order to formulate the problem in a practically solvable form. There are a variety of methods of formulating the problem, but care must be taken to insure that a consistent set of simplifying assumptions and nondimensionalizations are made.

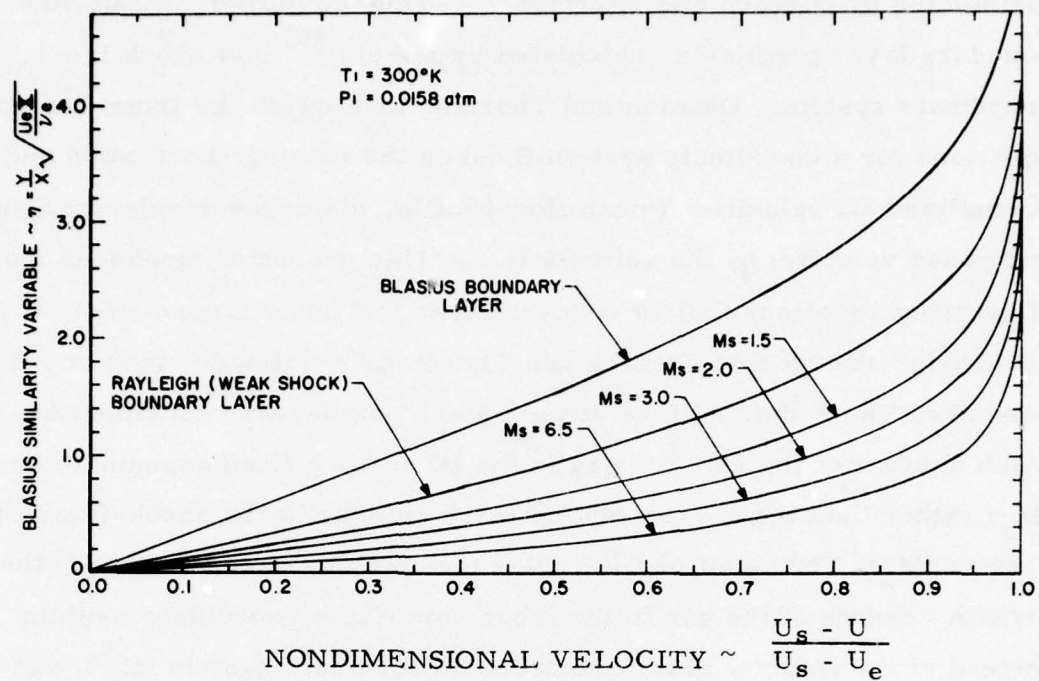


Figure 4. Representative Boundary Layer Mean Velocity Profiles.

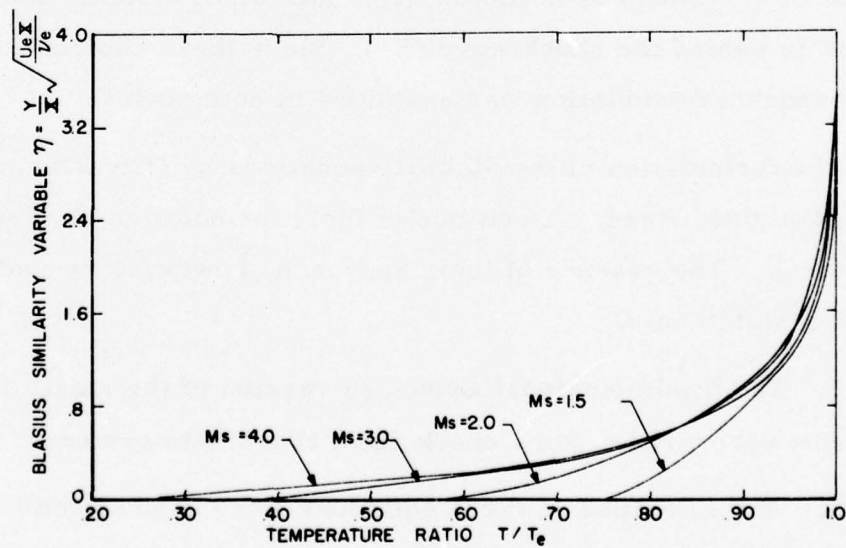


Figure 5. Representative Boundary Layer Mean Temperature Profiles.

The stability equations for shock induced boundary layer flow were formulated by Ostrach and Thornton⁽⁷⁾. They employed mean flow boundary layer profiles as calculated by Mirels⁽¹⁴⁾ in a shock fixed coordinate system. Ostrach and Thornton then wrote the Dunn-Lin stability equations for a coordinate system fixed on the moving shock wave and normalized all velocities (mean flow profile, disturbance velocity components, and phase velocity) by the velocity U_e^* . This procedure produced a set of stability equations that were identical to the Dunn-Lin equations** for steady flow except that Ostrach and Thornton "redefined" Mach and Reynolds numbers. The redefined free stream Mach number was considered to be the Mach number of the shocked gas in the laboratory fixed coordinate system (M_2) rather than the corresponding Mach number in the shock-fixed coordinate system (M_e). The redefined Reynolds number was based upon: (1) the free stream velocity of the gas in the laboratory-fixed coordinate system (U_2^*) instead of the velocity in the shock fixed coordinate system (U_e^*), and (2) a characteristic length equal to the distance traveled by a free stream fluid element in the laboratory fixed coordinate system (x^*) during the total time that the fluid element is in motion (t^*), instead of distance that the fluid element is behind the shock wave (X^*). Since these choices are not consistent, the subsequent formulation was examined in some detail.

The formulation of the stability equations by Ostrach and Thornton is not straightforward. A critique of their formulation is presented in Appendix A. The essence of their approach, however, is contained in the following statements.

1. The nondimensional Dunn-Lin version of the small disturbance equations were written for a shock fixed coordinate system.
2. The velocities in these equations were normalized with respect to the free stream velocity in a laboratory fixed coordinate system

** The Dunn-Lin equations are not a complete set of the small disturbance stability equations. Certain terms are omitted to permit 3-D solutions to be obtained from 2-D solutions.

(U_2^* , where $U_2^* = U_s^* - U_e^*$) rather than by the free stream velocity in the shock fixed coordinate system (U_e^*).

3. The characteristic length (ℓ^*) was taken to be proportional to the local boundary layer thickness in the shock fixed coordinate system, given by: $\ell^* = (2 X^* \nu_w^* / U_e^*)^{1/2}$.

4. The characteristic time (t_c^*) was given by, $t_c^* = \ell^* / (U_s^* - U_e^*)$.

5. Fluid, thermodynamic, and transport properties were non-dimensionalized with their corresponding free stream values.

When the dimensional Dunn-Lin small disturbance equations are non-dimensionalized using the characteristic quantities defined above, the final form of the Ostrach and Thornton stability equations is obtained (Equations 9a through 13a and Equation 14 in Reference 7).

The nondimensionalizations and normalizations described above effectively transformed the stability equation formulation out of the shock fixed coordinate system into the laboratory fixed coordinate system. However, the mean flow profiles as derived from Mirels' analysis (14) remained in the shock fixed coordinate system. The stability formulation was now inconsistent with the mean flow formulation. This inconsistency was resolved by "redefining" certain nondimensionalizations (such as Reynolds number). This "redefinition" effectively transformed the stability analysis back into shock fixed coordinates. The final formulation was therefore, entirely in shock fixed coordinates. A more detailed critique of this formulation is contained in Appendix A.

The final formulation of the stability equations by Ostrach and Thornton was unsuitable for use with existing computational programs at the University of Dayton which were constructed in a laboratory fixed coordinate system. Therefore, a different approach to formulating the stability equations was developed. This approach starts with the

linearized complete small disturbance equations in dimensional form (rather than the Dunn-Lin equations) written in a laboratory fixed coordinate system. Then both the parallel flow and quasi-steady approximations were invoked. Finally, all dependent variables were nondimensionalized with respect to free stream quantities and all spatial variables were nondimensionalized with respect to a scale length proportional to the boundary layer thickness. This procedure yields a system of stability equations which are identical to the Ostrach and Thornton stability equations except that all parallel flow terms are included and the Reynolds number (Re_l) is given by $(R_x)^{1/2}$ instead of $(2 R_x)^{1/2} (T_w^*/T_e^*)$. (The Ostrach-Thornton formulation includes only those terms contained in the Dunn-Lin stability equations.)

In summary, the stability equations used in the present analysis are the same as the stability equations for steady flow over a flat plate. The stability analysis is thus a stability analysis of a given mean flow profile and is valid over changes in distances and times that are small enough so that the change of profiles in both time and space can be ignored. The computer program which implements this formulation is described in Appendix B.

2.3 RANGE OF FLOWS ANALYZED

Eigensolutions to the linear stability equations, with the parallel flow assumption, were computed for both a quasi-steady flow shock tube system, and a steady flow wind tunnel system. The effects of wall cooling on boundary layer stability in shock tube type flows were examined for both subsonic ($M_s = 1.5$, $M_2 = 0.6027$ and supersonic ($M_s \leq 5.0$, $M_2 \leq 1.841$) flows. The effects of wall cooling on boundary layer stability for Mach numbers less than 0.9 in steady wind tunnel type flows were also investigated.

2.3.1 Shock Tube Flows

The shock Mach numbers considered in this analysis extended from $M_s = 2.50$ to $M_s = 5.00$ in increments of 0.25. In addition, treatment

was given to $M_s = 1.5$, as previously noted. These calculations were performed for the "standard" wall cooling ratios (T_w/T_e), as given in Table 1. The "standard" wall cooling is that which occurs when the shock tube walls remain at ambient temperature regardless of the temperature of the shocked gas. In addition, calculations were performed at shock Mach numbers of $M_s = 2.5$ and $M_s = 2.75$ with specified "nonstandard" amounts of wall cooling. Numerical solutions to all the above situations were generated for the case of two-dimensional disturbances. Three dimensional, oblique solutions were obtained for only the cases of $M_s = 1.5$ (subsonic) and $M_s = 3.0$ (supersonic) flows. The results of these calculations are presented in Section III.

It should be noted that the technique employed is valid only for shock tube flows where, in general, $M < 6.5$, as "real gas" effects have been ignored.

2.3.2 Subsonic Wind Tunnel Flows

Two and three dimensional disturbances in steady flow, wind tunnel type boundary layers were investigated for free stream Mach numbers of 0.603, 0.80, and 0.90. Surface cooling at each Mach number was varied from the insulated value of T_w/T_e (specified by the flow conditions), to $T_w/T_e = 0.620$. The streamwise wave angle of three dimensional disturbances was varied from 0° to 87.5° for each case. Results of these calculations are presented in Section IV.

TABLE 1
MOVING SHOCK WAVES-MEAN FLOW RESULTS
 $T_1 = 300^\circ\text{K}$
 $P_1 = 0.0158 \text{ atm}$

| M_s | M_e | T_e/T_w | U_s/U_e | $(\frac{dU}{d\eta})_w$ | θ_w | G_w | M_2 | T_w/T_e | η_δ | $T_2(^{\circ}\text{R})$ | $C_r(\hat{M}_w = -1)$ | $1 + \frac{1}{M_2}$ |
|-------|-------|-----------|-----------|------------------------|------------|--------|-------|-----------|---------------|-------------------------|-----------------------|---------------------|
| 1.00 | 1.000 | 1.000 | 1.000 | 1.000 | 0.000 | 0.000 | 0.000 | 1.000 | | 540.00 | ∞ | ∞ |
| 1.50 | 0.705 | 1.317 | 1.854 | -1.751 | -2.437 | 2.600 | 0.602 | 0.759 | 5.37 | 711.48 | 1.445 | 2.659 |
| 2.00 | 0.580 | 1.679 | 2.671 | -2.031 | -6.135 | 8.440 | 0.969 | 0.595 | 5.00 | 907.18 | 0.795 | 2.031 |
| 2.50 | 0.514 | 2.114 | 3.371 | -3.840 | -10.365 | 17.150 | 1.220 | 0.472 | 4.55 | 1141.77 | 0.563 | 1.819 |
| 2.75 | 0.493 | 2.359 | 3.677 | -4.884 | -12.524 | 22.122 | 1.320 | 0.423 | 4.42 | 1274.01 | 0.493 | 1.757 |
| 3.00 | 0.475 | 2.622 | 3.957 | -6.019 | -14.665 | 27.397 | 1.406 | 0.381 | 4.32 | 1455.88 | 0.439 | 1.710 |
| 3.25 | 0.461 | 2.902 | 4.215 | -7.239 | -16.773 | 32.900 | 1.482 | 0.344 | 4.21 | 1567.04 | 0.395 | 1.674 |
| 3.50 | 0.449 | 3.199 | 4.452 | -8.536 | -18.827 | 38.543 | 1.550 | 0.312 | 4.12 | 1727.50 | 0.360 | 1.645 |
| 3.76 | 0.438 | 3.513 | 4.671 | -9.904 | -20.825 | 44.281 | 1.611 | 0.284 | 4.05 | 1896.97 | 0.331 | 1.620 |
| 4.00 | 0.430 | 3.843 | 4.874 | -11.337 | -22.760 | 50.066 | 1.666 | 0.260 | 3.99 | 2075.35 | 0.306 | 1.600 |
| 4.25 | 0.422 | 4.190 | 5.062 | -12.831 | -24.628 | 55.855 | 1.715 | 0.238 | 3.93 | 2262.62 | 0.284 | 1.582 |
| 4.50 | 0.415 | 4.553 | 5.237 | -14.378 | -26.426 | 61.610 | 1.761 | 0.219 | 3.88 | 2458.79 | 0.266 | 1.567 |
| 4.75 | 0.409 | 4.933 | 5.399 | -15.975 | -28.153 | 67.302 | 1.802 | 0.202 | 3.83 | 2663.89 | 0.249 | 1.554 |
| 5.00 | 0.404 | 5.329 | 5.550 | -17.616 | -29.807 | 72.906 | 1.840 | 0.187 | 3.79 | 2877.97 | 0.235 | 1.533 |
| 5.50 | 0.395 | 6.172 | 5.822 | -19.774 | -32.904 | 79.168 | 1.907 | 0.162 | 3.75 | 3332.98 | 0.211 | 1.524 |
| 6.50 | 0.381 | 8.057 | 6.270 | -26.029 | -38.314 | 96.487 | 2.010 | 0.124 | 3.71 | 4351.13 | 0.175 | 1.497 |

$$\theta = \frac{h_t^* - h_e^*}{h_t^* - h_e^*}$$

$$G = \frac{\mu}{\sigma} \frac{d\theta}{d\eta}$$

SECTION III

RESULTS OF ANALYSIS OF SHOCK INDUCED FLOWS

As noted in Section 1.2, Boehman made his first attempt to determine higher mode solutions to the parallel flow stability equations for shock induced flows in 1972. These initial attempts were unsuccessful but higher mode solutions were obtained during the course of the present investigation. The results of the search for higher mode solutions are presented in this section. However, these higher mode solutions do not correlate with observed transition phenomena. It was also pointed out in Section 1.2 that the Ostrach-Thornton investigation of the stability of shock induced flow did not include an investigation of 3-D (oblique) disturbances. The search for 3-D unstable disturbances was included in the present effort but it was found that three dimensional disturbances were always more stable than two dimensional disturbances over the range of flow parameters considered.

The principal objective of the present effort was to determine higher mode and three dimensional solutions to the stability equations for shock induced flows in the expectation that these solutions would correlate with experimental observations of transition in shock induced flow. When it was found that this expectation was not to be realized, a search for other types of solutions to the stability equations was undertaken. A new type of solution was found for a supersonic incoming wave disturbance and qualitative correlation with Boison's measurements of transition; Reynolds number has been demonstrated. Before proceeding with the presentation and discussion of these new results, the flow conditions under which different types of disturbances can be expected are described.

3.1 SUBSONIC, SONIC, AND SUPERSONIC DISTURBANCES IN SHOCK INDUCED FLOWS

Three curves of phase velocity versus shock Mach number (M_s) are shown in Figure 6. The curve labeled $c_r(\hat{M}_w = -1)$ shows the minimum

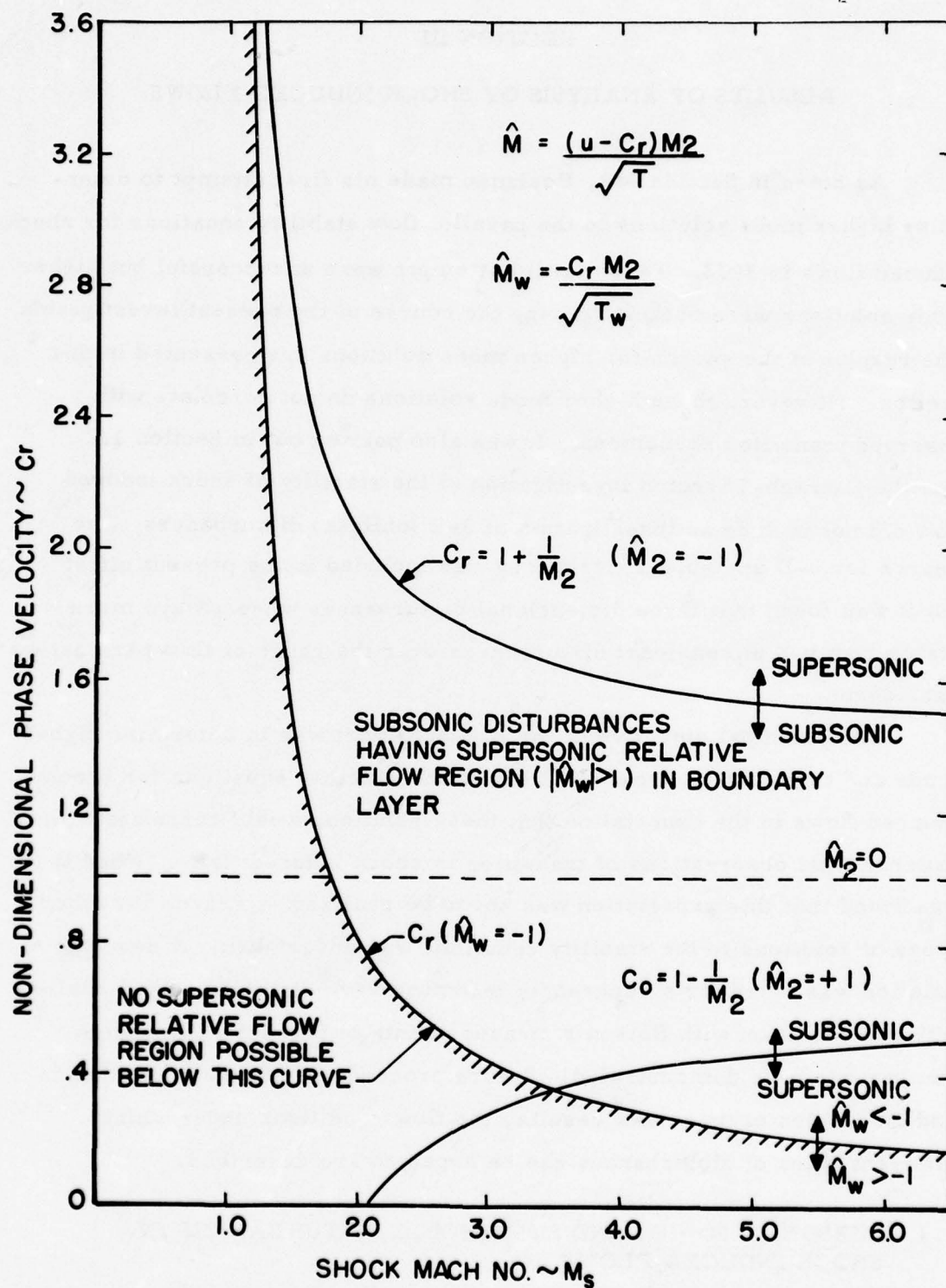


Figure 6. Phase Velocity Versus Shock Mach No. in Shock Tube Flows.

phase velocity that a disturbance must have in order to move supersonically relative to the flow at the wall. The second curve, labeled $c_r = 1 + 1/M_2$, shows the phase velocity that a disturbance must have to move sonically with respect to the disturbance (i. e., the free stream is moving in the upstream direction at $M = 1$ relative to an observer moving at the velocity $1 + 1/M_2$). The third curve, labeled $c_o = 1 - 1/M_2$, shows the phase velocity that a disturbance must have to allow the free stream to move sonically with respect to disturbance but with the relative velocity between the disturbance and the free stream being in the direction of flow. These three curves together form a region in which subsonic disturbances exist and the local Mach number of the flow at the wall is supersonic relative to the phase velocity. This region of phase velocities is the region in which subsonic higher mode disturbances can exist. Above $M_s = 3.5$, both subsonic and supersonic multiple mode solutions can exist.

3.2 INCOMING AND OUTGOING DISTURBANCES

It was noted in Section 1.1.3 and illustrated in Figure 1 that a pair of Mach waves are produced whenever a low amplitude supersonic disturbance exists in the free stream. Mack has noted that the two solutions to the inviscid stability equations for the flow in the free stream represent a pair of Mach waves ⁽⁶⁾. Thus, the stability equations produce solutions for supersonic disturbances which have a well-defined physical interpretation. One of these solutions represents a reflected or outgoing Mach wave and the other represents an incident or incoming Mach wave. In Reference 6 Mack shows that for neutral outgoing Mach waves, energy is transported in the direction of increasing y (i. e., into the free stream) whereas for neutral incoming waves, energy is transported in the direction of decreasing y , (i. e., into the boundary layer).

For subsonic disturbances, the inviscid free stream solutions no longer represent Mach waves, but instead represent two exponentially varying pressure fields caused by inviscid flow over a moving wavy wall. Thus for subsonic phase velocities, as well as for supersonic phase velocities,

the solutions to the inviscid stability equations have simple physical interpretations. A basic understanding of the mathematical nature of the solutions to the inviscid stability equations is helpful for understanding the discussion of results presented in this section. The solution to the inviscid stability equations for the free stream region of flow has the general form ⁽⁶⁾:

$$\pi(y) = Ae^{\lambda_1 \eta} + Be^{\lambda_2 \eta}, \quad (12)$$

where π represents the amplitude of the pressure oscillation, λ_1 and λ_2 are the two characteristic values of the second order ordinary differential equation which describes the behavior of π in the free stream when no viscous terms are included in the stability equations, η is the distance from the surface (Blasius similarity variable) and A and B are constants of integration. λ_1 and λ_2 are represented by ⁽⁶⁾:

$$\lambda_1 = -\alpha(1 - \hat{M}_2^2)^{1/2}, \quad (13)$$

and

$$\lambda_2 = -\lambda_1. \quad (14)$$

The fundamental difference in nature between subsonic and supersonic disturbances is described in the following sections in which the properties of the characteristic values of neutral disturbances ($c_i = 0$) for these two cases are examined.

3.2.1 Supersonic Disturbances ($|\hat{M}_2| > 1$)

For $|\hat{M}_2| > 1$, $1 - \hat{M}_2^2$ is a negative number and $(1 - \hat{M}_2^2)^{1/2}$ is a pure imaginary number. Thus λ_1 is given by:

$$\lambda_1 = \pm i\alpha(\hat{M}_2^2 - 1)^{1/2} \quad (15)$$

In the coordinate system moving with the phase velocity, the pressure fluctuation p' is given by ⁽⁶⁾:

$$p' = i\alpha \gamma \hat{M}_2^2 (1 - c_r) \exp\{i\alpha[x \mp (\hat{M}_2^2 - 1)^{1/2}(\eta - \eta_e)]\} \quad (16)$$

Thus, in the $x-\eta$ plane, the above equation will have a line of constant amplitude (constant phase) which is a Mach line of the flow relative to the phase velocity. The amplitude of the pressure fluctuation is independent of η . If $c_r > 1 + 1/M_2$, then the incoming wave will correspond to:

$$\lambda_1 = -i\alpha (\hat{M}_2^2 - 1)^{1/2} \text{ (incoming wave, } c_r > 1 + 1/M_2 \text{)}.$$

If $c_r < 1 - 1/M_2$, the incoming wave will correspond to:

$$\lambda_1 = +i\alpha (\hat{M}_2^2 - 1)^{1/2} \text{ (incoming wave, } c_r < 1 - 1/M_2 \text{)}.$$

3.2.2 Subsonic Disturbances ($-1 < \hat{M}_2 < 1$)

In the case of subsonic disturbances, $(1 - \hat{M}_2^2)^{1/2}$ is a real number; λ_1 is negative and λ_2 is positive. The pressure fluctuation p' is given by:

$$p' = i\alpha \gamma M_2^2 (1 - c_r) \exp(i\alpha x) \exp[\mp \alpha (1 - \hat{M}_2^2)^{1/2} (\eta - \eta_e)] \quad (17)$$

The solution whose characteristic value has a negative real part represents the pressure field over the moving wavy wall (outgoing solution). The solution whose characteristic value has a positive real part represents the pressure field under the moving wavy wall (incoming solution).

In the viscous theory, two of the independent solutions are almost identical to the inviscid solutions except for a small viscous decay term. Ordinarily in stability theory, the inviscid solution (or the viscous counterpart) whose characteristic value has a positive real part (incoming solution) is not used since this solution increases exponentially upwards from the boundary layer and thus does not satisfy the boundary conditions at infinity. In the following paragraphs it will be convenient to classify the results of the stability investigations in terms of incoming or outgoing subsonic or supersonic disturbances. Sonic disturbances have a singular character as explained in the next section.

3.3 FAMILIES OF SOLUTION

Perhaps one of the most important discoveries made by Mack was that two families of solutions can be obtained from the stability equations for compressible laminar boundary layer flows⁽⁶⁾. Mack characterized the two families on the basis of the behavior of the solutions at $\alpha = 0$. He called a set of solutions members of the c_o family of solutions if the phase velocity approached a value of $c_r = 1 - 1/M_\infty$ as α approached zero. He called a set of solutions members of the "regular" family of solution when the phase velocity approached a value of $c_r = 1 + 1/M_\infty$ as α approached zero.

Most of the stability results which are available in the literature for supersonic flows are subsonic solutions belonging to the c_o family of solutions. If the free stream Mach number is less than one (subsonic boundary layer flows), the c_o family of solutions has its origin at $c_r = 0$. Relatively few "regular" family solutions are available in the literature --those which do exist were determined by Mack or Boehman.

From the preceeding discussion it is evident that the two sonic phase velocities $c_r = 1 - 1/M_\infty$ and $c_r = 1 + 1/M_\infty$ define two separate families of solutions.

3.4 RESULTS FOR SHOCK INDUCED FLOWS

This section begins with a presentation of the results which were obtained from the first effort to reconduct the Ostrach-Thornton analysis. As was mentioned in Section 1.1, the effort was carried out before the present effort was undertaken but is included here for the sake of completeness.

3.4.1 Subsonic Outgoing Disturbances

As was mentioned in the Introduction, the first effort showed that very small integration step sizes are required to numerically integrate the stability equations for the shock-tube boundary layer when compared to step-size requirements for treating wind tunnel boundary layers. Figure 7 shows the neutral stability curve for 2-D disturbances which was obtained for the $M_s = 1.5$ boundary layer. One hundred and thirty-six integration

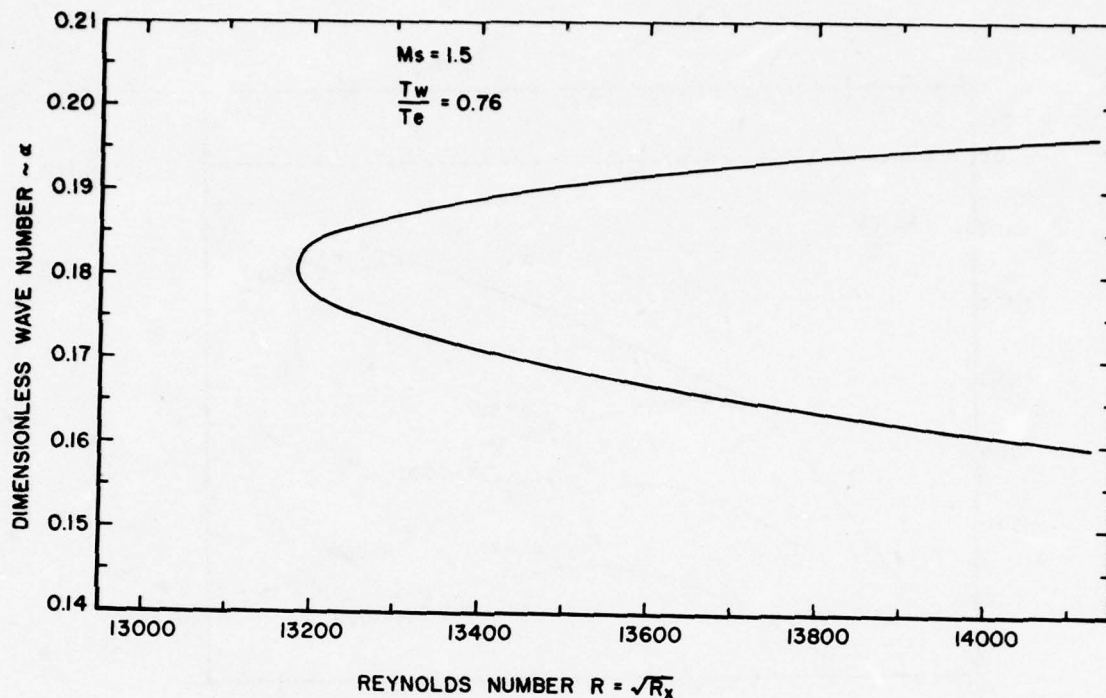


Figure 7. Two Dimensional Disturbance Neutral Stability Curve at $M_s = 1.5$ for Shock Tube Boundary Layer.

steps were required to obtain these results. The minimum critical Reynolds (R_{crit}) is seen to be 13,180 and compares to the Ostrach-Thornton value of 14,000 for the same value of M_s . These calculations as well as those of those of Ostrach and Thornton were for 2-D waves. A value of R_{crit} of 13,180 corresponds to a value of R_x of 1.737×10^8 which is about two orders of magnitude higher than measured transition Reynolds numbers for $M_s = 1.5$. The remainder of the results presented in this report were obtained as part of the current effort.

Since R_{crit} for 2-D disturbances at $M_s = 1.5$ obviously did not correlate with measured transition Reynolds numbers, 3-D disturbances were investigated at $M_s = 1.5$. The results are shown in Figures 8 and 9 for several Reynolds numbers. These results show that at $M_s = 1.5$, oblique disturbances are always more highly damped than 2-D disturbances. Similar calculations performed for $M_s = 3.0$ also show

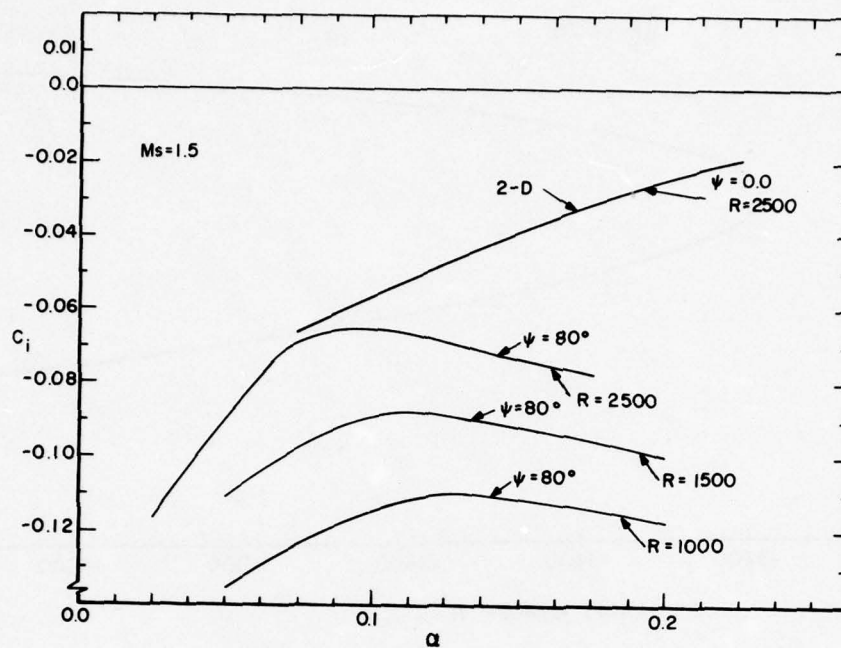


Figure 8. Effect of Wave No. (α) on Amplification (c_i) for Varying Reynolds No. (R). Wave Angle (ψ) = 80° , $M_s = 1.5$

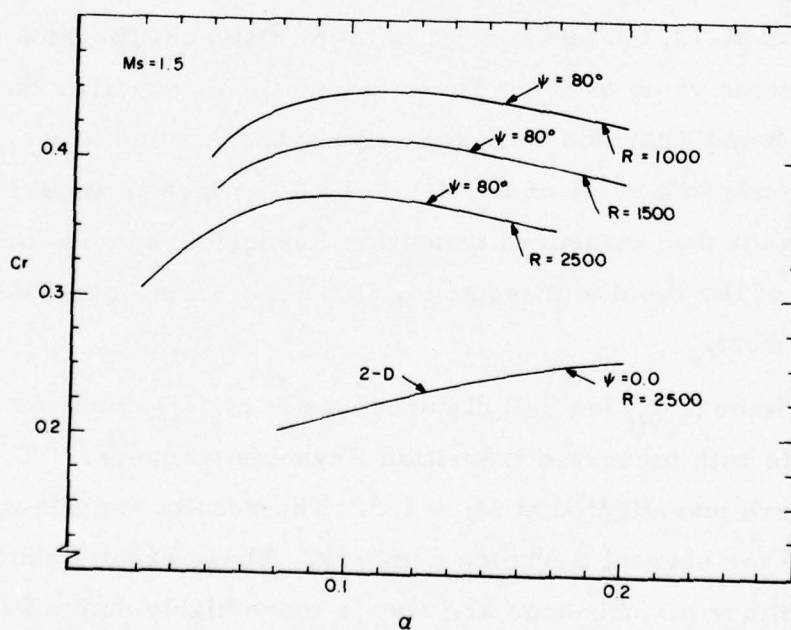


Figure 9. Effect of Wave No. (α) on Phase Velocity (c_r) for Varying Reynolds No. (R). Wave Angle $\psi = 80^\circ$, $M_s = 1.5$

that 3-D disturbances are more highly damped than 2-D disturbances. Typical results at $M_s = 3.0$ are shown in Figures 10 and 11. The results shown in Figures 8 - 11 are for disturbances belonging to the c_o family. No higher mode amplified solutions for this family of solutions are possible for shock tube boundary layers since the wall cooling is sufficient to remove the generalized inflection point from these boundary layers⁽⁶⁾.

First and higher-mode outgoing subsonic solutions belonging to the "regular" family of solutions, which are always amplified when $c_r \leq 1$, have been investigated. The regular family of solutions persist to low subsonic Mach numbers, since it is always possible to find a c_r large enough so that a supersonic relative flow region exists somewhere in the boundary layer, except at $M = 0$. In Figure 6, the curve labeled $c_r = 1 + 1/M_2$ ($\hat{M}_2 = -1$) shows the phase velocity which this family of solutions begins at ($\alpha = 0$) as a function of shock Mach number. For this family of solutions to have amplified solutions, $c_r < 1$ and for neutral solutions, $c_r = 1$ ⁽⁶⁾.

From Figure 6 can be seen that a supersonic relative flow region for subsonic disturbances with $c_r \leq 1$ can only exist when $M_s \leq 1.8$ in shock tube boundary layers. Thus, regular amplified subsonic solutions are not possible below this Mach number. Some typical regular family solutions are shown in Figures 12 and 13 for $M_s = 1.5, 2$, and 4. In Figure 12, the phase velocity (c_r) versus wave number (α) is shown for both viscous and inviscid solutions. As shown in Figure 13, the viscous solutions are all damped whereas the inviscid solutions are all neutral. The only exception is at $M_s = 4$ where the inviscid solutions show a very small amount of amplification for $\alpha > 3.5$. For $\alpha > 3.5$, the phase velocity (c_r) is less than one. According to Mack, a necessary condition for an amplified inviscid regular solution to exist is that c_r be less than 1. Calculations performed to date indicate that an amplified regular viscous solution can likewise only exist if $c_r < 1$. In Mack's terminology, the solution for $c_r = 1$ is called the regular neutral solution and the corresponding value of α is given the symbol

α_{11}

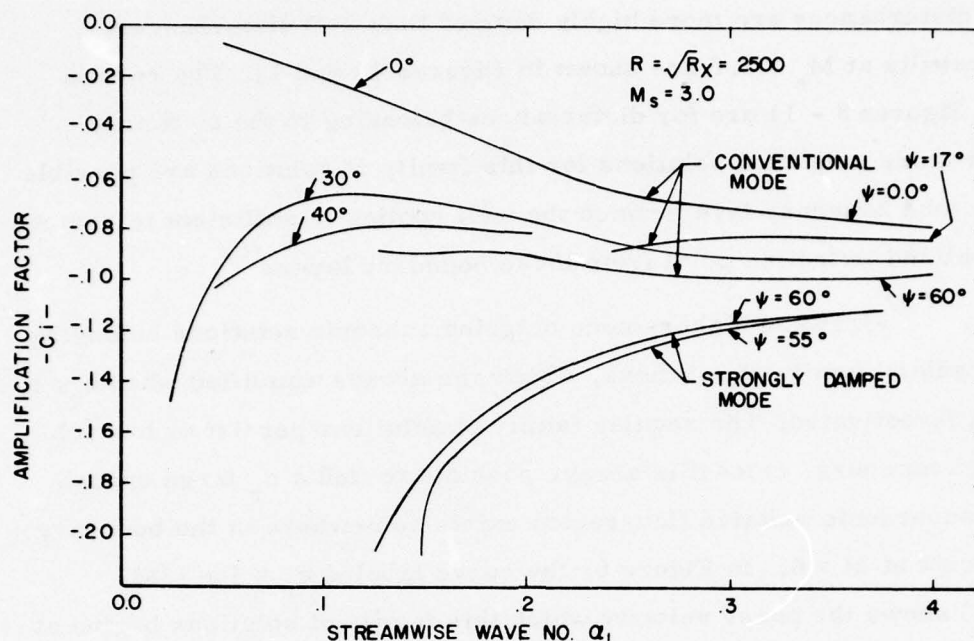


Figure 10. Effect of Wave Angle (ψ) on Amplification (c_i). $M_s = 3.0$

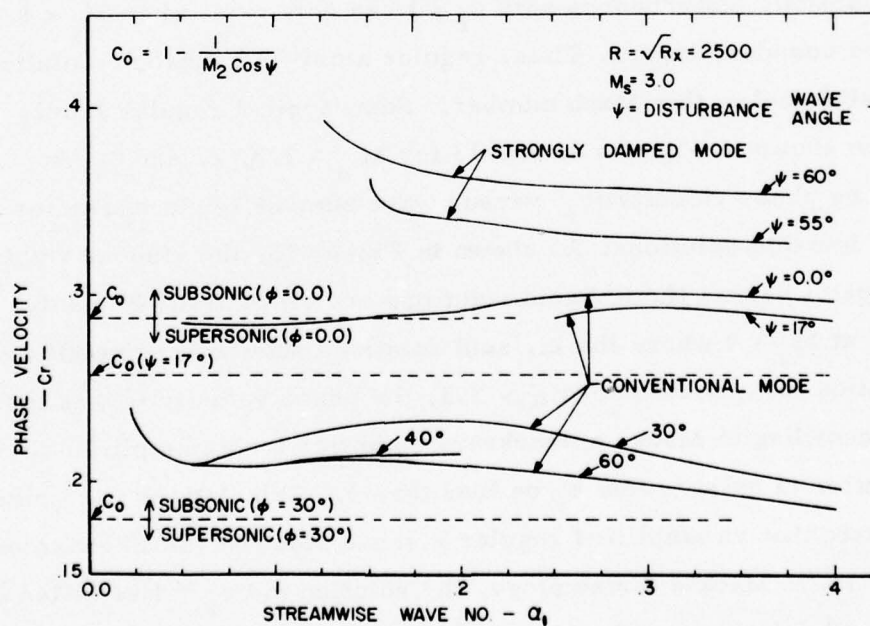


Figure 11. Effect of Wave Angle (ψ) on Phase Velocity (c_r). $M_s = 3.0$

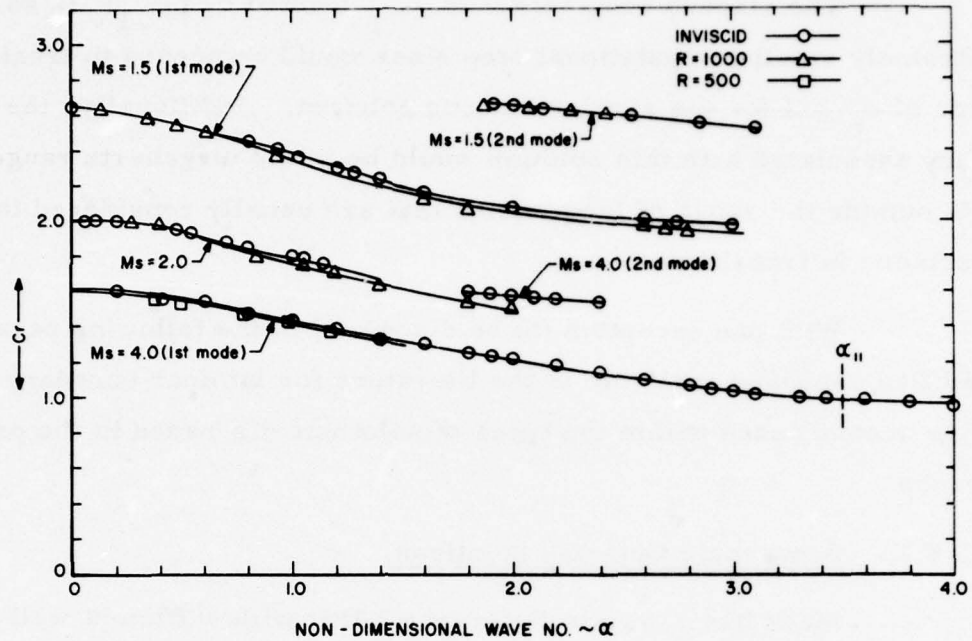


Figure 12. Phase Velocity (c_r) Versus Wave Number (α) for First and Second Mode Regular Subsonic Disturbances

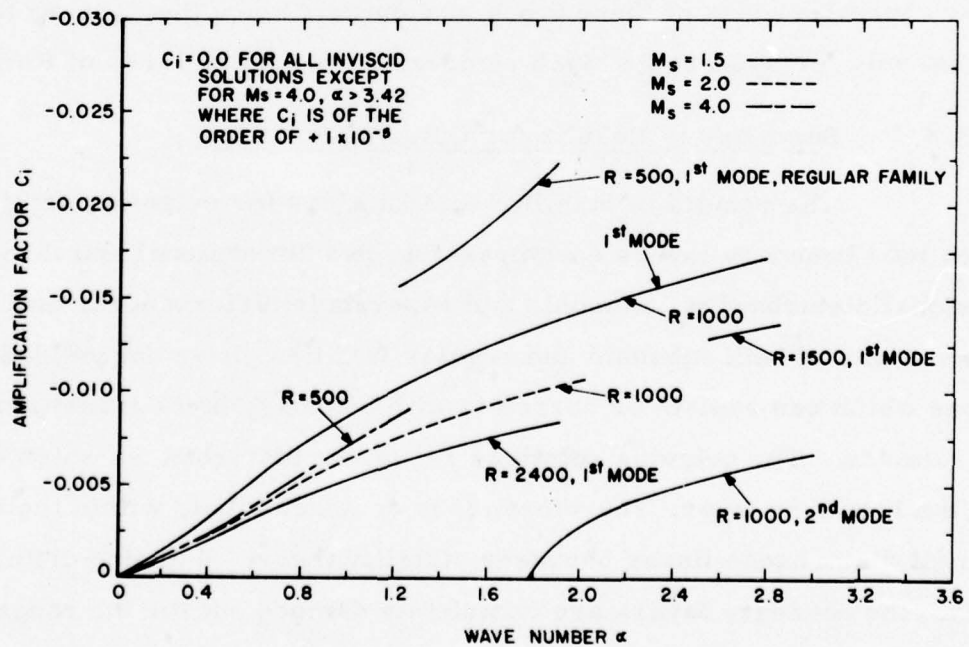


Figure 13. Amplification (c_i) Versus Wave Number for Subsonic Regular Family of Solutions. $M_s = 1.5, 2.0$ and 4.0

The viscous counterpart to α_{11} denoted by $(\alpha_{11})_v$ is so large that extremely small computational step sizes would be needed to treat a condition of $c_r \leq 1$ for the regular viscous solution. Additionally, the frequency associated with this solution would be in the megahertz range which is outside the range of frequencies that are usually considered to be of importance in transition.

With one exception (to be discussed in the following paragraphs), all amplified solutions available in the literature for laminar boundary layer flows are encompassed within the types of solutions discussed in the previous paragraphs.

3.4.2 Supersonic Outgoing Solutions

Mack has shown in Reference 6 that with sufficient wall cooling, amplified, supersonic, outgoing solutions belonging to the c_o family of solutions can exist. However, these solutions have wave numbers which are greater than α_{11} so that again, high frequency solutions are the only possible amplified solutions. Thus, no attempt was made to determine the stability characteristics of these types of solutions since they appear to be important only for hypersonic Mach numbers (see Figure 11.25 of Ref. 6).

3.4.3 Summary of Results for Outgoing Solutions

The results of stability computations for outgoing disturbances in shock tube boundary layers encompassing; two dimensional and three dimensional disturbances, subsonic and supersonic disturbances, and multiple mode solutions of both subsonic and regular families, have not yielded solutions which can explain or correlate with boundary layer transition measurements. The outgoing solutions represent disturbances which originate within the boundary layer. Therefore, it is concluded that, within the context of a small disturbance linear boundary stability theory, outgoing disturbances in shock tube boundary layers are completely damped out for the range of Mach numbers considered in this study ($M_g = 1.5$ to 5.0). It is further concluded, subject to the limitations on the validity of the linear theory, that

extremely high transition Reynolds numbers would be attainable if it were possible to eliminate all environmental disturbances in a shock tube. Even at a shock Mach number as low as 1.5, linear stability theory predicts a critical Reynolds number as high as approximately 1.7×10^8 .

3.4.4 Incoming Disturbances

A new type of solution to the stability equations was discovered during the course of the outgoing wave study. These solutions show some promise of providing a mechanism for explaining transition. These new solutions are incoming wave eigensolutions and were originally discovered when it was noted that certain damped supersonic incoming wave eigensolutions end abruptly in a c_r versus α plot unless one allows the sign of the real part of the characteristic value of the viscous solution (which is a counterpart to the inviscid free stream) to switch from negative to positive.

Before discussing amplified incoming supersonic disturbances, a number of related points should be made. First, Mack had never found any incoming neutral supersonic solutions. Second, he indicated that if they did exist, they would not have the importance of the outgoing neutral supersonic solutions (page 11-45 of Reference 6). Third, the amplitude of an incoming amplified supersonic disturbance would have to increase with increasing distance from the wall (page 10-34 of Reference 6). The third point posed some conceptual difficulties at first since only those solutions to the linear stability equations which are at least bounded at infinity are considered to be valid. This conceptual difficulty was resolved by recognizing that the boundary layer in a shock tube does not extend to infinity. In particular, surface roughness or turbulence on one sidewall in a shock tube, can influence the boundary layer on the opposite sidewall. Thus solutions which have amplitudes increasing with distance from the wall are permissible so long as the rate of growth is not excessive. This condition is generally satisfied by the viscous counterpart to the inviscid solution of the stability equations. The initial search for incoming amplified

disturbances was prompted by an unexpected finding made during investigation of the two dimension subsonic disturbance calculations for low Reynolds numbers and low wave numbers at $M_s = 3.0$. It was observed that as α was decreased from about 0.3 to 0.1 for a 2-D wave, the damping rate started to sharply decrease. However, 3-D waves ($\psi > 30^\circ$) show a gradual decrease in damping and then a sharp increase as α approaches zero as illustrated in Figure 10. The phase velocity of the 2-D subsonic disturbances shows a steady decrease first approaching and then dropping below $c_r = 1 - 1/M_2$. In contrast the 3-D, 30° wave showed a strong increase in c_r as α approaches zero (as shown in Figure 11). It was observed that the character of the 2-D disturbances changed from out-going to incoming as c_r dropped below $1 - 1/M_2$. Decreasing the Reynolds number from $R = 2500$ to 1500 showed that, as α dropped below 0.075, the damping at $R = 1500$ became less than the damping for $R = 2500$. These results provided the first clues that amplified incoming disturbances might exist. As α was decreased to about 0.05 and the Reynolds number decreased to 1000 it was observed that the real part of the eigenvalue corresponding to the inviscid solution had to be allowed to change sign from negative to positive as it passed through zero in order to maintain an incoming disturbance. A further decrease in α at $R = 1000$ yielded the first amplified incoming supersonic disturbances as shown in Figure 14 and 15. The results presented in Figure 14 clearly show that viscosity is destabilizing; that is the amplification factor decreases as the Reynolds number is increased. Thus these incoming solutions cannot be found from an inviscid stability analysis. Similar calculations were performed for $M_s = 3.25$ and 3.5. These results are shown in Figures 16, 17, 18, and 19.

As α is decreased at constant R , in Figure 16, the real part of the characteristic value of the viscous counterpart to the inviscid solution changes sign from negative to positive at the points labeled as a "transitional" region. For values of α greater than α at this "transitional region", the amplitude of the waves decreases as y increases; whereas, for α values less than α at this "transitional region", the amplitude of the waves increases as y increases. These new incoming wave eigensolutions must be interpreted

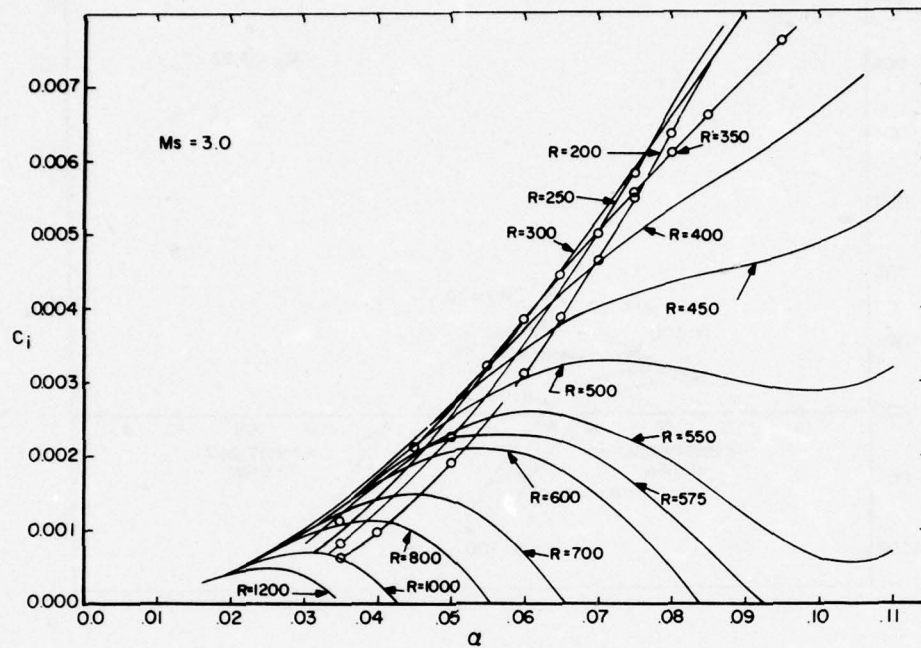


Figure 14. Effect of Streamwise Wave No. (α) on Amplification Factor (c_i) for Varying Reynolds No. ($R = \sqrt{R_x}$) (106 Integration Steps), $M_s = 3.0$

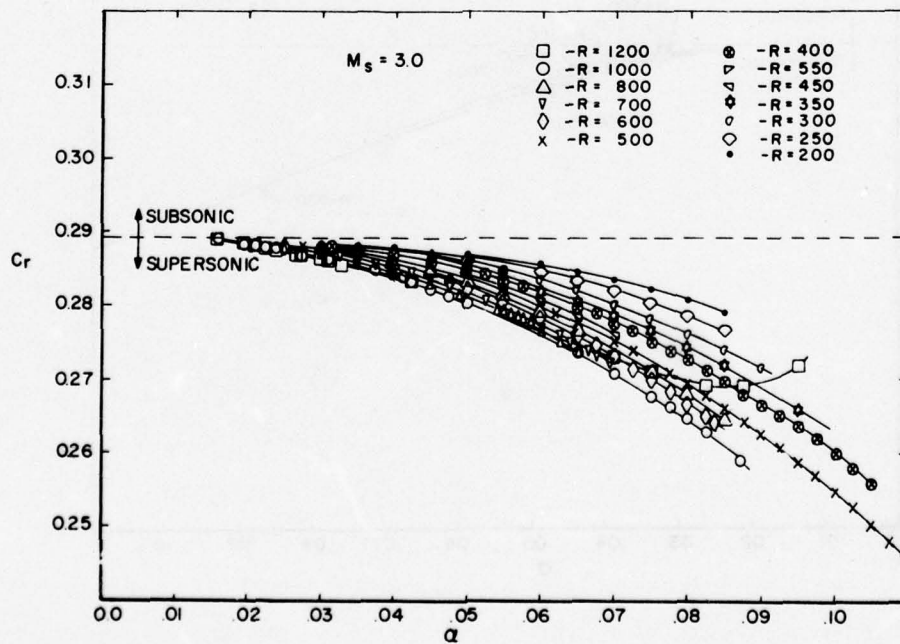


Figure 15. Phase Velocity (c_r) Vs. Streamwise Wave No. (α) at Varying Reynolds No. ($R = \sqrt{R_x}$). 106 Integration Steps, $M_s = 3.0$

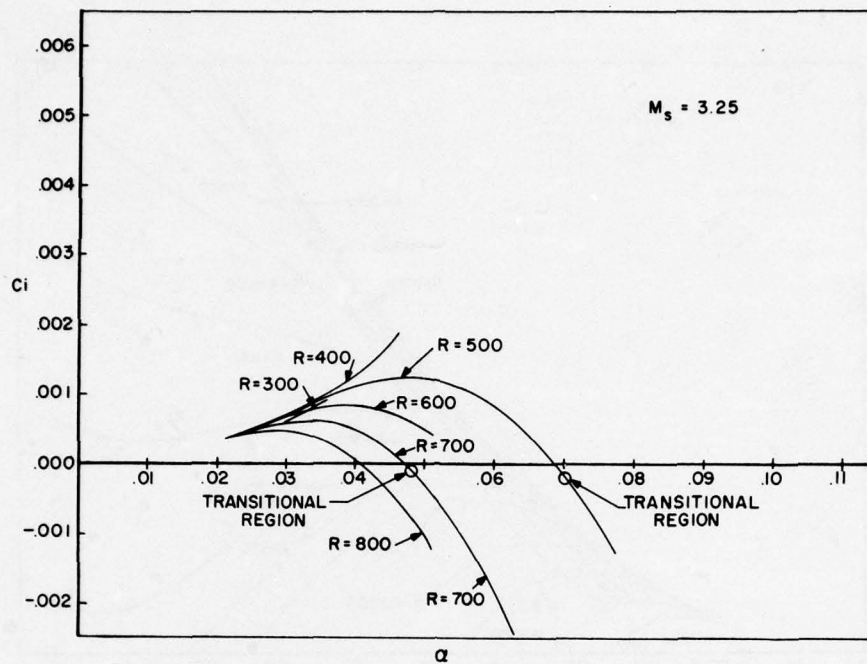


Figure 16. Effect of Wave Number (α) on Amplification (c_i), $M_s = 3.25$

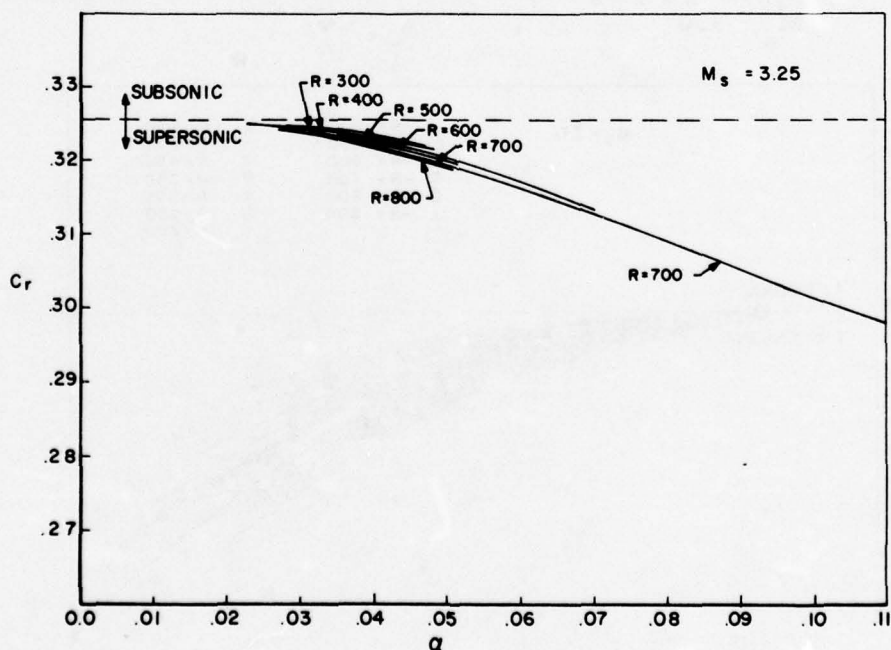


Figure 17. Effect of Wave Number (α) on Phase Velocity (c_r) for Varying Reynolds Number ($R = \sqrt{R_x}$), $M_s = 3.25$

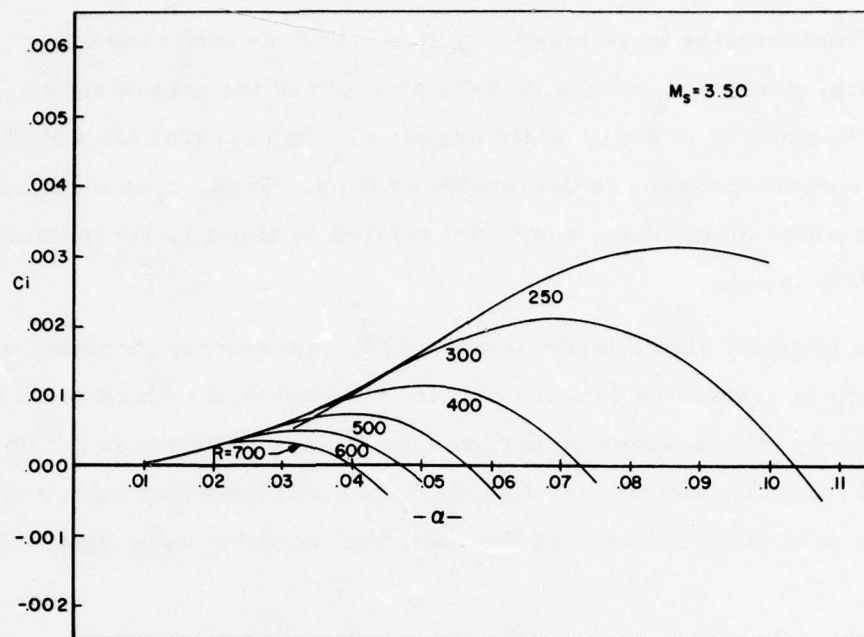


Figure 18. Effect of Wave No. (α) on Amplification Factor (c_i), $M_s = 3.5$

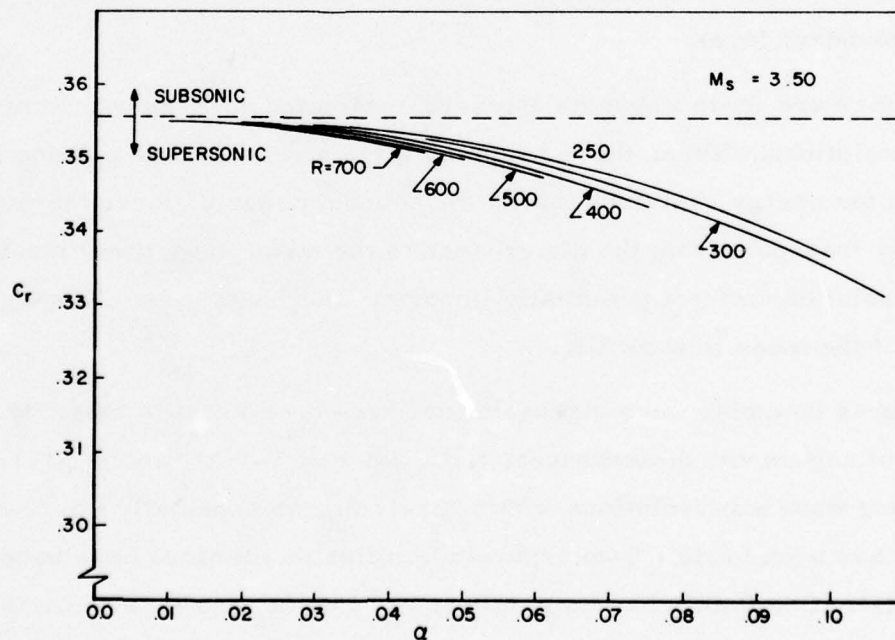


Figure 19. Effect of Wave No. (α) on Phase Velocity (c_r), $M_s = 3.5$

differently from outgoing wave eigensolutions. For the incoming wave eigensolutions, positive c_i means that the strength of the free-stream disturbance is growing in time, while negative c_i implies that the strength of the free-stream disturbance is decreasing in time. Thus, c_i is an attribute of the free-stream disturbance and is not related by itself to the instability of the boundary layer.

The physical significance of amplified, supersonic, incoming wave eigensolutions is associated with the special characteristic which these waves possess, namely, these waves do not produce a reflected wave in the boundary layer. That is, while an ordinary (noneigensolution) incoming wave requires the presence of a reflected wave at the wall, the incoming wave eigensolutions do not.

The important physical significance of these incoming wave eigensolutions is related to the energy transfer associated with the incoming wave. All of the energy transported into the boundary layer through the incoming wave remains in the boundary layer; there is no reflected wave to carry energy out of the boundary layer.

There are finite Reynolds stresses associated with these incoming wave eigensolutions. Thus, these incoming wave eigensolutions provide a mechanism for energy redistribution in the boundary layer. Since there is a net energy transport from the disturbance to the mean flow, these incoming wave eigensolutions offer a potentially important mechanism for changing the character of the mean flow profile.

These incoming wave eigensolutions have been found to exist for both types of supersonic disturbances, i. e., for $c_r \leq 1-1/M_2$ and $c_r \geq 1+1/M_2$. For incoming wave eigensolutions with $c_r \leq 1-1/M_2$, an especially interesting phenomena has been found. Two separate families of solutions have been found to exist. One family has its origin at $c_r = 1-1/M_2$ and $\alpha = 0$ while the other family originates from subsonic solutions. Above a certain Reynolds

number labeled "changeover Reynolds number" (R_{ch}), the two families switch their relative positions. This phenomena is shown in Figures 20 and 21 for $M_s = 3.25$. In Figure 22, the variation of R_{ch} is shown as a function of shock Mach number. The physical importance of this changeover Reynolds number appears to be that for Reynolds numbers less than the changeover Reynolds number the forced response analysis shows that a relatively strong reflected wave is present, i. e., significant energy is carried out of the boundary layer. For Reynolds numbers greater than R_{ch} , the strength of the reflected wave is relatively weak. Thus, when the Reynolds number is greater than R_{ch} , the boundary layer is more susceptible to mean flow profile modification than when $R < R_{ch}$.

The variation of R_{ch} versus M_s shown in Figure 22 does follow the general trend of the first transition reversal observed by Boison. Thus, it would appear that this "changeover Reynolds number" might have the same physical significance for incoming waves as the critical Reynolds number has for outgoing waves. That is, the "changeover Reynolds number" seems to represent a Reynolds number which must be reached before significant transition mechanisms can take effect.

The transition measurements shown in Figure 1 suggest that the changeover Reynolds number associated with supersonic and sonic waves having $c_r \leq 1 - 1/M_2$ may be responsible for the transition reversal which occurs in the vicinity of $T_w/T_e \sim .35$. Some other mechanism must be responsible for transition for $T_w/T_e > .35$. One possibility is that there may be a similar changeover Reynolds number phenomena associated with waves having $c_r \geq 1 + 1/M_2$. This possibility was not investigated.

3.5 FORCED RESPONSE ANALYSIS

Neutral incoming wave solutions (noneigen solutions) have been used in conjunction with neutral outgoing wave solutions by Mack⁽¹⁰⁾ to determine

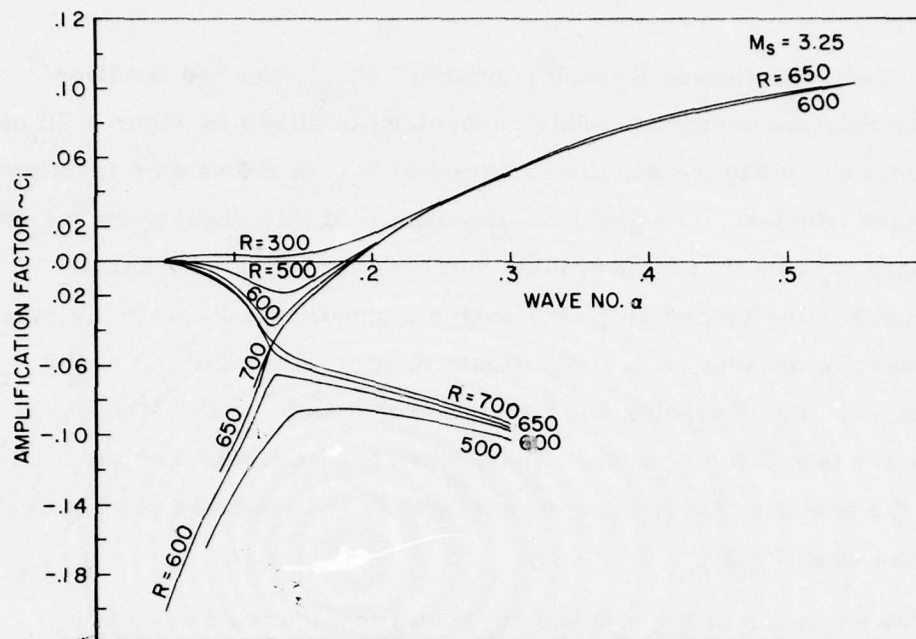


Figure 20. Effect of Wave No. (α) on Amplification Factor (c_i) for $M_s = 3.25$ for Varying Reynolds No.

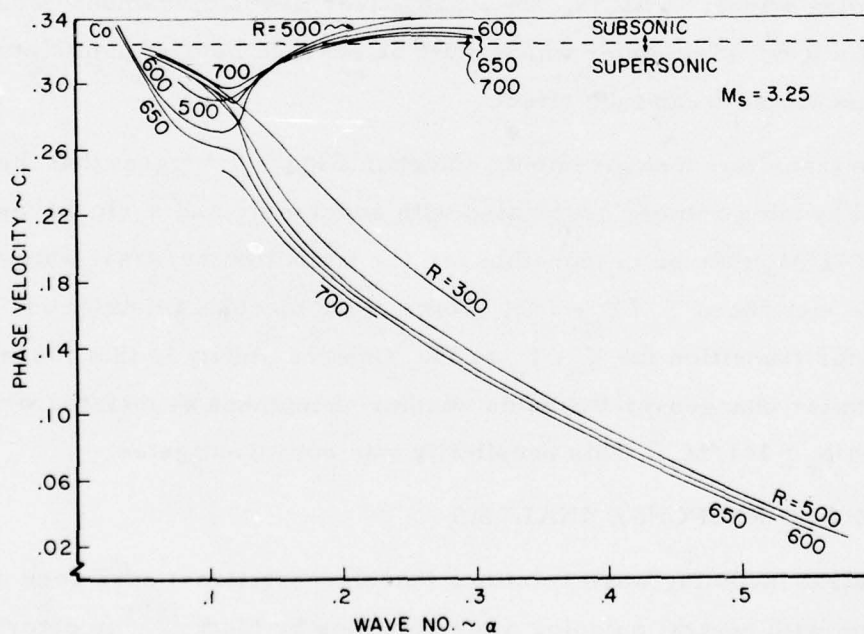


Figure 21. Effect of Wave No. (α) on Phase Velocity (c_p) for $M_s = 3.25$ for Varying Reynolds No.

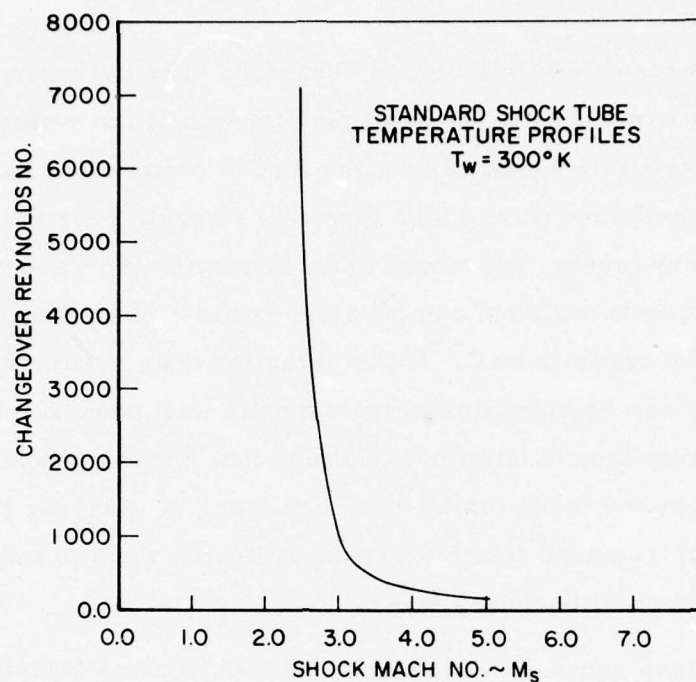


Figure 22. Effect of Shock Mach Number on "Changeover" Reynolds Number.

the forced response of the laminar boundary layer to free stream supersonic waves. A similar approach was applied to shock tube boundary layers in the present work. This effort was very limited in scope and cannot be considered complete at this point. To date no evidence has been found that the forced response analysis by itself can explain transition in shock tube boundary layer flows. Wall cooling has the same effect for shock tube boundary layer flows as it has for supersonic wind tunnel flows; that is, wall cooling tends to weaken the response of the boundary layer to forced oscillations. The forced response analysis however, yields a particularly interesting result which may have an important bearing on transition in shock tube flows.

Mack has shown that the peak response of the boundary layer to supersonic incoming waves of the noneigen solution type occurs very near the leading edge of the boundary layer. The limited results obtained in

the present effort also show this type of behavior. The response of the boundary layer is expressed in terms of the strength of the reflected wave produced by the incoming wave. Thus, the forced response of the boundary layer produces a reflected wave which grows in strength over the initial part of the boundary layer. In a shock tube, this reflected wave will impinge on the opposite wall and can possibly excite an incoming wave eigensolution at the opposite wall. If this situation does occur, then significant energy can be deposited in the opposite wall boundary layer. The intriguing possibility thus exists for explaining how boundary layer transition can be influenced by the diameter of the shock tube. The larger the shock tube, the longer the time required for the growing reflected wave to impinge on the opposite side wall boundary layer.

The preceding comments are purely speculative and obviously further investigation is needed to support this conjecture. A very recent set of experiments conducted by Golobic ⁽¹⁵⁾ definitely shows that the diameter of the shock tube does play an important role on boundary layer transition. Figure 23 shows the boundary layer transition measurements reported in Reference 15. The work reported in Reference 15 was performed in order to obtain transition data for the wall cooling range of $0.255 < T_w/T_e < 0.39$. The purpose of these experiments was to verify the existence of Boison's transition reversal loop. (see Section 1.2). As can be seen in Figure 23, the results of Golobic show a marked deviation from Boison's; that is from the expected results. The primary difference between Golobic's shock tube and Boison's was the diameter of the tube. Golobic's was 17 inches in diameter and Boison's was 4 inches in diameter. In general, Boison's experiments were conducted with a shock tube which should have provided a less hostile environment to the boundary layer than Golobic's since more precautions were taken to minimize wall roughness, alignment of the shock tube sections, etc. But since Golobic's transition measurements were higher than Boison's over the same wall cooling range it must be concluded that the difference in diameter of the shock tubes had an important effect on the differences in transition in these two shock tubes.

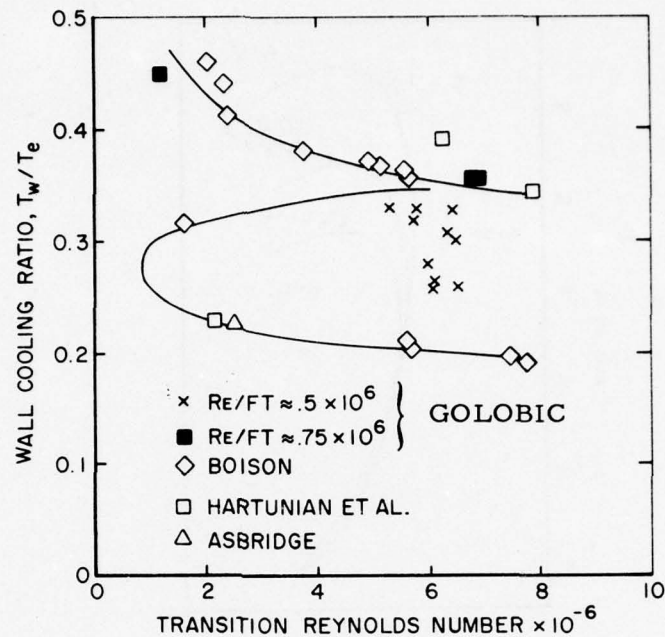
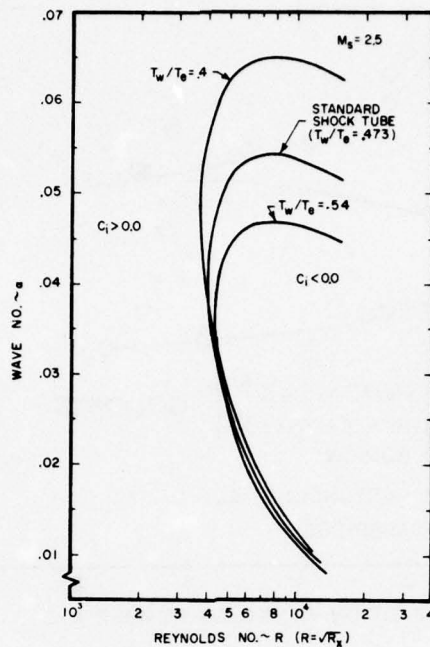


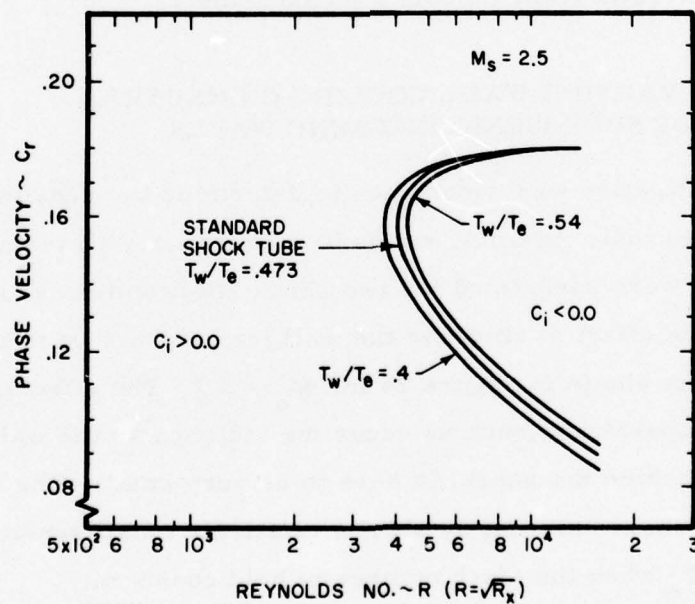
Figure 23. Transition Reynolds Number Correlation Showing Results from Golobic's Measurements (15).

3.6 EFFECT OF VARYING WALL COOLING ON NEUTRAL STABILITY OF SUPERSONIC INCOMING WAVES

A brief investigation was undertaken to determine the sensitivity of the stability of supersonic incoming waves to a change in wall temperature. These calculations were performed for two shock Mach numbers, $M_s = 2.5$ and $M_s = 2.75$. The effect of changing the wall temperature on neutral stability ($c_i = 0.0$) is shown in Figure 24 for $M_s = 2.5$. The effects of small changes in wall temperatures, such as occur for instance as the wall becomes heated by the flow behind the shock, is seen to be very small. The results for $M_s = 2.75$ (not shown) similarly show a relatively small sensitivity to changes in T_w/T_e when the Mach number is held constant.



(a)



(b)

Figure 24. The Effect of Wall Cooling on Neutral Stability Conditions for 2-D Disturbances at $M_s = 2.5$; (a) Wave Number, (b) Phase Velocity.

SECTION IV

APPLICATION OF ANALYSIS TO SUBSONIC WIND TUNNEL BOUNDARY LAYERS

Skin friction drag, caused by turbulence in compressible boundary layers, comprises a significant portion of the total aerodynamic drag experienced by subsonic aircraft. This drag component can be reduced considerably if the boundary layers can be maintained laminar. Hence, phenomena affecting boundary layer transition in subsonic flows are of major importance, especially if they point the way toward developing technology for controlling transition and delaying its onset. The stability analysis for shock-induced boundary layers described in Section III have been extended to treat boundary layers in steady, subsonic flows such as are produced in conventional wind tunnels and in subsonic flight. A description of this analysis and its results follows.

4.1 FORMULATION OF THE PROBLEM

Solution of the linear stability equations for steady flow subsonic wind tunnel boundary layers is similar to that discussed in Section II for shock tube boundary layers. The major difference is in the shape of the mean flow profiles. The shock tube profiles are of the Rayleigh type and the wind tunnel profiles are of the Blasius type (see Figures 4 and 5).

Computer generation of these cooled steady flow mean flow profiles presents no significant difficulties. All that is required is specification of the dimensionless enthalpy at the wall (θ_w) given by;

$$\theta_w = (h_w^* - h_e^*) / (h_{oe}^* - h_e^*) ,$$

where,

$$h_w^* = \text{enthalpy at the wall,}$$

$$h_e^* = \text{enthalpy in the free-stream,}$$

$$h_{o_e}^* = \text{stagnation enthalpy of the free-stream.}$$

Once these mean flow profiles have been determined, they are used as input to the linear stability computer program.

4.2 RESULTS

Neutral stability solutions were obtained for two dimensional and three dimensional disturbances in $M = 0.603$, and $M = 0.80$, and $M = 0.90$ steady flow laminar boundary layers. Calculations were performed for the following thermal conditions:

1. insulated surface,
2. $T_w/T_e = 0.824$,
3. $T_w/T_e = 0.759$,
4. $T_w/T_e = 0.620$.

In the present study, second mode eigensolutions to the viscous linear stability equations were not considered since the dimensional frequencies associated with these solutions are in the megahertz range. Such high frequencies are not physically significant for subsonic flows. Only neutral stability calculations were performed since these provide a good indication of the general stability of the viscous boundary layer. Both 2-D and 3-D disturbances were considered.

4.2.1 Two Dimensional Disturbances

Results indicate that for neutrally stable two-dimensional subsonic disturbances, surface cooling increases the "critical Reynolds number" (R_{crit}). Typical results are shown in Figures 25 and 26. Figures 25 (a) and 26 (a) show the variation of the neutral stability wave number (α) with

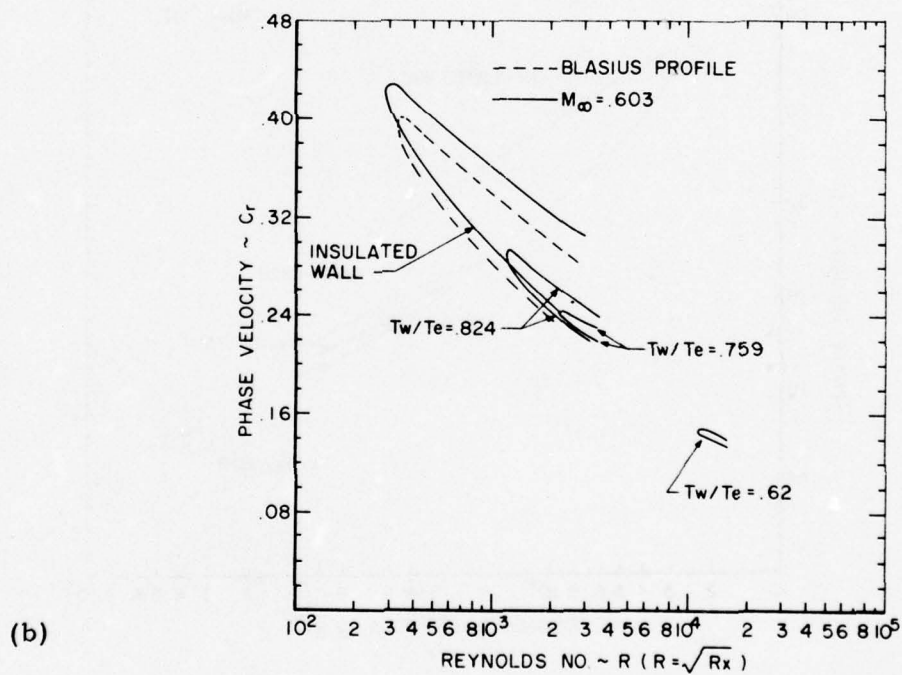
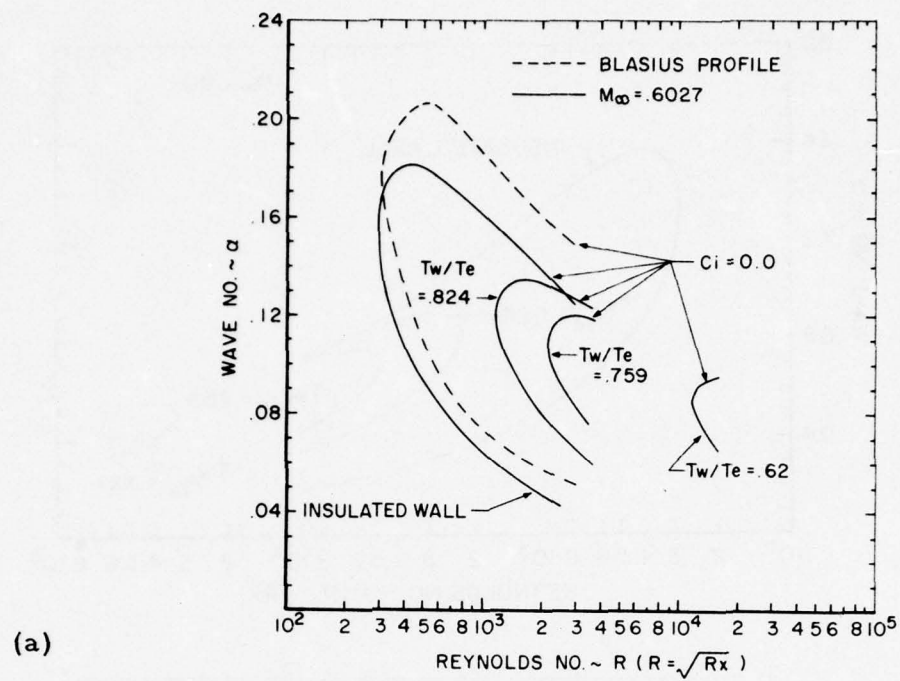


Figure 25. Effect of Wall Cooling on Neutral Stability Conditions for 2-D Disturbances at $M_\infty = 0.603$; a) Wave Number, b) Phase Velocity.

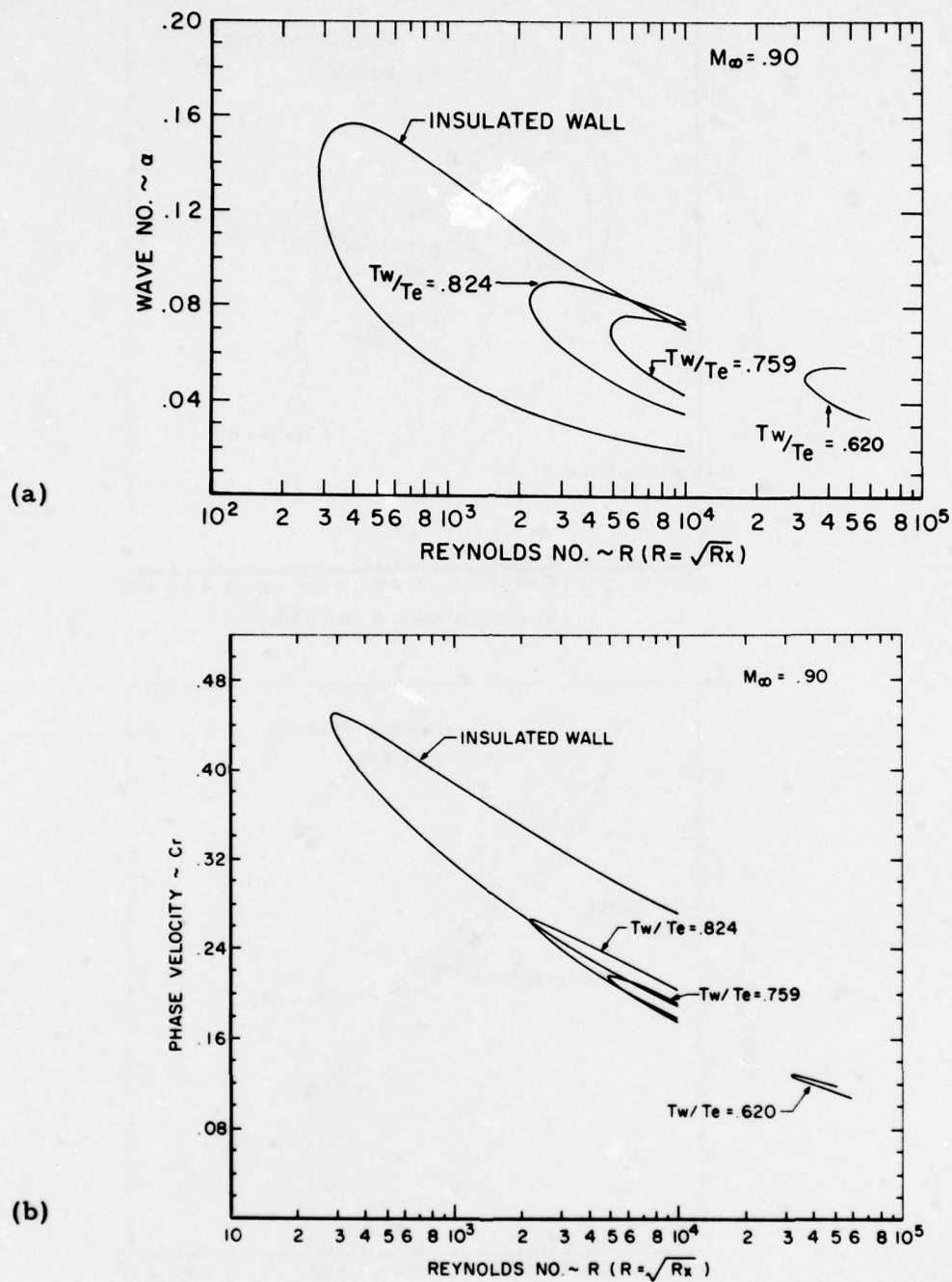


Figure 26. Effect of Wall Cooling on Neutral Stability Conditions for 2-D Disturbances at $M = 0.90$; a) Wave Number; b) Phase Velocity.

Reynolds number for Mach numbers of $M = 0.603$ and 0.90 respectively. Figures 25 (b) and 26 (b) denote the variation of phase velocity, c_r , with Reynolds number at the same Mach numbers. For either case, as the ratio of T_w/T_e is decreased, the critical Reynolds number increases monotonically from approximately $R = 300$ (insulated surface) to approximately $R = 20,000$ ($T_w/T_e = 0.620$). This behavior was found to be characteristic of this Mach number range.

Dimensional frequencies typical of the first mode neutral disturbances found in the Mach number range from 0.6 to 0.9 are presented in Figure 27 for $M = 0.9$. In general, the boundary condition that results in the highest degree of neutral instability, is an insulated surface. This also results in the highest neutral disturbance frequency (on the order of 200 kHz).

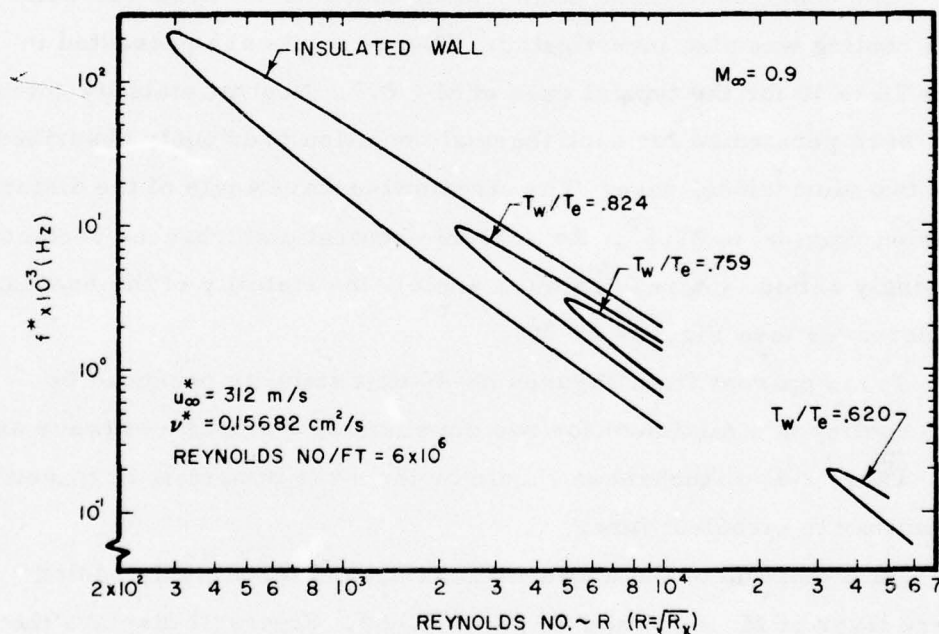


Figure 27. Effect of Wall Cooling on the Neutral Stability Frequency for 2-D Disturbances at $M_\infty = 0.9$

An increase in surface cooling (or a decrease in the temperature ratio (T_w/T_e)) decreases the maximum neutral disturbance frequency. Physically, this suggests that it is possible to limit the frequency spectrum of potentially unstable disturbances by increasing surface cooling. Insulated surface boundary layers are relatively unstable, since the spectrum of disturbance frequencies that are potentially unstable is large. Highly cooled boundary layers are more stable, since the spectrum of potentially unstable disturbances is reduced. Therefore, if the frequency spectrum of disturbances is large and random ("white noise"), a cooled boundary layer will be more stable since only a small frequency band is potentially unstable.

4.2.2 Three Dimensional Disturbances

The behavior of three dimensional subsonic disturbances with surface cooling was also investigated. These results are presented in Figures 28 to 30 for the typical case of $M = 0.9$. Neutral stability calculations were performed for each thermal condition previously described for the two dimensional case. The streamwise wave angle of the disturbance was varied from 0° to 87.5° . As subsonic neutral disturbances become increasingly oblique (increasing wave angle), the stability of the boundary layer increases (see Figures 28-30).

It is apparent from Figures 28-30 that stability produced by surface cooling is a minimum for two dimensional disturbances (wave angle of 0°). Thus, 2-D disturbances should be the most important in transition from laminar to turbulent flow.

An exception to the above findings occurs for a highly cooled boundary layer at $M_\infty = 0.9$ and $T_w/T_e = 0.620$. Figure 31 displays the results for this case. The most unstable disturbance is no longer two dimensional, but three dimensional, and occurs at a streamwise wave angle in the vicinity of 30° to 45° . This result is significant in that it differs from Mack's findings⁽⁶⁾. Mack proposed that three dimensional disturbances

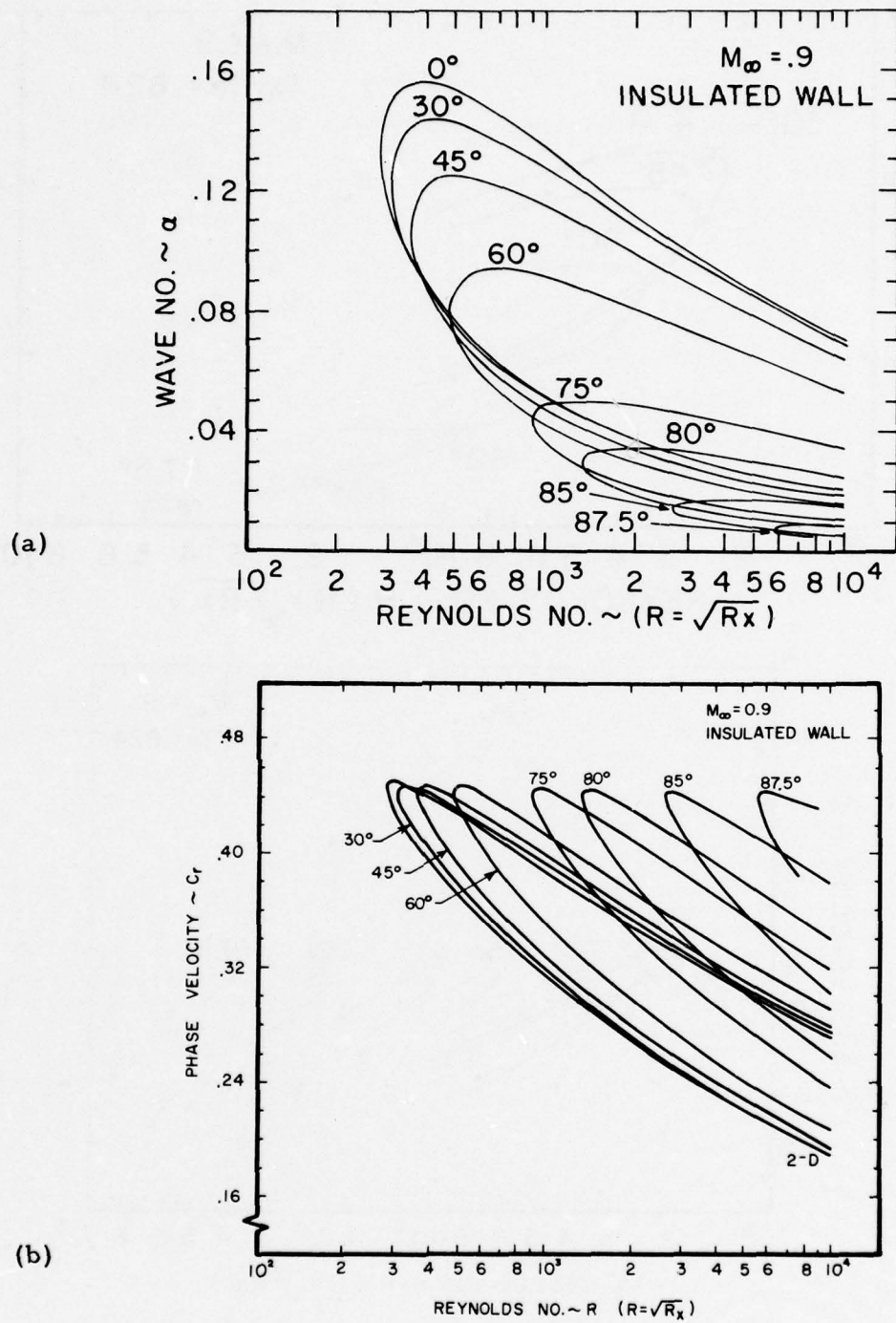


Figure 28. Effect of Streamwise Wave Angle on Neutral Stability Conditions for 3-D Disturbances for Insulated Wall at $M_\infty = 0.90$; a) Wave Number, b) Phase Velocity.

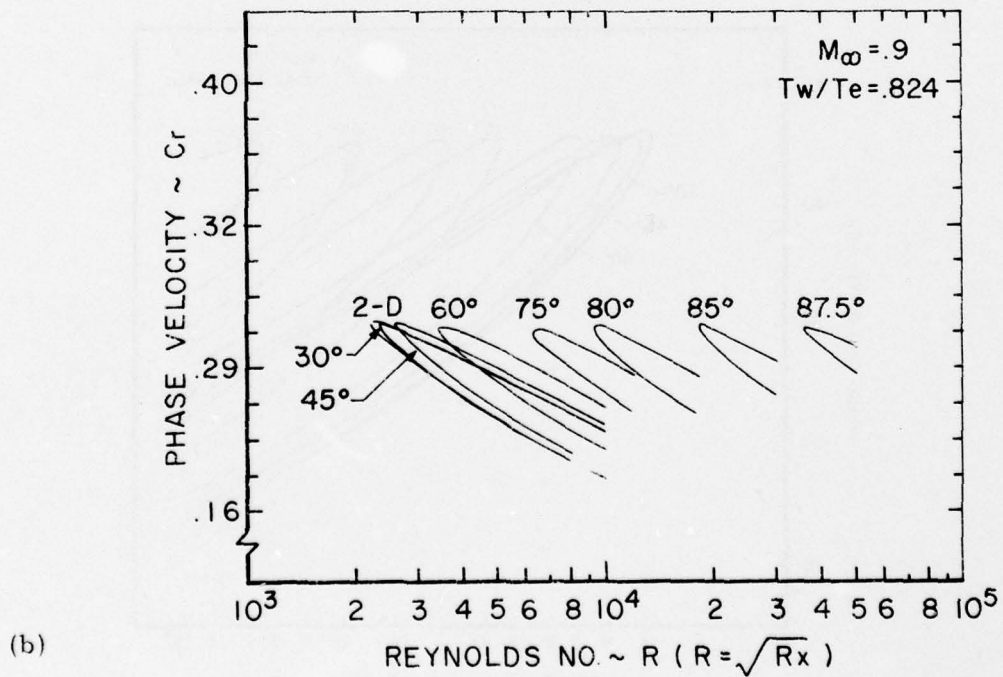
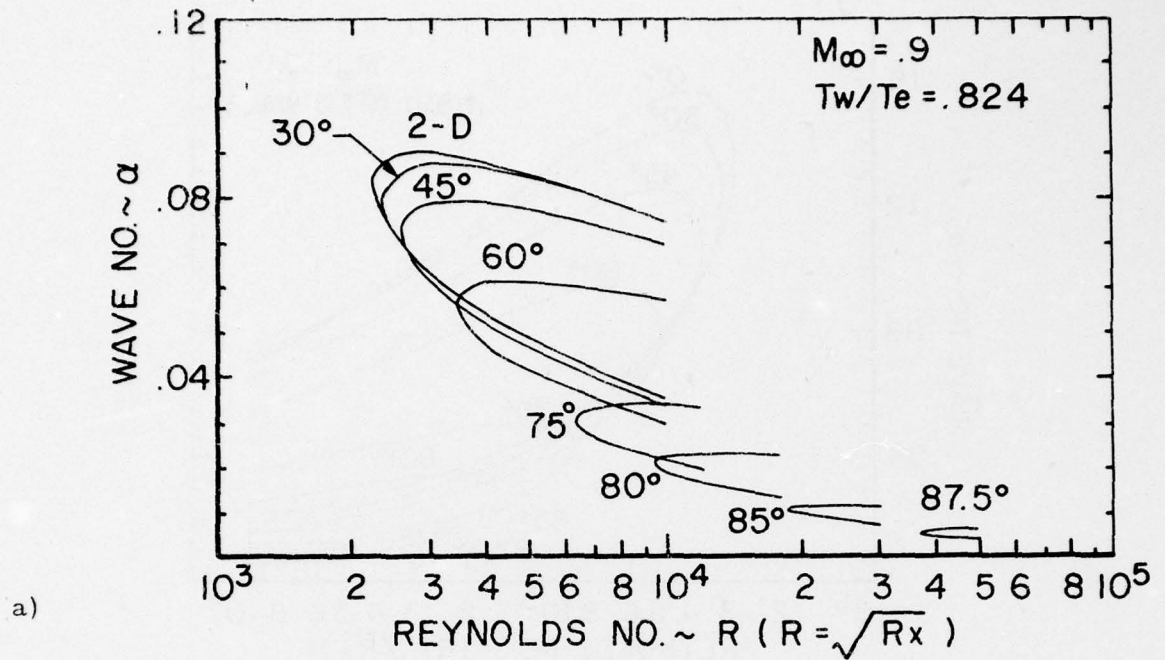


Figure 29. Effect of Streamwise Wave Angle on Neutral Stability Conditions for 3-D Disturbances at $M_\infty = 0.90$ and $T_w/T_e = 0.824$; a) Wave Number, b) Phase Velocity.

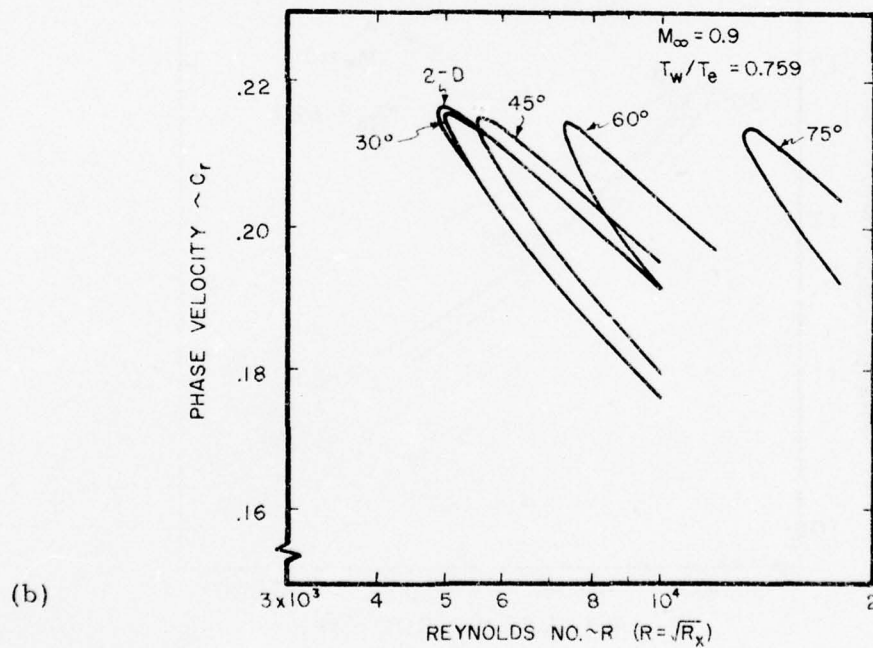
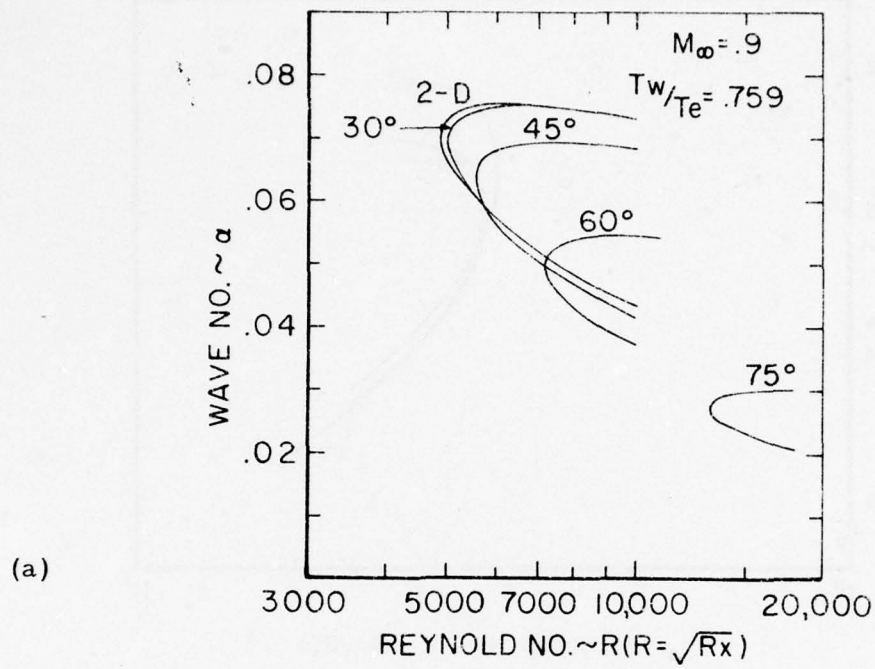


Figure 30. Effect of Streamwise Wave Angle on Neutral Stability Conditions for 3-D Disturbances at $M_\infty = 0.90$ and $T_w/T_e = 0.759$;
a) Wave Number, b) Phase Velocity.

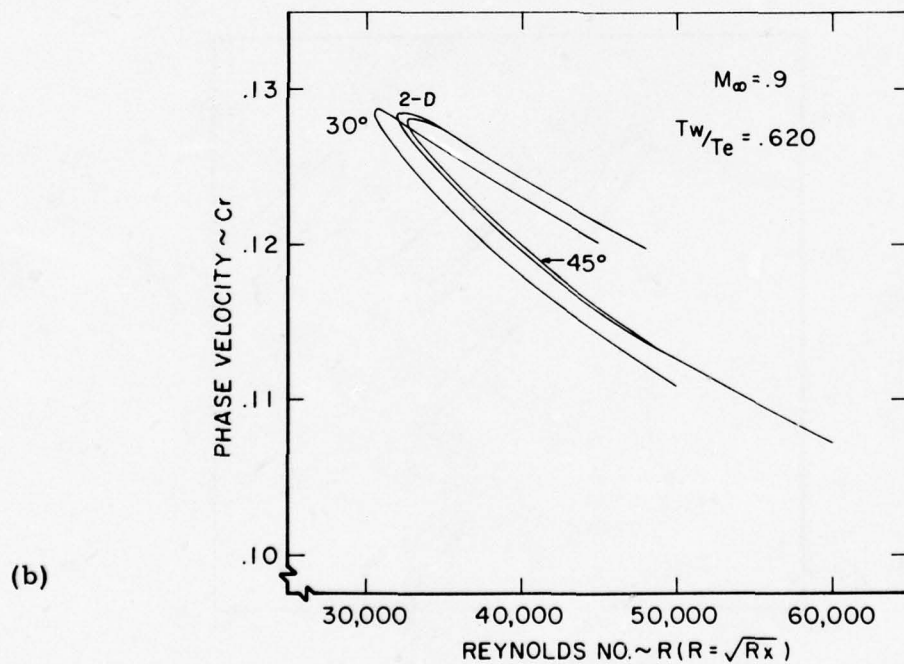
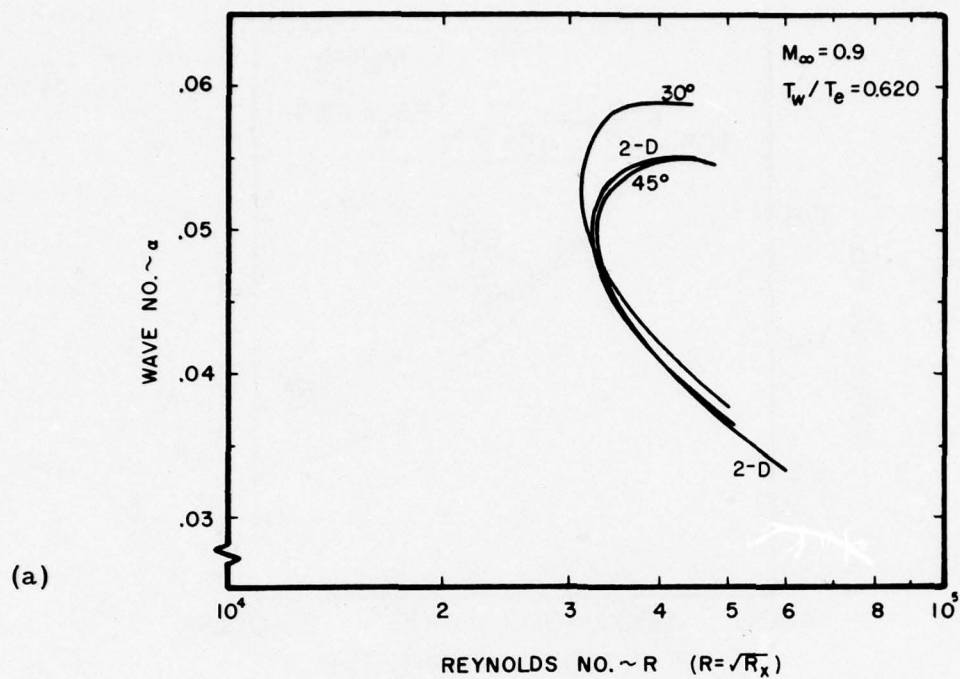


Figure 31. Effect of Streamwise Angle on Neutral Stability Conditions for 3-D Disturbances at $M_\infty = 0.90$ and $T_w/T_e = 0.620$; a) Wave Number, b) Phase Velocity.

become the predominantly unstable disturbances for cooled boundary layers for Mach numbers of about 0.7 or 0.8. This appears, however, not to be the case. At $M = 0.80$ (not shown) two dimensional disturbances were found to be the most unstable for all values of T_w/T_e analyzed. At $M = 0.9$, three dimensional disturbances, which were only slightly oblique (i.e. wave angle of about 30°), were found to be the most unstable (and only at $T_w/T_e = 0.620$).

Figure 32 is a typical neutral stability frequency versus Reynolds number distribution for oblique disturbances at $M_\infty = .90$ and for an insulated surface. Here the limiting condition on the maximum neutral stability frequency is the two dimensional disturbance. For disturbances which are increasingly oblique, the frequency spectrum available to a potentially unstable disturbance becomes narrower. This behavior is

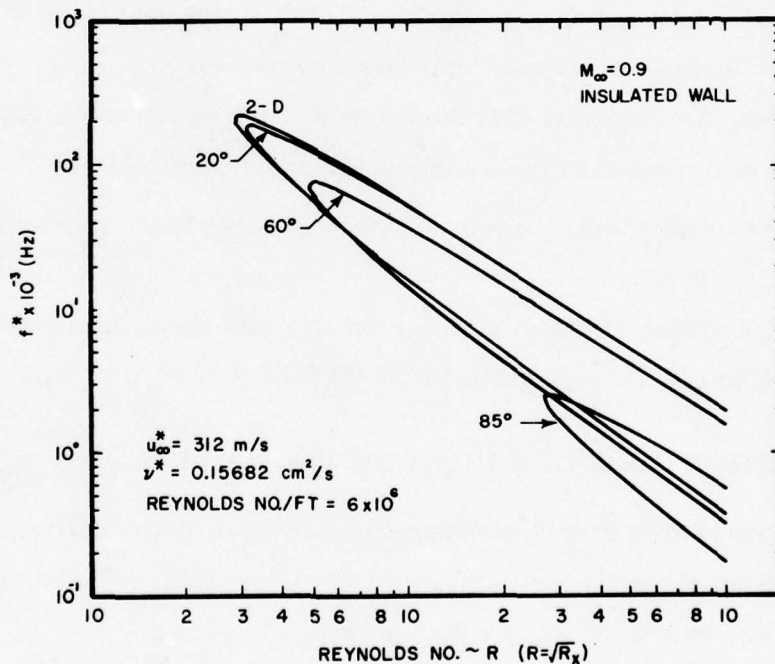


Figure 32. Effect of Wave Angle on the Neutral Stability Frequency for Three Dimensional Neutral Disturbances.

similar to the effect of wall cooling on two dimensional disturbances. Three dimensional disturbances of constant frequency react to changes in wave angle in a manner analogous to the reaction of two dimensional disturbances to changes in surface cooling. The results tend to confirm the hypotheses of other investigators such as Dunn and Lin⁽⁸⁾ and Mack⁽⁶⁾. Most of the work reported by Mack concerning the effects of surface cooling on stability was conducted with an inviscid linear stability theory and supersonic flow. He concluded that increasing the surface cooling in the boundary layer serves to stabilize 2-D and 3-D first mode disturbances. Higher mode disturbances are increasingly unstable with increasing surface cooling.

In summary, the linear stability analysis of cooled subsonic wind tunnel boundary layers indicates that:

1. Wall cooling has a pronounced stabilizing effect on two and three dimensional first mode disturbances.
2. Two dimensional disturbances are more unstable than three dimensional disturbances for Mach numbers of $M = 0.90$ or less, and surface cooling ratios greater than approximately $T_w/T_e = 0.62$.
3. The effect of Mach number on two and three dimensional disturbances is negligible for $0.60 < M < 0.90$.

4.3 COMPARISON TO SHOCK INDUCED FLOW RESULTS

For purposes of general comparison between the stability of cooled subsonic wind tunnel boundary layers, and shock induced subsonic boundary layers, two particular cases were considered:

1) $M_\infty = 0.603$, wind tunnel flow and, 2) $M_s = 1.5$, $M_2 = 0.603$, shock tube flow. The behavior of both cases was investigated over a range of wall cooling conditions. Results of these calculations for points of neutral

stability are presented in Figure 33. The subsonic shock induced boundary layer is more stable, possessing a higher critical Reynolds number for a given wall cooling ratio than its wind tunnel counterpart. This difference is attributable to the differences in mean flow profiles. The shock tube profile has higher gradients, and hence transfers more energy out of the boundary layer than the steady-flow Blasius type profile. (This phenomena was also observed by Ostrach and Thornton⁽⁷⁾.) Stability is influenced not only by boundary layer cooling, but to an even greater extent, by the gradients of the mean flow profile. Thus, direct correlation between experimental transition data obtained in wind tunnels and that obtained in shock tubes is not expected.

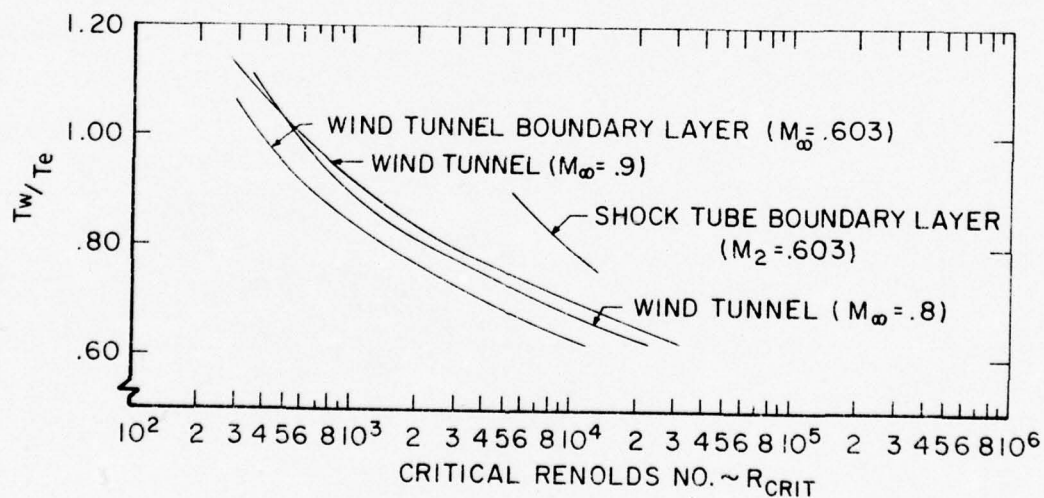


Figure 33. Comparison of the Relative Stability of Shock Tube and Wind Tunnel Boundary Layers, as a Function of Critical Reynolds Number and Wall Cooling Ratio.

4.4 EFFECT OF WALL COOLING ON LOCAL SKIN FRICTION COEFFICIENT

A comparison between laminar and turbulent skin friction values for the specific flow parameters under consideration, is presented in Table I. The following definitions apply:

- μ_w - Dimensionless viscosity at the surface
- $\left. \frac{dU}{d\eta} \right|_{\eta=0}$ - Dimensionless velocity gradient at the surface
- $C_{f_L} \sqrt{R_x}$ - Laminar skin friction parameter
- $C_{f_T} \sqrt{R_x}$ - Approximate turbulent skin friction parameter

It is apparent that, although laminar skin friction increases with wall cooling, it is still an order of magnitude less than the turbulent skin friction at the same Reynolds number. A potential thus exists to significantly reduce aerodynamic drag on aircraft surfaces by providing sufficient cooling to delay the onset of transition.

TABLE 2

LOCAL SKIN FRICTION COEFFICIENT COMPARISON FOR LAMINAR AND TURBULENT FLOW

| M_∞ | T_w ($^{\circ}\text{K}$) | T_e ($^{\circ}\text{K}$) | T_w/T_e | μ_w | $\frac{dU}{d\eta} \Big _{\eta=0}$ | $C_{f_L} \sqrt{R_x}$ | $C_{r_T} \sqrt{R_x}$ |
|------------|------------------------------|------------------------------|-----------|---------|-----------------------------------|----------------------|----------------------|
| .603 | 418.72 | 395.3 | 1.059 | 1.042 | .3168 | .6602 | \uparrow |
| .603 | 325.8 | 395.3 | 0.824 | 0.867 | .3873 | 0.6715 | 7.3 |
| .603 | 300.4 | 395.3 | 0.759 | 0.815 | .4141 | 0.6749 | \downarrow |
| .603 | 245.0 | 395.3 | .620 | 0.694 | .4918 | 0.6826 | |
| .800 | 332.0 | 300.0 | 1.107 | 1.079 | .3047 | .6575 | \uparrow |
| .800 | 247.2 | 300.0 | 0.824 | 0.858 | .3900 | .6692 | 7.3 |
| .800 | 227.7 | 300.0 | 0.759 | 0.803 | .4189 | .6727 | \downarrow |
| .800 | 186. | 300.0 | 0.620 | 0.675 | .5106 | .6893 | |
| .90 | 340.5 | 300.0 | 1.135 | 1.101 | .2984 | .6570 | \uparrow |
| .90 | 247.2 | 300.0 | .824 | 0.858 | .3898 | .6688 | 7.3 |
| .90 | 227.7 | 300.0 | .759 | 0.803 | .4186 | .6722 | \downarrow |
| .90 | 186. | 300.0 | .620 | 0.675 | .5012 | .6766 | |

SECTION V

SUMMARY, CONCLUSIONS, AND RECOMMENDATIONS

5.1 SUMMARY

The work described in this report ^{shows} ~~has shown~~ that wall cooling can be an effective means of increasing the stability of laminar boundary layer flows. The stability of two general classes of cooled boundary layer flows was investigated; shock tube induced boundary layers, and cooled subsonic steady flow boundary layers (such as that on a cooled aerodynamic surface in free flight or in a wind tunnel).

A distinguishing feature of wall boundary layers in shock tubes is that the wall temperature is less than the temperature at the edge of the boundary layer for all shock Mach numbers. In this report, shock Mach numbers ranging from 1.5 to 5.0 were investigated. The results showed that the cooling of the boundary layer in this type of flow is sufficient to suppress the ordinary types of disturbances (2-D and 3-D subsonic disturbances) considered in boundary layer stability theory. Higher mode solutions to the stability equations of the type first discovered by Mack were found to exist in shock tube boundary layer flows. The frequencies associated with these higher mode solutions were found to be so high (in the megahertz range) that they were considered to be unimportant in establishing the stability of shock tube boundary layers.

The primary objective of the reported effort was to determine whether or not three-dimensional and/or higher mode solutions correlate with transition measurements in shock tubes, particularly those of Boison⁽⁴⁾. When it was determined that these types of solutions would not correlate with transition measurements, a search for other types of solutions which might show correlation was undertaken. Two new classes of disturbance solutions were discovered which are unstable in highly cooled boundary layers. Both classes

originate in the free stream in the form of supersonic disturbances. One class corresponds to supersonic disturbances which travel slower than the free stream ($c_r \leq 1 - 1/M_\infty$) and the other class corresponds to disturbances which travel faster than the free stream ($c_r \geq 1 + 1/M_\infty$). Since both classes of disturbances originate in the free stream, these unstable disturbances are not important for determining the stability of cooled boundary layers in a disturbance-free environment such as free flight. Conversely, these types of disturbances are of fundamental importance to the stability of shock tube boundary layers, since free stream disturbances always exist in shock tube flows. Free stream disturbances also exist in all wind tunnel flows so that supersonic incoming disturbances are also of importance in determining the stability of boundary layers on models in wind tunnels. This factor is especially important for cooled models when the cooling is sufficient to suppress the subsonic disturbances which would otherwise control boundary layer stability.

The wall cooling required to suppress subsonic disturbances was determined for steady subsonic flow over flat plates with no pressure gradient. The Mach number range investigated was $0.603 \leq M_\infty \leq 0.9$ and the wall temperatures range extended from insulated wall conditions to $T_w = 0.62 T_e$. The increase in critical Reynolds number with decreasing T_w/T_e is dramatic, as is shown in Figure 33. Thus, even a moderate amount of wall cooling should lead to a significant increase in transition Reynolds number. It was also found that two-dimensional disturbances are more unstable (have a lower critical Reynolds number) than three-dimensional disturbances over this range of M_∞ and T_w/T_e , except at $M_\infty = 0.9$ and $T_w/T_e = 0.62$ where an oblique wave having a wave angle of about 30° was found to have the lowest critical Reynolds number. In addition, it was shown in Section 4.4, that wall cooling does not significantly increase the local skin friction coefficient for laminar flow.

5.2 CONCLUSIONS

The conclusions cover a wider range of information than that contained in this report in order to obtain the widest possible perspective on the effect of wall cooling on boundary layer stability. The conclusions do not; however, extend beyond the range of flow parameters considered in this report.

The first five conclusions are concerned with the effect of wall cooling on subsonic disturbances:

1. With little or no wall cooling, subsonic disturbances are the principal cause of transition.
2. Surface cooling stabilizes subsonic disturbances and delays transition over all Mach numbers investigated ($M_\infty < 2$).
3. Subsonic disturbances cause transition on aerodynamic surfaces in wind tunnel flows and free flight unless sufficient surface cooling is imposed.
4. Shock tube flows always have significant wall cooling.
5. Amplification of subsonic disturbances in shock tube wall boundary layer flows is delayed well beyond the location of measured transition.

The wall cooling associated with shock tube flows was found to be so effective in suppressing both two-dimensional and three-dimensional disturbances that these types of disturbances did not provide any correlation between boundary layer instability and measured transition Reynolds numbers. Therefore, a search for other types of unstable waves, which could account for earlier transition, was undertaken. The investigation identified a class of supersonic disturbances.

From a study of the behavior of these disturbances it was concluded that;

6. Unstable outgoing supersonic disturbances exist, but their characteristic frequencies are too high to affect boundary layer stability.

7. Incoming supersonic disturbances always exist and have unstable regions over all flow conditions investigated.
8. Unstable incoming supersonic disturbances control transition in shock tube flows.

5.3 RECOMMENDATIONS

The results in this report show that wall cooling in subsonic and low supersonic Mach number ($M < 2$) has a significant potential for reducing skin friction drag on flight vehicles by delaying transition from laminar to turbulent flow. The results of this investigation were obtained for flows with no pressure gradient. Obviously, it will be necessary to determine if wall cooling can prevent laminar flow separation and transition in regions of adverse pressure gradient before an estimate can be made of the total aerodynamic drag reduction which can be achieved through wall cooling on flight vehicles (skin friction drag + pressure drag).

The following program for further research will be necessary to determine the overall feasibility of boundary layer control through wall cooling.

1. A Wind Tunnel Investigation of Boundary Layer Transition on Cooled Flat Plates with no pressure Gradient for subsonic Mach numbers.
2. A Linear Stability Theory Investigation of Subsonic Laminar Boundary Layers on Cooled Surfaces with Adverse Pressure Gradient.
3. An Experimental Investigation of The Effect of Wall Cooling on Lift and Drag on Airfoils at Subsonic Conditions. This program should include both wind tunnel and flight testing.
4. A Systems Analysis to Determine the Overall Payoff Which Can be Achieved by Integrating Cooled Aerodynamic Surfaces, Supporting Hardware, and the Use of Cryogenic Fuels Such as Hydrogen into a Flight Vehicle.

APPENDIX A

A CRITIQUE OF OSTRACH-THORNTON ANALYSIS

APPENDIX A

CRITIQUE OF OSTRACH-THORNTON ANALYSIS

The mean flow field in a shock tube is basically an unsteady flow. In an experiment, the instrumentation is fixed in the laboratory coordinate system and so one wants to understand the flow from the point of view of an observer fixed in space. However, from the point of view of an observer riding on the shock wave, the flow is steady (neglecting small changes in the free stream conditions of the shocked gas due to the presence of a growing boundary layer and attenuation of the shock speed itself). Thus, the analytical formulation of both the boundary layer equations for the mean flow and the small disturbance equations is simpler when done in the moving coordinate system where the mean flow is constant in time and all of the unsteadiness of the flow is due to disturbances. The correlation of boundary layer stability and transition data with analytical predictions however is easier done in the fixed coordinate system since all available data are obtained with sensors fixed in the laboratory coordinate system. In the present analysis the mean flow is solved in the shock-fixed coordinate system and then transformed back into the laboratory-fixed coordinate system. The entire stability analysis is formulated in the laboratory-fixed coordinate system.

In the Ostrach-Thornton investigation ⁽⁷⁾ the entire analysis was carried out in the shocked-fixed coordinate system. The small disturbance equations were first nondimensionalized with free stream quantities of the shocked gas (U_e^* , T_e^* , etc.). Then, basically in the interests of expediency, they normalized the mean flow velocity profile and phase velocity in a manner so as to reduce the problem to one in which the normalized velocity profile had a value of zero at the wall and 1 in the free stream corresponding to the classical stability analyses. They defined new quantities, Ω , Ω' , and \bar{c} as follows

$$\Omega = \frac{u - u_w}{1 - u_w} = \frac{U_e^* - U_w^*}{U_e^* - U_w^*}$$

$$\Omega' = \frac{u'}{1 - u_w} = \frac{U_e^{*'}}{U_e^* - U_w^*} \quad (A-1)$$

$$\bar{c} = \frac{c - u_w}{1 - u_w} = \frac{C^* - U_w^*}{U_e^* - U_w^*}$$

where capital letters refer to dimensional quantities and lower case letters refer to quantities nondimensionalized by U_e^* and ()' signifies differentiation with respect to η , the Blasius similarity variable. Note that the operation of dividing velocities by $(1 - u_w)$ when these velocities were originally nondimensionalized by U_e^* is equivalent to nondimensionalizing the velocities by $U_e^* - U_w^*$ in the first place.

The disturbance velocities in the Ostrach-Thornton analysis were originally nondimensionalized by U_e^* and then subsequently divided by $1 - u_w$. As an example, the normalized value of the amplitude of the velocity fluctuation in the streamwise direction f^* (their notation) became

$$f^* = \frac{f/U_e^*}{(1 - u_w)} = \frac{f}{(U_e^* - U_w^*)} \quad (A-2)$$

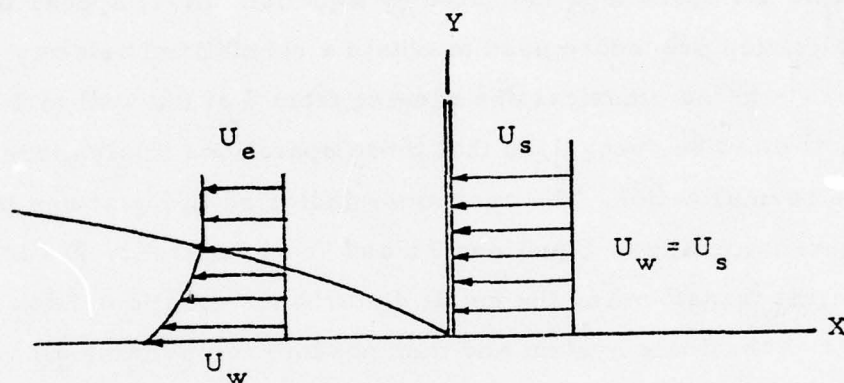
where here f represents a dimensional quantity.

Referring to Equation (A-1) above, it should be noted that the operations performed by Ostrach and Thornton as indicated in Equation (A-1) are really equivalent to transforming the mean flow velocity and phase velocity back into a lab-fixed coordinate system. This transformation is performed when U_w^* is subtracted from the mean flow velocity. Then they simply nondimensionalized all velocities by the velocity of the fluid

relative to the wall ($U_e^* - U_w^*$). These operations clearly lead to changes in the sign of the quantities $\Omega - \bar{c}$ and Ω' compared to $u - c$ and u' respectively. If originally $u - c$ was positive, then, after the operations of subtracting u_w individually from u and c and dividing by $1 - u_w$, $\Omega - \bar{c}$ becomes negative and vice versa if $u - c$ was originally negative. The sign of Ω' is also changed from that of u' when u' is divided by $1 - u_w$. Therefore, while the operations indicated by Equation (A-1) appear to be simply a normalization procedure used to obtain a normalized velocity profile that corresponds to the classical one ranging from 0 at the wall to 1 in the free-stream, it must be recognized that these operations imply more than just a simple normalization. The operations indicated in Equations (A-1) and (A-2) (corresponding to Equations 7a and 7b in Reference 7) really correspond to first transforming the small disturbance equations back into the laboratory coordinate system and then nondimensionalizing all velocities by the velocity of the fluid relative to the wall. Therefore, in evaluating the Ostrach and Thornton analysis, it must be kept clearly in mind which coordinate system each of the quantities related to velocities is defined in. Ω and \bar{c} are properly defined in a laboratory fixed coordinate system and thus \bar{c} is the nondimensional phase velocity relative to a stationary observer. That \bar{c} is thus defined is not stated or immediately evident in Reference 7.

It is very easy to become thoroughly confused when reading Reference 7 since all quantities related to velocities seem to have the wrong sign. Ostrach and Thornton apparently recognized that these quantities did not have the correct sign for they invented new sign conventions in order to "make things come out right". They defined a new wave number $\alpha = -\bar{\alpha}$ and the Reynolds number Re_1 , was defined as $|1 - u_w| Re$ instead of $(1 - u_w) Re$. They do not state it but in their analysis the wave number in the transverse direction β would also have to be defined with a negative sign. Had they considered 3-D waves instead of only 2-D waves, it is quite probable that noticeably incorrect results would have resulted and steps taken to correct the analysis.

It is now clear to us that the Ostrach-Thornton analysis is basically properly posed (within the accuracy of the Dunn-Lin approach) if one untangles all of the sign inconsistencies. One then finds that they have really stated the problem (equations 1a through 5a in Reference 7) for the situation pictured in the following sketch



and that all disturbances are left running waves. In the above sketch then, α , β , c , U_e^* , U_w^* , and U_w^* would all be negative quantities as they, of course, should be for this physical situation. The input mean flow profile would then be input as negative numbers for u and positive numbers for u' . Then upon nondimensionalizing with respect to $U_e^* - U_w^*$ (a positive number) Ω and \bar{c} would be positive and $\Omega - \bar{c}$ would have the correct sign. ^{**} \bar{c} would indeed

^{**} It appears that O-S used a positive velocity profile for U^* with U^* negative (corresponding to their Figure 7 for steady flow system) but considered U_w^* and U_e^* also to be positive quantities. They considered \bar{c} to be positive, but again U_w^* and U_e^* were considered to be positive. Thus, their $\Omega - \bar{c}$ and Ω' had the incorrect sign for our sketch. But then they redefine their disturbance velocity amplitudes to have negative values which tended to undo the incorrect signs on $\Omega - \bar{c}$ and Ω' . Finally, after they invented a negative sign for α (and by implication negative signs for β and c), their equations 1a through 5a became applicable to the physical situation shown above. When they wrote their final equations (Eqns. 9a through 14 in Reference 7), they had in essence retransformed their disturbance velocities and redefined α and R_{e1} to correspond to the flow situation which is just the opposite of our sketch, but corresponds to their Figure 7.

be the phase velocity relative to an observer in the laboratory-fixed coordinate system corresponding to the sketch which is really what the Ostrach-Thornton phase velocities \bar{c} are.

In Figure 34, the movement of a given particle is tracked in the two different coordinate systems corresponding to the shock-fixed coordinate system for which the Ostrach-Thornton analysis is really applicable. This figure is particularly useful for visualizing the basis for the development of the Reynolds number based on velocity of a particle relative to the wall and length equal to the total distance that a particle is in motion relative to the wall at a given time t . Note that for a time interval $\Delta t = t_2 - t_1$ after the shock has passed a given position (x_g) the particle that is at the position x_g has been in motion for the time t_2 and has covered the distance equal to $U_2 t_2$. Also, note that (all quantities are considered to be dimensional in what follows)

$$\Delta t = \frac{x_{s2} - x_{s1}}{U_s} = \frac{x_{s2} - x_g}{U_s} = \tau^*$$

$$\text{and that } \Delta t = \frac{x_{p2} - x_{p1}}{U_2} = \frac{x_g - x_{p1}}{U_2} = \tau^*$$

where τ^* is the time after the shock moves past a given point on the shock tube wall. Equating these two expressions for Δt yields

$$\frac{U_s}{U_2} = \frac{x_{s2} - x_g}{x_g - x_{p1}} = \frac{t_2(U_s - U_2)}{U_2 \Delta t}$$

$$\text{or } t_2 = \frac{U_s}{(U_s - U_2)} \Delta t = \frac{U_s}{U_e} \Delta t$$

which states that in the time Δt after the shock passes a given point on the shock tube wall, the particle at position x_g at time t_2 has been in motion for the time given by

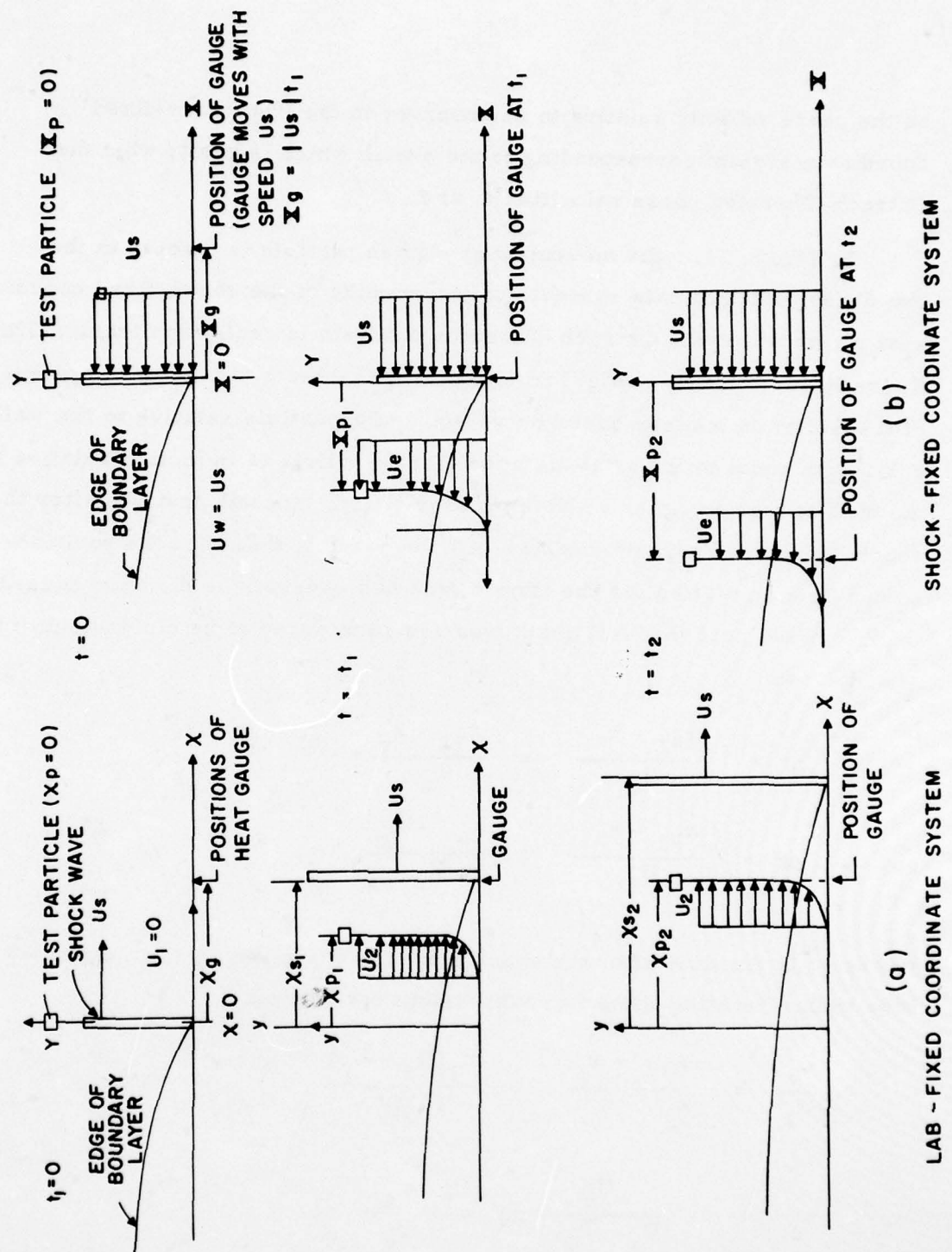


Figure 34. Motion of a Test Particle in Stationary and Moving Coordinate System.

$$t_2 = \frac{U_s}{U_e} \Delta t$$

and the distance covered by the particle is

$$x_{p2} = U_2 \cdot \frac{U_s}{U_e} \Delta t = (U_s - U_e) \frac{U_s}{U_e} \Delta t .$$

If Δt is the time to transition after the shock passes a given point, then x_{p2} represents the total distance that a particle travels relative to the wall to reach transition.

In the shock-fixed coordinate system $X_{p2} = U_e t_2$ which represents the total distance covered by a particle in time t_2 . But in this same time, the wall has traveled a distance $U_w t_2 = U_s t_2$. The distance that the particle has traveled relative to the wall is then $(U_s - U_e)t_2 = U_2 t_2$. But again

$$\frac{t_2}{\Delta t} = \frac{x_g / U_e}{x_g / U_s}$$

or

$$t_2 = \frac{U_s}{U_e} \Delta t$$

Note that in the Ostrach-Thornton analysis the Reynolds number Re_X was based on

$$Re_X = \frac{(U_s - U_e)^2 X_{p2}}{U_e \nu_e}$$

but $X_{p2} = U_e t_2 = U_e \cdot \frac{U_s}{U_e} \Delta t = U_s \Delta t$

$$\text{or } Re_X = (U_s - U_e)^2 U_s \Delta t / U_e$$

which is the same as the Reynolds number based on the total distance that a particle travels and its velocity in the laboratory-fixed coordinate system.

Therefore, it appears that the end result of the Ostrach-Thornton formulation of the stability equations is correct within the accuracy of the Dunn-Lin approach if one interprets their phase velocity \bar{c} as the phase velocity in a shock-fixed coordinate system. It is very clear that their formulation of the stability equation does lead to the correct form of the parameters, Mach number and Reynolds number, for a stability analysis of the boundary layer formed behind a moving shock wave.

APPENDIX B

DESCRIPTION OF THE BOUNDARY LAYER STABILITY COMPUTER PROGRAM

B.1 STABILITY EQUATIONS FOR THE VISCOUS STABILITY COMPUTER PROGRAM

The complete parallel flow linear stability equations used to generate the results presented in this report can be found in Reference 16. The stability equations presented in Reference 16 contain terms which arise because of non-parallelism of a boundary layer. These terms were not included in the version of the stability computer program used to generate the results presented in this report. The terms included in Reference 16 which are not included for parallel flow investigation are as follows:

- (a) All terms involving V (mean flow component of velocity in the y -direction) and all derivatives of V .
- (b) All streamwise derivatives of mean flow quantities.

The stability equations in Reference 16 also include the effect of the bulk coefficient of viscosity, denoted by ξ . In the present investigation ξ was taken to be zero.

The complex amplitude functions of the flow variables are defined by

$$(u', v', w', p') = (f, \alpha \phi, h, \pi) \exp [i(\alpha_1 x + \alpha_3 z - \omega t)] \quad (\text{B. 1})$$

When equations of the type expressed by Equation B. 1 are substituted into the linearized small disturbance equations for parallel flow, an eighth order system of linear differential equations is obtained. The eighth order system is setup as follows:

$$\sum_{j=1}^8 a_{ij} Z_j' = \sum_{j=1}^8 b_{ij} Z_j \quad (i=1, 2, \dots, 8) \quad (\text{B. 2})$$

where

$$Z_1 = f, \quad Z_2 = f' = Z_1', \quad Z_3 = \emptyset, \quad Z_4 = \pi / M_\infty^2, \quad Z_5 = \theta$$

$$Z_6 = \theta' = Z_5', \quad Z_7 = h, \quad Z_8 = h' = Z_7'$$

and where the row index, i , in Equation (B. 2) is set up in the following order

| <u>Row Index</u> | <u>Equation</u> |
|------------------|-------------------------------|
| 1 | $Z_1' = Z_2$ |
| 2 | First momentum (x-direction) |
| 3 | Continuity |
| 4 | Second momentum (y-direction) |
| 5 | $Z_5' = Z_6$ |
| 6 | Energy |
| 7 | $Z_7' = Z_8$ |
| 8 | Third momentum (z-direction) |

The above formulation of the stability equations given above is identical to Mack's except that he defines $Z_4 = \pi / \gamma M_\infty^2$. His system of stability equations also has one further minor difference and that difference involves the definition of the bulk viscosity coefficient. Mack uses the Lees-Lin definition which is 3/2 times the usually defined value, ξ .

The system of equations (Equation (1)) is written in the form

$$Z_i' = \sum_{j=1}^8 D_{ij} Z_j \quad (i=1, \dots, 8) \quad (\text{B. 3})$$

where

$$D_{ij} = \sum_{k=1}^8 d_{ik} b_{kj} \quad (\text{B. 4})$$

$$d_{ik} = [a_{ik}]^{-1}$$

For the parallel flow version of the stability equations, the D_{ij} can be obtained analytically whereas for the non-parallel flow version the D_{ij} must be obtained numerically. The values for the parallel flow stability equations are given below.

The Z_1' equation has one non-zero coefficient

$$D(1,2) = 1 \quad (B.5)$$

The Z_2' equation has six non-zero coefficients

$$D(2,1) = (\alpha_1^2 + \alpha_3^2) + \frac{i \alpha_1 R (U-c)}{\mu T} \quad (B.6)$$

$$D(2,2) = - \frac{T'}{\mu} \frac{d\mu}{dT} \quad (B.7)$$

$$D(2,3) = \frac{\alpha_1 U R}{\mu T} - \left[\frac{1}{\mu} \frac{d\mu}{dT} + \left(\frac{1}{3} + \kappa \right) \frac{1}{T} \right] i \alpha_1^2 T' \quad (B.8)$$

$$D(2,4) = - \left(\frac{1}{3} + \kappa \right) \alpha_1^2 M_\infty^2 (U-c) + \frac{i \alpha_1^2 R}{\gamma \mu} \quad (B.9)$$

$$D(2,5) = \frac{\alpha_1^2}{T} (U-c) \left(\frac{1}{3} + \kappa \right) - U'' \frac{T'}{\mu} \frac{d^2\mu}{dT^2} - \frac{U''}{\mu} \frac{d\mu}{dT} \quad (B.10)$$

$$D(2,6) = - \frac{U'}{\mu} \frac{d\mu}{dT} \quad (B.11)$$

The Z_3' equation has 5 non-zero coefficients

$$D(3,1) = -i \quad (B.12)$$

$$D(3,3) = T'/T \quad (B.13)$$

$$D(3,4) = -i(U-c) M_\infty^2 \quad (B.14)$$

$$D(3,5) = \frac{i}{T} (U-c) \quad (B.15)$$

$$D(3,7) = -i \frac{\alpha_3}{\alpha_1} \quad (B.16)$$

The Z_4' equation has no non-zero coefficients. The coefficients are written in terms of the factor L , defined as

$$L = \frac{R}{\alpha_1 \gamma \mu} + i \left(\frac{4}{3} + \kappa \right) M_\infty^2 (U-c) \quad (B.17)$$

The coefficients are

$$D(4,1) = \frac{-i}{L} \left[\frac{2 T'}{\mu} \frac{d\mu}{dT} + \left(\frac{4}{3} + \kappa \right) \frac{T'}{T} \right] \quad (B.18)$$

$$D(4,2) = -\frac{i}{L} \quad (B.19)$$

$$D(4,3) = \frac{1}{L} \left[-(\alpha_1^2 + \alpha_3^2) + \left(\frac{4}{3} + \kappa \right) \frac{(T')^2}{\mu} \frac{d\mu}{dT} + \frac{T''}{T} - i \frac{R \alpha_1}{\mu T} (U-c) \right] \quad (B.20)$$

$$D(4,4) = \frac{1}{L} \left(\frac{4}{3} + \kappa \right) \left[D(3,4) \left(\frac{T'}{\mu} \frac{d\mu}{dT} + \frac{T'}{T} \right) - i U' M_\infty^2 \right] \quad (B.21)$$

$$D(4,5) = \frac{1}{L} \left[\left(\frac{4}{3} + \kappa \right) \frac{T'}{\mu} \frac{d\mu}{dT} D(3,5) + i U' \left(\frac{1}{\mu} \frac{d\mu}{dT} + \frac{\left(\frac{4}{3} + \kappa \right)}{T} \right) \right] \quad (B.22)$$

$$D(4,6) = \frac{i}{L} \left(\frac{4}{3} + \kappa \right) \frac{(U-c)}{T} \quad (B.23)$$

$$D(4,7) = D(4,1) \frac{\alpha_3}{\alpha_1} \quad (B.24)$$

$$D(4,8) = D(4,2) \frac{\alpha_3}{\alpha_1} \quad (B.25)$$

The Z_5' equation has a single non-zero coefficient.

$$D(5,6) = 1 \quad (B.26)$$

The Z_6' equation has five non-zero coefficients.

$$D(6,2) = -2\sigma(\gamma-1) M_\infty^2 U' \quad (B.27)$$

$$D(6,3) = \alpha_1 \frac{R}{\mu} \sigma \frac{T'}{T} - 2i\sigma(\gamma-1) \alpha_1^2 M_\infty^2 U' \quad (B.28)$$

$$D(6,4) = -i\alpha_1 \frac{R}{\mu} \sigma \frac{(\gamma-1)}{\gamma} (U-c) M_\infty^2 \quad (B.29)$$

$$D(6,5) = (\alpha_1^2 + \alpha_3^2) - \frac{T''}{\mu} \frac{d\mu}{dT} - \frac{(T')^2}{\mu} \frac{d^2\mu}{dT^2} \\ - \sigma(\gamma-1) \frac{M_\infty^2}{\mu} \frac{d\mu}{dT} (U')^2 + i\alpha_1 \frac{R\sigma}{\mu} \frac{(U-c)}{T} \quad (B.30)$$

$$D(6,6) = -2 \frac{T'}{\mu} \frac{d\mu}{dT} \quad (B.31)$$

The Z_7' equation has a single non-zero coefficient.

$$D(7,8) = 1 \quad (B.32)$$

The Z_8' equation has 5 non-zero coefficients.

$$D(8,3) = -i\alpha_1 \alpha_3 T' \left(\frac{1}{\mu} \frac{d\mu}{dT} + \left(\frac{1}{3} + \kappa \right) / T \right) \quad (B.33)$$

$$D(8,4) = - \left(\frac{1}{3} + \kappa \right) \alpha_1 \alpha_3 (U-c) M_\infty^2 + i \frac{\alpha_3}{\gamma} \frac{R}{\mu} \quad (\text{B. 34})$$

$$D(8,5) = \left(\frac{1}{3} + \kappa \right) \alpha_1 \alpha_3 \frac{(U-c)}{T} \quad (\text{B. 35})$$

$$D(8,7) = \left(\alpha_1^2 + \alpha_3^2 \right) + i \alpha_1 \frac{R}{\mu} \frac{(U-c)}{T} \quad (\text{B. 36})$$

$$D(8,8) = - \frac{T'}{\mu} \frac{d\mu}{dT} \quad (\text{B. 37})$$

In these equations

$$\kappa = \xi / \mu \quad (\text{B. 38})$$

and is a constant.

The boundary conditions are

$$Z_1(0) = 0, Z_3(0) = 0, Z_5(0) = 0, Z_7(0) = 0 \quad (\text{B. 39})$$

and as $\eta \rightarrow \infty$, the amplitude functions must be bounded, or for the case incoming supersonic waves, the amplitude functions must be bounded for $\eta \gg \eta_\delta$.

The problem as formulated above is such that the boundary conditions themselves are not sufficient to establish any solution of the eight differential equations other than the trivial solution of zero. Therefore, the problem is an eigenvalue problem, that is, nonzero solutions which satisfy the boundary conditions exist only for certain combinations of the parameters α_1 , α_3 , R , c . The general method used to determine the eigenvalues and eigensolutions to

the above system of equations is given in the next section. The computer program used to implement the solution is given in Section B. 3.

B. 2 METHOD OF SOLUTION

The difficulties of solving the boundary layer stability equations are well known. Chapter III of Reference 17 can provide the reader with an elementary understanding of the main difficulty involved in numerically integrating the system of equations represented by Equation B. 3. The main difficulty is associated with the problem of controlling parasitic error growth in the solution of two-point boundary value problems. In the BLSTAB program, the Gram-Schmidt orthogonalization procedure is used to overcome this problem. The reader is referred to Reference 18 (pp. 98-103) for a concise demonstration of the problem of parasitic error growth and how it can be overcome by the use of the Gram-Schmidt orthogonalization procedure. Chapter IV of Reference 19 also demonstrates the use of the Gram-Schmidt orthogonalization procedure for solving two-point boundary value problems. The details of the use of the Gram-Schmidt orthogonalization procedure to determine the eigenvalues and eigensolutions of Equations B. 3 have been presented in Reference 11.

The method used to determine the eigenvalues of Equations B. 3 is outlined as follows. Four linearly independent solutions to Equations B. 3 are generated. These four independent solutions are chosen to satisfy the boundary conditions at $\eta \gg \eta_\delta$. A linear combination of the four independent solutions is then determined such that the velocity amplitudes are zero at $\eta=0$ and the pressure amplitude at $\eta=0$ is 1.0. Using this same linear combination, the value of $\theta(0)$ is evaluated. If $\theta(0)$ is sufficiently close to zero, the values of α_1 , α_3 , R , and c which were used to generate the four independent solutions constitute an eigenvalue set. The details of the methods outlined above are discussed in the following paragraphs.

B. 2. 1 Free Stream Solution

In the free stream $U=T=\mu=1$ and $U'=U''=T'=T''=0$. All of the coefficients in Equations B. 3 are constant and only the following coefficients are non-zero: $D(2, 1)$, $D(2, 4)$, $D(2, 5)$, $D(3, 1)$, $D(3, 4)$, $D(3, 5)$, $D(3, 7)$, $D(4, 2)$, $D(4, 3)$, $D(4, 6)$, $D(4, 8)$, $D(5, 6)$, $D(6, 4)$, $D(6, 5)$, $D(8, 4)$, $D(8, 5)$, and $D(8, 7)$. An analytic solution to Equation B. 3 can be obtained by elementary methods. The easiest way to obtain the analytic solution is to rewrite Equations B. 3 as a system of four second order equations in terms of Z_1 , Z_4 , Z_5 , and Z_7 . This system of four second order equations has the form

$$W_i'' = \sum_{j=1}^4 b_{ij} W_j \quad (i=1, \dots, 4) \quad (B. 40)$$

where $W_1=Z_1$, $W_2=Z_4$, $W_3=Z_5$, and $W_4=Z_7$ and the non-zero b_{ij} are given in terms of the D_{ij} by:

$$b_{11} = b_{44} = D(2, 1) \quad (B. 41)$$

$$b_{12} = D(2, 4) \quad (B. 42)$$

$$b_{13} = D(2, 5) \quad (B. 43)$$

$$b_{22} = D(2, 4) \times D(4, 2) + D(3, 4) \times D(4, 3) + D(6, 4) \times D(4, 6) + D(8, 4) \times D(4, 8) \quad (B. 44)$$

$$b_{23} = D(2, 5) \times D(4, 2) + D(3, 5) \times D(4, 3) + D(6, 5) \times D(4, 6) + D(8, 5) \times D(4, 8) \quad (B. 45)$$

$$b_{32} = D(6, 4) \quad (B. 46)$$

$$b_{33} = D(6, 5) \quad (B. 47)$$

$$b_{42} = D(8, 4) \quad (B. 48)$$

$$b_{43} = D(8, 5) \quad (B. 49)$$

$$b_{44} = D(8, 7) \quad (B. 50)$$

AD-A036 210

DAYTON UNIV OHIO RESEARCH INST
STABILITY OF HIGHLY-COOLED COMPRESSIBLE LAMINAR BOUNDARY LAYERS--ETC(U)
OCT 76 L I BOEHMAN, M G MARISCALCO
UDRI-TR-76-70 AFFDL-TR-76-148 F33615-74-C-3067
NL

UNCLASSIFIED

2 OF 2

AD
A036210



END

DATE
FILMED

3-77

The characteristic values of the system of Equations B.40, which are the same as the characteristic values of Equations B.3, are given by

$$\lambda_1 = -(b_{11})^{1/2} = -[(\alpha_1^2 + \alpha_3^2) + i\alpha_1 R(1-c)]^{1/2} \quad (\text{B. 51})$$

$$\lambda_2 = \lambda_1 \quad (\text{B. 52})$$

$$\lambda_3 = - \left\{ 1/2(b_{22} + b_{33}) + [1/4(b_{22} - b_{33})^2 + b_{32} b_{23}]^{1/2} \right\}^{1/2} \quad (\text{B. 53})$$

$$\lambda_4 = - \left\{ 1/2(b_{22} + b_{33}) - [1/4(b_{22} - b_{33})^2 + b_{32} b_{23}]^{1/2} \right\}^{1/2} \quad (\text{B. 54})$$

$$\lambda_5 = -\lambda_4 \quad (\text{B. 55})$$

$$\lambda_6 = -\lambda_3 \quad (\text{B. 56})$$

$$\lambda_7 = \lambda_8 = -\lambda_1 \quad (\text{B. 57})$$

In order to study incoming supersonic waves it is necessary to determine which of the above characteristic values represent the viscous counterparts to the inviscid solution as given by Equations 13, 14, and 15 on page 24. To this end, it is instructive to evaluate b_{22} and b_{23} for the special case of $\kappa = 0$ and $\sigma = 3/4$. From Equation B.45 it can be shown that

$$b_{23} = \alpha_1 R(1-c)^2 (1 - 4/3 \sigma - \kappa \sigma) \quad (\text{B. 58})$$

and from Equation B.44 it can be shown that

$$b_{22} = (\alpha_1^2 + \alpha_3^2) - \frac{\alpha_1^2 M_\infty^2 (1-c)^2 [\gamma - (4/3 + \kappa) \sigma (\gamma - 1)]}{[1 + i \frac{\alpha_1}{R} \gamma M_\infty^2 (1-c) (4/3 + \kappa)]} \quad (\text{B. 59})$$

For the case of $\kappa = 0$ and $\sigma = 3/4$, Equation B.58 reduces to

$$b_{23} = 0 \quad (\text{B. 60})$$

and from Equation B.53

$$\lambda_3 = -(b_{22})^{1/2} \quad (\text{B. 61})$$

and from Equation B. 54

$$\lambda_4 = -(b_{33})^{1/2} \quad (\text{B. 62})$$

Combining equations B. 61 and B. 59 yields the following expression for λ_3 when $\kappa = 0$ and $\sigma = 3/4$

$$\lambda_3 = - \left\{ (\alpha_1^2 + \alpha_3^2) - \frac{\alpha_1^2 M_\infty^2 (1-c)^2}{[1 + i \frac{\alpha_1}{R} \frac{4}{3} \gamma M_\infty^2 (1-c)]} \right\}^{1/2} \quad (\text{B. 63})$$

which for large R reduces to

$$\lambda_{3_{R \rightarrow \infty}} = -\alpha_1 \left\{ [1 - M_\infty^2 (1-c)^2] + \alpha_3^2 / \alpha_1^2 \right\}^{1/2} \quad (\text{B. 64})$$

Thus, λ_3 and λ_6 are the viscous counterparts to the inviscid characteristic solutions (Note that Equations 13-15 on page 24 are valid only for 2-D waves whereas Equation B. 64 is a 3-D wave result). From Equations B. 62, B. 47, and B. 30 it is easy to show that λ_4 is given by

$$\lambda_4 = -[(\alpha_1^2 + \alpha_3^2) + 3/4 i \alpha_1 R (1-c)]^{1/2} \quad (\text{B. 65})$$

when $\kappa = 0$ and $\sigma = 3/4$.

The characteristic vectors corresponding to each of the eight characteristic values can most easily be obtained by first determining the characteristic vector components corresponding to Z_1 , Z_4 , Z_5 , and Z_7 from Equations B. 40-B. 50, and then using the relations $Z_2 = Z_1'$, $Z_6 = Z_5'$, $Z_8 = Z_7'$ and the continuity equation to define the other components. Let $B^{(j)}$ represent the characteristic vector corresponding to the characteristic value λ_j . Then from Equations B. 40-B. 50 the following system of equations for the $B^{(j)}$ are obtained:

$$(b_{11} - \lambda_j^2) B_1^{(j)} + b_{12} B_2^{(j)} + b_{13} B_3^{(j)} = 0 \quad (\text{B. 66})$$

$$(b_{22} - \lambda_j^2) B_2^{(j)} + b_{23} B_3^{(j)} = 0 \quad (B.67)$$

$$b_{32} B_2^{(j)} + (b_{33} - \lambda_j^2) B_3^{(j)} = 0 \quad (B.68)$$

$$b_{42} B_2^{(j)} + b_{43} B_3^{(j)} + (b_{44} - \lambda_j^2) B_4^{(j)} = 0 \quad (B.69)$$

For the first characteristic value, $\lambda_1 = -(b_{11})^{1/2} = -(b_{44})^{1/2}$, $B_1^{(1)}$ is arbitrary as is $B_4^{(1)}$. Therefore, $B_2^{(1)}$ and $B_3^{(1)}$ must both be zero. Observe that λ_1 is a double root to the characteristic determinant. However, since only one (and not two) of the Equations B.66-B.69 is a linear combination of the other equations for $\lambda_j = \lambda_1$, it follows that even though there is a double root, there are still two linearly independent characteristic vectors corresponding to the double root. Thus, $B^{(1)}$ and $B^{(8)}$ are defined as $(1, 0, 0, 0)$ while $B^{(2)}$ and $B^{(7)}$ are defined as $(0, 0, 0, 1)$. The remaining characteristic vectors are given by the following relations:

$$B_3^{(j)} = -D(6, 4) \quad (B.70)$$

$$B_2^{(j)} = D(6, 5) - \lambda_j^2 \quad (B.71)$$

$$B_1^{(j)} = \frac{D(2, 4) \times B_2^{(j)} - D(2, 5) \times D(6, 4)}{\lambda_j^2 - D(2, 1)} \quad (B.72)$$

$$B_4^{(j)} = \frac{D(8, 4) \times B_2^{(j)} + D(8, 5) \times B_3^{(j)}}{\lambda_j^2 - D(8, 7)} \quad (B.73)$$

The characteristic vectors for the eighth order system $A^{(j)}$ are then defined as follows:

$$A_1^{(j)} = B^{(j)} / \lambda_j \quad (B.74)$$

$$A_2^{(j)} = B^{(j)} \quad (B.75)$$

$$A_3^{(j)} = [D(3, 1) \times B_1^{(j)} + D(3, 4) \times B_2^{(j)} + D(3, 5) \times B_3^{(j)} + D(3, 7) \times B_4^{(j)}] / \lambda_j^2 \quad (B.76)$$

$$A_4^{(j)} = B_2^{(j)} / \lambda_j \quad (\text{B. 77})$$

$$A_5^{(j)} = B_3^{(j)} / \lambda_j \quad (\text{B. 78})$$

$$A_6^{(j)} = B_3^{(j)} \quad (\text{B. 79})$$

$$A_7^{(j)} = B_4^{(j)} / \lambda_j \quad (\text{B. 80})$$

$$A_8^{(j)} = B_4^{(j)} \quad (\text{B. 81})$$

The analytic free stream solutions provide the initial conditions for four linearly-independent solutions. The characteristic vectors corresponding to the characteristic values having negative real parts ($\lambda_1, \lambda_2, \lambda_3$, and λ_4) are then integrated, each separately, across the boundary layer to produce four linearly-independent solutions. Each of these four solutions approach zero as $\eta \rightarrow \infty$. When amplified incoming supersonic waves are being considered, λ_6 and it's characteristic vector must be used instead of λ_4 and it's characteristic vector in order that the pressure amplitude have the characteristics of an incoming Mach wave.

B. 2. 2 Solution Inside the Boundary Layer

With initial conditions at $\eta = \eta_0$ specified by the analytic solutions, the Equations B. 3 are then numerically integrated across the boundary layer from $\eta = \eta_0$ to $\eta = 0$. A standard fourth order Runge-Kutta technique is used to carry out the numerical integration. The four separate integrations are carried out in parallel across a specified number of integration steps. Then the Gram-Schmidt orthogonalization procedure is performed; both on the initial conditions as well as on the current solutions. When the wall ($\eta = 0$) is reached, a final Gram-Schmidt orthogonalization is performed and then a linear combination of the solutions is obtained satisfying the boundary conditions at the wall ($Z_1(0) = Z_3(0) = Z_7 = 0$ and $Z_4(0) = 1.0$). $\theta(0)$ is then obtained where θ is given by

$$\theta = C_1 Z_5^{(1)} + C_2 Z_5^{(2)} + C_3 Z_5^{(3)} + C_4 Z_5^{(4)} \quad (B.82)$$

where the C_j are the combining coefficients obtained by satisfying the wall boundary conditions. If $\theta(0)$ is zero within a specified tolerance, an eigenvalue has been found. If $\theta(0) \neq 0$, the Newton-Raphson search procedure is used to find a combination of α_1 , α_3 , R , and c which will yield an eigenvalue.

B.3 LISTING OF THE BLSTAB COMPUTER PROGRAM

The computer program which implements the methods discussed in Section B.2 is called the Boundary Layer STABility Computer Program. The input data for the program are as follows. The data on the first card are:

FIRST CARD (all quantities in I10 format)

Columns 1-10. NSTEPS--the number of integration steps.

Columns 11-20. ITSTEP--the number of integration steps between Gram-Schmidt orthogonalizations;

Columns 21-30. ORDER--the order of the differential equation system which is eight (8) for the version of the program described in this report.

Columns 31-40. NPNTDA--if not equal to zero, the input mean flow profiles will be printed out.

MEAN FLOW PROFILE INPUT CARDS

The program requires that the mean flow quantities U , U' , U'' , T , T' , and T'' be specified at the wall and at equal intervals of one-half of the integration step size ($H/2$). Thus, the mean flow profile data must be available at $2 \times \text{NSTEPS} + 1$ locations equally spaced across the boundary layer at intervals of $H/2$. Two input cards are used to prescribe the mean flow profile data at each point. The first card contains U , U' , and U'' in a 3E14.7 format in the order given. The second card in each set contains T , T' , and T'' and Y , the location within the boundary layer at which the data are given. T , T' , and T'' are in a 3E14.7 format. Y is in columns

71-80 in a F10.3 format. The order in which the mean flow profile data must appear is in ascending order of Y , that is, the first two cards give the data at $Y=0$ ($\eta=0$), the next two cards give the data at $H/2$, and so on, with the last two cards giving data at $\eta=\eta_\delta$. The last data set is used in subroutine EIGEN to determine the analytic solution for the free stream. Therefore, the last two cards must show $U(\eta_\delta)=1.0$, $U'(\eta_\delta)=U''(\eta_\delta)=0$ on the second last card and $T(\eta_\delta)=1.0$, $T'(\eta_\delta)=0$, $T''(\eta_\delta)=0$, and $Y=\eta_\delta$ on the last card. H , the integration step size is calculated within the program by dividing η_δ by NSTEPS. The user must insure that the number of integration steps divided by ITSTEP is an integer.

DATA AND PARAMETERS REQUIRED FOR EACH PROBLEM SET

A set of four cards is required for each problem.

First Card of a Problem Set

Columns 1-20. EPS, the tolerance of $\theta(0)$. If $|\theta(0)| < \text{EPS}$, an eigenvalue has been found. E20.1 format.

Columns 21-30. NOIT2, the number of iterations of the Newton-Raphson search procedure which are permitted to find an eigenvalue; I10 format.

Columns 31-40. NPRINT, a diagnostic output parameter. If NPRINT $\neq 0$, the results of intermediate computations associated with obtaining the free stream solution are printed out each time a trial solution is carried out; I10 format.

Columns 41-50. NPRINT1, another diagnostic output parameter to be used in conjunction with NPRINT. If only the characteristic values of the free stream solution are desired for each individual solution, then NPRINT1 $\neq 0$ and NPRINT=0. I10 format.

Second Card of a Problem Set (all quantities in an F11.5 format)

Columns 1-11. M, Mach number of the free stream. For shock induced flows, enter the Mach number of the flow behind the moving shock wave in a laboratory-fixed coordinate system.

- Columns 12-22. GAMMA, specific heat ratio c_p/c_v at free stream temperature (assumed to be constant throughout the flow).
- Columns 23-33. SIGMA, Prandtl number of the free stream (assumed to be constant throughout the flow).
- Columns 34-44. TINF, temperature of the free stream in degrees Rankine.
- Columns 45-55. MU2, bulk viscosity (denoted by κ in Sections B.1 and B.2).

Third Card of a Problem Set (all quantities in an F11.5 format)

- Columns 1-11. (ALPHA1)_r; real part of α_1
- Columns 12-22. (ALPHA1)_i; imaginary part of α_1
- Columns 23-33. (ALPHA3)_r; real part of α_3
- Columns 34-44. (ALPHA3)_i; imaginary part of α_3
- Columns 45-55. R, Reynolds number ($R = \sqrt{R_x}$)
- Columns 56-66. (PHV)_r; real part of phase velocity, c_r
- Columns 67-77. (PHV)_i; imaginary part of phase velocity, c_i

Fourth Card of a Problem Set (all quantities in an I10 format)

- Columns 1-10. IX1 The seven numbers on the third card are stored in an array called X. IX1 denotes one of the two parameters which will be varied in carrying out the Newton-Raphson search procedure.
- Columns 11-20. IX2 Denotes the second of the two parameters which will be varied in carrying out the Newton-Raphson search procedure.
- Columns 21-30. ITEST. α_3 can be input in two ways. If ITEST equals 1, the input number for α_3 is considered to be α_3/α_1 . If ITEST \neq 1, then the numbers read in for α_3 are considered to be α_3 . The option of ITEST=1 is used to study waves which have a constant oblique angle.
- Columns 31-40. INT. If INT \neq 0, the eigensolution for the region inside the boundary layer will be computed and printed out after an eigenvalue has been found.

Columns 41-50. INTOBL. If INTOBL \neq 0, the eigensolution for the region outside of the boundary layer will be computed and printed out.

Multiple problem sets can be included in the input data. This concludes the description of the input data for the program. The listing of the program is given in the next section.

```

1  PROGRAM ELSTAB (INPUT=200,OUTPUT=200,TAPES=INPUT,TAPE6=OUTFUT,TAPE1
2  $0)
3
4  * * * * *
5
6  BOUNDARY LAYER STABILITY COMPUTER PROGRAM. DEVELOPED BY LR. L. I.
7  BOEHMAN, MECHANICAL ENGINEERING DEPT., UNIVERSITY OF DAYTON, DAYTON
8  OHIO 45469. THIS VERSION DETERMINES THE STABILITY OF A 2-D COMPRESSI-
9  BILE LAMINAR BOUNDARY LAYER TO PLANE OBLIQUE (3-D) DISTURBANCES.
10 THIS PROGRAM IS A NEW VERSION THAT MINIMIZES STORAGE. ONLY THOSE
11 COEFFICIENTS IN THE SYSTEM OF DIFFERENTIAL EQUATIONS ARE STORED
12 WHICH ARE NEEDED TO INTEGRATE ACROSS ONE INTEGRATION STEP.
13
14 * * * * *
15
16 INTEGER ORDER,ORDER1
17 CCOMPLEX C, DET,D(8,8),CM(4),EIGVEC(8,8),EIGVAL(8),
18 XTS1(4,1),CMX(4,1), TMP(8),Z(8,4),TS(4,4)
19 CCOMPLEX RSTR8,RK,RX,RY,IE,PHV,STORE(8,4),STORE1(8,4),
20 X ALPHA1,CON2,ALPHA3,SUM
21 REAL M,JAC,G(8,2),MU2
22 DIMENSION X(7),DATA(6,530)
23 COMMON/CT/C(5,8,4)/PROFIL/DATA/PARAM/ITEST,ITSTEP,
24 1IX1,IX2/CCNST/M,GAMMA,SIGMA,TINF,NS4,X,MU2,H
25 EQUIVALENCE (CMX(1,1),CM(1)),(CMX(2,1),CM(2)),(CMX(3,1),CM(3))
26 EQUIVALENCE (CMX(4,1),CM(4))
27 EQUIVALENCE (X(1),ALPHA1),(X(3),ALPHA3),(X(5),R),(X(6),PHV)
28 DATA IE/(0.,1.)/
29
30 * * * * *
31 READ IN TABLE OF VALUES FOR W, AND T FUNCTIONS, AND OTHER CONSTANTS
32 * * * * *
33
34 READ ( 5,1001) NSTEPS,ITSTEP,ORDER,NPNTDA
35 FORMAT (8I10)
36 ORDER1 = ORDER / 2
37 NS4=2*NSTEPS+1

```

```

38 IF (NPNTA.EQ.0) GO TO 3
39 WRITE (6,1009)
40 1009 FORMAT (5H1 Y,14X,1HW,18X,2HWP,16X,3HWPP,22X,1HT,18X,2HTP,16X,
41 $3HTPP//)
42 3 DC 5 J=1,NS4
43 IF (NPNTA.EQ.0) GO TO 4
44 IF (MOC(J,58).EQ.0) WRITE(6,1009)
45 4 READ ( 5,1006) (DATA(I,J),I=1,6) ,Y
46 IF (NPNTA.EQ.0) GO TO 5
47 WRITE (6,1010) Y, (DATA(I,J),I=1,6)
48 5 CONTINUE
49 1006 FORMAT (3E14.7/3E14.7,28X,F10.3)
50 1010 FORMAT (F7.3,E18.8,2E19.8,5X,3E19.8)
51 1011 FORMAT (F7.3,E12.4,2E13.4)
52 DELTA=Y
53 H=DELTA/FLCAT(NSTEPS)
54 MORD=ORDER1-1
55 MCRD1=CORDER1+1
56 6 READ (5,1005) EPS,NOIT2,NPRINT,NPRNT1
57 IF (EOF (5)) 351,10
58 10 CCNTINUE
59 1005 FORMAT (E20.1,3I10)
60 WRITE (6,1003) EPS,NSTEPS,ITSTEP,NOIT2,DELTA,H
61 1003 FORMAT (//18H1CONTROL CONSTANTS,12X,22HINTEGRATION PARAMETERS/2X,
62 $4HEPS=,E14.3,11X,7HNSTEPS=,I7,5X,7HITSTEP=,I4/2X,6HNCIT2=,I12,12X,
63 $6HDELTA=,F8.4,9X,2HH=,F9.5//)
64 READ (5,1002) M,GAMMA,SIGNA,TINF,MU2
65 1002 FORMAT(7F11.5)
66 READ (5,1002) ALPHA1,ALPHA3,R,PHV
67 READ(5,1001) IX1,IX2,ITEST,INT,INTOBL
68 WRITE (6,1007) M,GAMMA,SIGNA,TINF,MU2,ITEST,INT,INTOBL
69 1007 FORMAT(19H CCNSTANTS THIS RUN//3X,2HH=,F10.5,10X,6HGAMMA=,F6.3,
70 $10X,6HSIGNA=,F6.3,10X,5HTINF=,F9.3,10X,4HNU2=,F8.3/16X,6HITEST=,
71 $I2,15X,4HINT=,I2,15X,7HINTOBL=,I2//)
72 WRITE (6,1008) ALPHA1,ALPHA3,R,PHV
73 1008 FORMAT (16H INITIAL GUESSES//12X,6HALPHA1,28X,6HALPHA3,20X,
74 $ 15HREYNOLDS NUMER,12X,14HPHASE VELOCITY/3X,2F12.8,10X,2F12.8,

```



```

75      #10X,F12.3,10X,2F12.8/)
76      NX=0
77      JA=1
78
79      C * * * * *
80      C * * * * *
81      C * * * * *
82      1
83      CONTINUE
84      CALL CCEF(NS4,ORDER,0)
85      DO 15 I=1,ORDER
86      DC 15 J=1,ORDER
87      15 D(I,J)=0.0
88      DC 21 J=1,ORDER
89      DC 20 I=2,ORDER,2
90      20 D(I,J)=C(I/2,J,4)
91      21 D(3,J)=C(MORD1,J,4)
92      D(1,2)=1.0
93      D(5,6)=1.0
94      D(7,8)=1.0
95      IF (NPRINT.EQ.0) GO TO 9000
96      WRITE(6,1050) ((D(I,J), J=1,ORDER), I=1,ORDER)
97      1050 FORMAT(/41X,8HC(DELTA)//16(8F15.5//))
98      C * * * * *
99      C * * * * *
100      C * * * * *
101      C * * * * *
102      C * * * * *
103      C * * * * *
104      C * * * * *
105      C * * * * *
106      C * * * * *
107      C * * * * *
108      C * * * * *
109      C * * * * *
110      C * * * * *
111      C * * * * *

```

SOLVE DIFFERENTIAL EQUATION FOR Y BEYOND THE BOUNDARY LAYER.
(WHERE CCEFFICIENTS OF MATRIX C ARE CONSTANT.) USE THIS SOLUTION
AND BOUNDARY CONDITIONS AT INFINITY TO FIND BOUNDARY CONDITIONS
AT Y=DELTA

FIND EIGENVALUES AND EIGENVECTORS OF MATRIX D (AT Y=DELTA).

```

9000  EC 55 I=1,ORDER
      DC 55 J=1,ORDER
      55 EIGVEC(I,J)=D(I,J)
      C

```

```

C
CALL EIGEN (EIGVEC, EIGVAL, ORDER)
IF (NPRINT.EQ.0) GO TO 9004
WRITE (6,1055) EIGVAL(1), EIGVAL(5), EIGVAL(2), EIGVAL(6), EIGVAL(3),
EIGVAL(7), EIGVAL(4), EIGVAL(8)
1055 FORMAT (55X, 11HEIGENVALUES/4 (2E25.14, 15X, 2E25.14/))
9004 IF (NPRINT.EQ.0) GO TO 9001
WRITE (6,35)
35 FORMAT (1H, 6X, 11HEIGENVALUES, 48X, 12HEIGENVECTORS/)
DO 43 I=1, ORDER
WRITE (6,354) EIGVAL(I), (EIGVEC(J,I), J=1, ORDER)
43 CONTINUE
354 FORMAT (1H, 2E17.9, 8E12.4/35X, 8E12.4)
C
C DETERMINE THE ACCURACY OF THE ANALYTIC SOLUTION FOR THE FREE-
C STREAM REGION. PRINT OUT THE LARGEST RESIDUAL.
C
9001 AMAX=0.0
IF (NPRINT.EQ.0) GO TO 9002
WRITE (6,1056)
1056 FORMAT (/10H RESIDUALS/)
9002 DC 62 I=1, ORDER
DC 59 J=1, ORDER
SUM=0.
CCN2=D(J,J)
D(J,J)=CCN2-EIGVAL(I,
DC 58 K=1, ORDER
SUM=SUM+D(J,K)*EIGVEC(K,I)
D(J,J)=CCN2
CON1=AMAX1 (ABS(REAL(SUM)), ABS(AIMAG(SUM)))
IF (CON1.GT.AMAX) AMAX=CON1
TMP(J)=SUM
59 IF (NPRINT.EQ.0) GO TO 62
WRITE (6,1060) (TMP(J), J=1, ORDER)
1060 FORMAT (8E15.3)
62 CONTINUE
WRITE (6,1065) AMAX

```



```

135      DC 135 I=1,ORDER1
      RSTR8=RSTR8+CM(I)*STORE1(5,I)
      WRITE(6,136) RSTR8
136      FORMAT (/7H RSTR8=,2E20.12/)
      DO 220 I=1,ORDER
      SUM=0.
231      DO 231 J=1,ORDER1
      SUM=SUM+CM(J)*STCRE(I,J)
220      TMP(I)=SUM
      DC 217 J=1,ORDER
      SUM=0.
216      DC 216 I=1,ORDER1
      SUM=SUM+CM(I)*STCRE1(J,I)
217      Z(J,1)=SUM
      GC TO 300
C
C
C      PRINT CONVERGED SOLUTION.
240      WRITE (6,1012) EFS,NSTEPS,ITSTEP,MOIT2,DELTA,H
1012      FORMAT (//18H CONTROL CONSTANTS,12X,22HINTEGRATION PARAMETERS/2X,
      $4HEPS=,E14.3,11X,7HNSTEPS=,I7,5X,7HITSTEP=,I4/2X,6HNCIT2=,I12,12X,
      $6HDELTA=,F8.4,9X,2HH=,F9.5/)
      WRITE (6,1007) M,GAMMA,SIGNA,TINF,MU2,ITEST,INT,INTCBL
      WRITE (6,1055) EIGVAL(1),EIGVAL(5),EIGVAL(2),EIGVAL(6),EIGVAL(3),
      1EIGVAL(7),EIGVAL(4),EIGVAL(8)
      DO 222 J=1,ORDER
      IF (AIMAG(Z(J,1)).EQ.0.0.AND.REAL(Z(J,1)).EQ.0.0) GO TO 221
      G(J,1)=CABS(Z(J,1))
      G(J,2)=ATAN2(AIMAG(Z(J,1)),REAL(Z(J,1)))
      G(J,2)=G(J,2)*57.295778
      GC TO 222
221      G(J,1)=0.0
      G(J,2)=0.0
222      CCNTINUE
      WRITE(6,223) (Z(J,1),G(J,1),G(J,2),J=1,ORDER)
223      FCENMAT (/14X,4H2(0),24X,9HHMAGNITUDE,19X,
      C16HCPHASE ANGLE(DEC)/8(2E16.7,5X,E16.6,17X,F10.4/))

```

```

223 DO 142 J=1,ORDER
224 IF (AIMAG(TMP(J)).EQ.0.0.AND.REAL(TMP(J)).EQ.0.0)GO TO 140
225 G(J,1)=CABS(TMP(J))
226 G(J,2)=ATAN2(AIMAG(TMP(J)),REAL(TMP(J)))
227 G(J,2)=G(J,2)*57.295778
228 GC TO 142
229 G(J,1)=0.0
230 G(J,2)=0.0
231 CCNTINUE
232 WRITE(6,218) (TME(J),G(J,1),G(J,2),J=1,ORDER)
233 218 FORMAT (1H,9X,8HZ(DELTA),25X,9H MAGNITUDE,
234 C19X,16HPHASE ANGLE(DEG)/8(2E16.7,5X,E16.6,17X,F10.4/))
235 WRITE(6,1231) (CM(I),I=1,ORDER1)
236 1231 FORMAT (/2X,6H CM(1)=,2E16.8,7X,6H CM(2)=,2E16.8,
237 $/2X,6H CM(4)=,2E16.8/)
238 WRITE(6,1332) (X(I),I=1,7)
239 WRITE(6,1012) EFS,NSTEPS,ITSTEP,NOIT2,DELTA,H
240 WRITE(6,1007) M,GAMMA,SIGMA,TINF,MU2,ITEST,INT,INTOBI
241 DO 360 I=1,ORDER1
242 WRITE(6,5000)
243 5000 FORMAT (1H,17X,4HZ(0),40X,21HPUR. INIT. CONDITIONS,20X,
244 X 27HINITIAL COND. (EIGENVECTOR))
245 DO 360 J=1,ORDER
246 WRITE(6,5001) STORE1(J,I),STORE(J,I),EIGVEC(J,I)
247 360 CONTINUE
248 5001 FORMAT(2E20.5,6X,2E20.5,6X,2E20.5)
249 IF (INT.EQ.0) GO TO 350
250 C
251 C
252 C
253 DETERMINE EIGENSCLUTION CORRESPONDING TO CONVERGED SCLUTION.
254 DC 225 I=1,ORDER1
255 Z(2*I-1,1)=0.
256 Z(2*I,1)=CM(I)
257 T3=0.0
258 T2=DELTA
259 CALL DIFF(T3,T2,NSTEPS,Z,ORDER,L1,ITSTEP,STORE,STORE1,0)
DO 250 I=1,ORDER

```



```

C * * * * *
C
300 GC TO (310,320,330),JA
310 RK=RSTR8
    X1=X(IX1)
    Y1=X(IX2)
    NX=NX+1
    IF (CAES(RK).LT.EPS) GO TO 240
    IF (NX.GT.NOIT2) GO TO 350
    T2=AMAX1(AES(REAL(RSTR8)),ABS(AIMAG(RSTR8)))
    DX=.005
    IF (T2.GT.1.E+7) GO TO 350
    IF (T2.LE.1.E+4) LX=.005
    IF (T2.LE.1.E+2) DX=0.001
    IF (T2.LE.1.E+1) EX=.0005
    X(IX1)=X1+DX*X1
    WHITE(6,1330) IX1,DX,(X(I),I=1,7)
    JA=2
    GC TO 1
    RX=RSTR8
    IF ((IX1.EQ.6.AND.IX2.EQ.7).OR.(IX1.EQ.1.AND.IX2.EQ.2)) GO TO 330
    X(IX1)=X1
    X(IX2)=Y1+DX*Y1
    WRITE(6,1330) IX2,DX,(X(I),I=1,7)
    JA=3
    GO TO 1
    RY=RSTR8
    RX=(RX-RK)/DX/X1
    IF ((IX1.EQ.6.AND.IX2.EQ.7).OR.(IX1.EQ.1.AND.IX2.EQ.2)) GO TO 331
    RY=(RY-RK)/DX/Y1
    GC TO 332
    RY=IE*EX
    JAC=REAL(RX)*AIMAG(RY)-AIMAG(RX)*REAL(RY)
    X(IX1)=X1-(REAL(RK)*AIMAG(RY)-AIMAG(RK)*REAL(RY))/JAC
    X(IX2)=Y1-(REAL(RX)*AIMAG(RK)-AIMAG(RX)*REAL(RK))/JAC
    WHITE(6,1332) (X(I),I=1,7)
    IF ((X(1).LE.0.).OR.(X(6).LT.0.)) GO TO 350

```

```

334 IF(X(1).GT.5.0) GO TO 350
335 JA=1
336 GO TO 1
337 1330 FORMAT(/46H INCREMENTED GUESSES-FRACTIONAL INCREASE IN X(,I1,2H)=,
338 $ P9.6/
339 $ 15HREYNOLDS NUMER,12X,14HPHASE VELOCITY/3X,2F12.8,10X,2F12.8,
340 #10X,F12.3,10X,2F12.8/)
341 1332 PCRMAT(1H1,////2X,48HNEW GUESSES FROM NEWTON-RAPHSON SEARCH PROC
342 $ DURE//12X,6HALPHA1,28X,6HALPHA3,20X,
343 $ 15HREYNOLDS NUMER,12X,14HPHASE VELOCITY/3X,2F12.8,10X,2F12.8,
344 #10X,F12.3,10X,2F12.8/)
345 350 GO TO 6
346 351 STCP
347 END

```

```

1  SUBROUTINE COEF(JK,ORDER,NV)
2  INTEGER ORDER,ORDER1
3  COMPLEX C(5,8,4),D(8,8),
4  1IE,CON4,EHV,ALPHA1,ALPHA3,CON2,ALPHA,CCM9,ZL
5  DIMENSION X(7),DATA(6,530)
6  COMMON/CT/C/PROFIL/DATA/FARAM/ITEST,ITSTEP,
7  1IX1,IX2/CONST/N,GAMMA,SIGMA,TINF,NS4,X,MU2,H
8  REAL N,MU2
9  EQUIVALENCE(X(1),ALPHA1),(X(3),ALPHA3),(X(5),R),(X(6),EHV)
10 DATA IE/(0.,1.),/
11 ORDER1=ORDER/2
12 MORD=ORDER1-1
13 MCRD1=ORDER1+1
14 DO 2 I=1,ORDER
15 DC 2 J=1,ORDER
16 2 D(I,J)=0
17 IF(ITEST.EQ.1) ALPHA3=ALPHA3*ALPHA1
18 IF(JK.EQ.NS4.AND.NV.EQ.1)GO TO 5
19 IF(JK.EQ.NS4.AND.NV.EQ.0)GO TO 6
20 N1=2
21 N2=3
22 DC 31 J=1,ORDER
23 DO 30 I=2,ORDER,2
24 30 C(I/2,J,1)=C(I/2,J,3)
25 31 C(MORD1,J,1)=C(MCRD1,J,3)
26 GC TO 100
27 5 DC 41 J=1,ORDER
28 DO 40 I=2,ORDER,2
29 40 C(I/2,J,1)=C(I/2,J,4)
30 41 C(MORD1,J,1)=C(MCRD1,J,4)
31 N1=2
32 N2=3
33 GC TO 100
34 6 N1=1
35 N2=1
36 100 DC 50 J1=N1,N2
37 II=JK-(J1-1)

```



```

38 Y=H*PLCAT(II-1)/2.
39
40 * * * * *
41 * SET UP MATRIX D FOR SOME VALUE CP Y.
42 * * * * *
43 * * * * *
44
45 W= DATA(1,II)
46 WP= DATA(2,II)
47 WFP= DATA(3,II)
48 TP =DATA(4,II)
49 TFF=DATA(5,II)
50 TFF=DATA(6,II)
51 IF (TINF.LE.198.6) GO TO 13
52 U=SQRT(T)*T*(1.+198.6/TINF)/(T+198.6/TINF)
53 DUDT=U/T*(.5+1./(1.+T*TINF/198.6))
54 GC TO 18
55 IF (T.LE.198.6/TINF) GO TO 15
56 U=SQRT(198.6*T/TINF)*T/(T+198.6/TINF)*2.
57 DUDT=U/T*(.5+1./(1.+T*TINF/198.6))
58 GC TO 18
59
60 U=T
61 DUDT=1.0
62 D2UDT2=0.0
63 CON1=R/U
64 CON2=ALPHA1*ALPHA1
65 CON9=CON2+ALPHA3*ALPHA3
66 CCN5=DUDT/U
67 CON3=TF/I
68 CON6=H*H
69 CCN7=(TFF-TP*TP/T)/I
70 CON8=MU2+1./3.
71 CCN4=ALPHA1*W-PHV*X(1)
72 IF(X(2).NE.0.) CCN4=ALPHA1*W-PHV
73 ALPHA=CSQRT(CCN9)
74 CON10=CON8+1.
75 D(3,1)=-IE
76 D(3,3)=TF/T

```

| | |
|---|-----|
| D(3,4) = -CON4*CCN6*IE/ALPHA1 | 75 |
| D(3,5) = CCN4*IE/(ALPHA1*T) | 76 |
| D(3,7) = -IE*ALPHA3/ALPHA1 | 77 |
| D(1,2) = 1.0 | 78 |
| D(5,6) = 1.0 | 79 |
| D(7,8) = 1.0 | 80 |
| D(2,1) = IE*CON4*CCN1/T+CON9 | 81 |
| D(2,2) = -TP*CCN5 | 82 |
| D(2,3) = ALPHA1*WP*CON1/T - (CON5+CON8/T)*CON2*TP*IE | 83 |
| D(2,4) = ALPHA1*CON1*IE/GAMMA-CON8*ALPHA1*CCN6*CON4 | 84 |
| D(2,5) = -WPP*CON5-WP*TP*D2UDT2/U+ALPHA1*CON4*CON8/T | 85 |
| D(2,6) = -WP*CCN5 | 86 |
| EL=CON1/(ALPHA1*GAMMA)+CON10*CON6*CON4*IE/ALPHA1 | 87 |
| D(4,1) = -(2.*TP*CCN5+CCN10*CON3)*IE/EL | 88 |
| D(4,2) = -IE/EL | 89 |
| D(4,3) = (-CON9+CON10*(TP*CON3*CON5+TFF/T)-CON4*CON1*IE/T)/EL | 90 |
| D(4,4) = CCN10*(D(3,4)*(TP*CON5+CON3)-CON6*WP*IE)/EL | 91 |
| D(4,5) = (WP*IE*(CCN5+CCN10/T)+CON10*TP*CON5*D(3,5))/EL | 92 |
| D(4,6) = (CON10*CON4*IE/(ALPHA1*T))/EL | 93 |
| D(4,7) = (D(4,1)*ALPHA3/ALPHA1) | 94 |
| D(4,8) = (D(4,2)*ALPHA3/ALPHA1) | 95 |
| D(6,2) = -2.*SIGNA*(GAMMA-1.)*CON6*WP | 96 |
| D(6,3) = ALPHA1*CCN1*SIGNA*CON3-2.*WP*(GAMMA-1.)*CON6*CON2*SIGNA*IE | 97 |
| D(6,4) = -IE*CCN4*CCN1*SIGNA*(GAMMA-1.)*CON6/GAMMA | 98 |
| D(6,5) = CON9+IE*CCN4*CCN1*SIGNA/T-TP*CCN5-TP*TP*D2UDT2/U-SIGNA* | 99 |
| X (GAMMA-1.)*CON6*CON5*WP*WP | 100 |
| D(6,6) = -2.*TP*CON5 | 101 |
| D(8,3) = -ALPHA1*ALPHA3*(CON5+CON8/T)*TP*IE | 102 |
| D(8,4) = IE*ALPHA3*CON1/GAMMA-CON4*ALPHA3*CON8*CON6 | 103 |
| E(8,5) = CON4*ALPHA3*CON8/T | 104 |
| D(8,7) = CCN9+IE*CCN4*CCN1/T | 105 |
| D(8,8) = -TP*CCN5 | 106 |
| C | 107 |
| C | 108 |
| C | 109 |
| C | 110 |
| C | 111 |

112
113
114
115
116
117
118
119
120
121

MM=J1
IF (NV.EC.0) MM=4
DC 21 J=1,ORDER
EC 20 I=2,ORDER,2
20 C(I/2,J,MM)=C(I,J)
21 C(MORD1,J,MM)=D(3,J)
50 CCINUE
IF (ITEST.EQ.1) ALPHA3=ALPHA3/ALPHA1
RETURN
END


```

1  SUPROUTINE EIGEN(A,EIGVAL,N)
2  COMPLEX A(8,8),E(4,8),EIGVAL(8),D(8,8),ALAMDA(8),E3,E4(8),E1,E2
3  DC 10 I=1,N
4  DC 10 J=1,N
5  D(I,J)=A(I,J)
6  * * * * *
7  COMPUTE EIGENVALUES
8  * * * * *
9  E1=(D(2,4)*D(4,2)+D(4,3)*D(3,4)+D(4,6)*D(6,4)+D(8,4)*D(4,8))
10 E2=(D(2,5)*D(4,2)+D(3,5)*D(4,3)+D(4,6)*D(6,5)+D(8,5)*D(4,8))
11 E3=(E1-D(6,5))*(E1-D(6,5))
12 ALAMDA(1)=-CSQRT(D(2,1))
13 ALAMDA(2)=ALAMDA(1)
14 ALAMDA(3)=-CSQRT(.5*(E1+D(6,5))+CSQRT(.25*E3+(E2*D(6,4))))
15 ALAMDA(4)=-CSQRT(.5*(E1+D(6,5))-CSQRT(.25*E3+(E2*D(6,4))))
16 ALAMDA(5)=-ALAMDA(4)
17 ALAMDA(6)=-ALAMDA(3)
18 ALAMDA(7)=-ALAMDA(1)
19 ALAMDA(8)=-ALAMDA(1)
20 DC 45 I=1,N
21 E4(I)=ALAMDA(I)*ALAMDA(I)
22 EIGVAL(I)=ALAMDA(I)
23 * * * * *
24 COMPUTE EIGENVECTORS
25 * * * * *
26 DC 50 I=1,4
27 DC 50 J=1,8
28 E(I,J)=0.0
29 B(1,1)=1.0
30 B(1,8)=1.0
31 B(4,2)=1.0
32 B(4,7)=1.0
33 DC 21 J=3,6
34 B(1,J)=(D(2,4)*D(6,5)-E4(J))-D(2,5)*D(6,4))/(E4(J)-D(2,1))
35 B(2,J)=D(6,5)-E4(J)
36 B(3,J)=-D(6,4)
37 21 B(4,J)=(D(8,4)*E(2,J)+D(8,5)*B(3,J))/(E4(J)-D(8,7))

```

38
39
40
41
42
43
44
45
46
47
48
49

```
DO 41 J=1,N
  A(1,J)=B(1,J)/ALAMDA(J)
  A(2,J)=B(1,J)
  A(3,J)=(C(3,1)*B(1,J)+D(3,4)*B(2,J)+D(3,5)*B(3,J)+D(3,7)*E(4,J))/
    $E4(J)
  A(4,J)=E(2,J)/ALAMDA(J)
  A(6,J)=E(3,J)
  A(5,J)=B(3,J)/ALAMDA(J)
  A(7,J)=E(4,J)/ALAMDA(J)
  41 A(8,J)=E(4,J)
  RETURN
  END
```

```

1  SUBROUTINE DIFF(X0,XN,N,A,ORDER,JK,NM,Z,Z2,NP)
2  CCMPLX Y(8,4),F(8,4),E(8,4),ZBAR(8,533),Z(8,4),
3  1 VN,Z1(8,533),Z2(8,4),CH(4),P(4,533),SUM,A(8,4)
4  INTEGER CORDER,ORDER1,OP
5  REAL XI(8,2)
6  ORDER1=CORDER/2
7  OP=ORDER1
8  JK=1
9  N4=N/NM
10 H=(XN-X0)/FLCAT(N)
11 IF (NP.EC.0) GO TO 210
12 DC 200 I=1,ORDER1
13 DO 200 J=1,ORDER
14 200 Z(J,I)=A(J,I)
15 ICCUNT=1
16 JK=2*N+1
17 GC TO 205
18 210 WRITE(6,997)
19 997 FCBAT(1H1)
20 DO 990 J=1,ORDER1
21 990 CH(J)=A(2*J,1)
22 OP=-OP
23 I=XM
24 ICCUNT=ICCUNT-1
25 H= H*FLOAT(NM)
26 GC TO 175
27 205 DO 171 JI=1,N4
28 C
29 C*****RUNGA-KUTTA METHOD*****
30 C
31 DO 46 HHH=1,NM
32 SUM=0.0
33 H=HOD(HHH-1,2)+1
34 I=HCD(HHH,2)+1
35 CALL CCEP(JK,ORDER,1)
36 DO 45 IN=1,ORDER1
37 DC 5 J=1,ORDER

```



```

38 5 Y(J,M)=A(J,IN)
39 CALL FCT(Y,F,M,JK,ORDER,1)
40 DC 10 J=1,ORDER
41 E(J,1)=H*F(J,M)
42 Y(J,I)=Y(J,M)+E(J,1)/2.
43 CALL FCT(Y,F,I,JK-1,ORDER,2)
44 DC 20 J=1,ORDER
45 E(J,2)=H*F(J,I)
46 Y(J,I)=Y(J,M)+E(J,2)/2.
47 CALL FCT(Y,F,I,JK-1,ORDER,2)
48 DC 30 J=1,ORDER
49 E(J,3)=H*F(J,I)
50 Y(J,I)=Y(J,M)+E(J,3)
51 CALL FCT(Y,F,I,JK-2,ORDER,3)
52 DC 40 J=1,ORDER
53 E(J,4)=H*F(J,I)
54 SUN=(E(J,1)+2.*E(J,2)+2.*E(J,3)+E(J,4))/6.
55 Y(J,I)=Y(J,M)+SUN
56 DC 42 J=1,ORDER
57 A(J,IN)=Y(J,I)
58 42 CONTINUE
59 JK=JK-2
60 46 CONTINUE
61
62 * * * * *
63 * * * * *
64 * * * * *
65 * * * * *
66
67 DC 171 NH=1,ORDER1
68 P(NH,ICOUNT)=1.
69 IF (NH.EQ.1) GO TO 250
70 ITEMP=ICOUNT-1
71 DC 80 II=2,NH
72 SUM=0.
73 P(NH,ITEMP)=0.
74 DO 90 J=1,ORDER
90 SUM=SUM+A(J,NH)*2*EAR(J,ITEMP)

```

```

75 IT=NM-II+1
76 F(IT,ICOUNT)=-SUM
77 DO 110 J=1,CEDEB
78 Z(J,NM)=Z(J,NM)-SUM*Z1(J,ITEMP)
79 A(J,NM)=A(J,NM)-SUM*ZBAR(J,ITEMP)
80 ITEMP=ITEMP-1
81 VN=0.
82 DO 310 J=1,ORDER
83 VN=VN+A(J,NM)*A(J,NM)
84 VN=CSQRT(VN)
85 DO 320 J=1,ORDER
86 A(J,NM)=A(J,NM)/VN
87 ZBAR(J,ICOUNT)=A(J,NM)
88 DC 321 J=1,NM
89 P(J,ICOUNT)=P(J,ICOUNT)/VN
90 DC 323 J=1,ORDER
91 Z(J,NM)=Z(J,NM)/VN
92 Z1(J,ICOUNT)=Z(J,NM)
93 IF(NM.EQ.ORDER1) GO TO 390
94 GC TO 170
95 NM=NM-1
96 DC 391 J=1,NM
97 IT=ICOUNT-ORDER1+J
98 IF=IT+1
99 DC 391 II=IP,ICOUNT
100 P(J,II)=F(J,II)*F(J,IT)
101 F(J,ICOUNT-1)=P(1,ICOUNT-1)+P(2,ICOUNT-1)*P(1,ICOUNT-2)
102 * /P(2,ICOUNT-2)
103 P(1,ICOUNT)=F(1,ICOUNT)+P(2,ICOUNT)*P(1,ICOUNT-2)/P(2,ICOUNT-2)
104 * +P(3,ICOUNT)*P(1,ICOUNT-1)/P(3,ICOUNT-1)
105 P(2,ICOUNT)=F(2,ICOUNT)+P(3,ICOUNT)*P(2,ICOUNT-1)/P(3,ICOUNT-1)
106 170 ICOUNT=ICOUNT+1
107 171 CCINUE
108 JK=1
109 DC 115 I=1,ORDER1
110 DC 115 J=1,ORDER
111 115 Z2(J,I)=A(J,I)

```

```

112      RETURN
113
114      * * * * *
115      THE FOLLOWING SECTION IS USED TO DETERMINE THE EIGENSOLUTION
116      AFTER AN EIGENVALUE HAS BEEN FOUND.
117      * * * * *
118
119      DC 180 JL=1,M4
120      DC 410 II=1,ORDER
121      SUM=0.
122      DO 400 J=1,ORDER1
123      IC=ICOUNT-ORDER1+J
124      SUM=SUM+ZBAR(II,IC)*CH(J)
125      Y(II,1)=SUM
126      IF(MOD(JL,5).EQ.0) WRITE(6,997)
127      XE=H*PLCAT(JL)-H
128      DO 999 J=1,ORDER
129      IF(AIHAG(Y(J,1)).EQ.0.0.AND.REAL(Y(J,1)).EQ.0.0) GO TO 996
130      XX(J,1)=CAES(Y(J,1))
131      XX(J,2)=ATAN2(AIHAG(Y(J,1)),REAL(Y(J,1)))
132      XX(J,2)=XX(J,2)*57.295778
133      GO TO 999
134      XX(J,1)=0.0
135      XX(J,2)=0.0
136      CCNTINUE
137      WRITE(6,998) IN,(Y(J,1),XX(J,1),XX(J,2),J=1,ORDER)
138      FORHAT(180,9HZ(Y)AT Y=,F5.2,24X,9H MAGNITUDE,13X,
139      * 21HPHASE ANGLE (DEGREES)/8(2E14.5,E21.6,9X,E16.6/))
140      DO 420 II=1,ORDER1
141      SUM=0.
142      DO 430 J=1,ORDER1
143      IC=ICOUNT-ORDER1+J
144      SUM=SUM+F(II,IC)*CH(J)
145      Y(II,1)=SUM
146      DO 431 J=1,ORDER1
147      CH(J)=Y(J,1)
148      ICOUNT=ICOUNT+OF

```


149
150
151
152
153
154
155

180 CCNTINUE
JK=1
116 DC 117 I=1,ORDER1
A(2*I-1,1)=0.0
117 A(2*I,1)=CH(I)
RETURN
END

1
2
3
4
5
6
7
8
9
10
11
12
13
14
15
16

```
SUBROUTINE PCT(Z,ZP,N,K,ORDER,IA)
  CCNEX Z(8,4),ZF(8,4),C,CSUM
  INTEGER CRDER
  COMMON /CT/C(5,8,4)
  M=CRDER/2+1
  DO 20 I=1,M
    CSUM=0.
    DO 10 J=1,ORDER
      CSUM=CSUM+Z(J,N)*C(I,J,IA)
      IF(I.EQ.M) GC TO 20
      ZP(2*I,N)=CSUM
      ZP(2*I-1,N)=Z(2*I,N)
    CONTINUE
    ZP(3,N)=CSUM
  RETURN
  END
```

10

20

```

1 SUBROUTINE CSCLVE(A,E,X,M,N,DET,NECWS)
2 SCIVE THE MATRIX EQUATION AX=B. INPUT IS THE N BY N MATRIX A, THE
3 N BY M MATRIX B, THE VALUES OF M AND N, AND A CONSTANT NECWS WHICH
4 IS EQUAL TO THE NUMBER OF ROWS ALLOCATED THE MATRIX A IN ITS
5 DIMENSION STATEMENT. OUTPUT IS THE N BY M MATRIX X AND THE VALUE
6 OF THE DETERMINANT OF A. IF THE MATRIX A IS SINGULAR, THE VALUE
7 RETURNED FOR THE DETERMINANT WILL BE 0 AND NO VALUES FOR X WILL BE
8 RETURNED. **NOTE: THE MATRICES A AND B ARE DESTROYED BY THIS
9 SUBROUTINE.
10 METHOD USED IS GAUSSIAN ELIMINATION WITH PIVOTAL CONDENSATION. AN
11 ARRAY PCNTRL IS CONSTRUCTED DURING THE TRIANGULARIZATION SC
12 THAT IT WILL CONTAIN THE ORDER IN WHICH EACH ROW WAS USED AS A
13 PIVCT. THIS ARRAY THEN CONTROL THE ORDER IN WHICH THE BACKSUB-
14 STITUTION IS DONE. A LOGICAL ARRAY PVTCHK IS USED TO SAVE TIME IN
15 DETERMINING WHETHER A PARTICULAR ROW HAS BEEN USED AS A PIVCT YET.
16 WHEN A ROW IS USED AS A PIVOT, THE CORRESPONDING ELEMENT OF PVTCHK
17 IS SET TO .TRUE..
18 COMPLEX A(NROWS,N),B(NROWS,M),X(NROWS,M),DET,ALRG,S,SUM
19 LOGICAL PVTCHK(8)
20 INTEGER PCNTRL(8)
21
22 * * * * *
23 INITIALIZE PVTCHK, DET.
24 * * * * *
25
26 DET=1.0
27 DO 5 I=1,N
28 PVTCHK(I)=.FALSE.
29
30 TRIANGULARIZATION ROUTINE
31
32 N1=N-1
33 DO 30 I=1,N1
34
35 FIND LARGEST ELEMENT IN COLUMN, WHICH WILL BE USED AS THE PIVCT.
36
37 ALRG=0.0

```


| | |
|--|----|
| DC 10 J=1,N | 38 |
| IF (PVTCHK(J)) GC TO 10 | 39 |
| IF (CAES(A(J,I)).LE.CABS(ALRG)) GC TO 10 | 40 |
| ALRG=A(J,I) | 41 |
| INDEX=J | 42 |
| CCONTINUE | 43 |
| DET=DET*ALRG | 44 |
| IF (CAES(ALRG).EQ.0.0) GO TO 120 | 45 |
| STORE ROW NUMBER OF PIVOT IN PCNTL. SET FLAG IN PVTCHK. | 46 |
| PCNTL(I)=INDEX | 47 |
| PVTCHK(INDEX)=.TRUE. | 48 |
| ELIMINATE COLUMN I. | 49 |
| DC 30 J=1,N | 50 |
| IF (PVTCHK(J)) GC TO 30 | 51 |
| IF (CAES(A(J,I)).EQ.0.0) GO TO 30 | 52 |
| S=A(J,I)/A(INDEX,I) | 53 |
| I1=I+1 | 54 |
| DC 20 K=I1,N | 55 |
| A(J,K)=A(J,K)-S*A(INDEX,K) | 56 |
| DC 25 K=1,M | 57 |
| B(J,K)=B(J,K)-S*B(INDEX,K) | 58 |
| CCONTINUE | 59 |
| DETERMINE WHICH ROW WAS NOT USED AS A PIVOT. PUT ROW NUMBER IN PCNTL(N). | 60 |
| DC 40 I=1,N | 61 |
| IF (.NOT.PVTCHK(I)) GC TO 45 | 62 |
| CCONTINUE | 63 |
| PCNTL(N)=I | 64 |
| DET = DET*A(I,N) | 65 |
| IF (CABS(DET).EQ.0.0) GO TO 120 | 66 |
| | 67 |
| | 68 |
| | 69 |
| | 70 |
| | 71 |
| | 72 |
| | 73 |
| | 74 |

| | | |
|-----|--|----|
| C | BACKSUBSTITUTION ROUTINE. | 75 |
| C | | 76 |
| | DO 70 I=1,M | 77 |
| | J=PCNTRL(N) | 78 |
| | X(N,I)=B(J,I)/A(J,N) | 79 |
| | DC 70 K=2,N | 80 |
| | KK=N-K+1 | 81 |
| | J=PCNTRL(KK) | 82 |
| | JJ=KK+1 | 83 |
| | SUM=0.0 | 84 |
| | DC 60 L=JJ,M | 85 |
| 60 | SUM=SUM+A(J,L)*X(L,I) | 86 |
| 70 | X(KK,I)=(E(J,I)-SUM)/A(J,KK) | 87 |
| C | | 88 |
| C | DETERMINE SIGN OF DET. (COUNT NUMBER OF IMPROPER PRECEDENCES | 89 |
| C | IN PCNTRL.) | 90 |
| C | | 91 |
| | INDEX=0 | 92 |
| | DO 80 I=2,N | 93 |
| | DC 80 J=1,I | 94 |
| | IF (PCNTRL(I).LT.PCNTRL(J)) INDEX=INDEX+1 | 95 |
| 80 | CCONTINUE | 96 |
| | DET=(-1.)**INDEX*DET | 97 |
| 120 | RETURN | 98 |
| | END | 99 |

REFERENCES

1. Mack, L. M., "On the Application of Linear Stability Theory to the Problem of Supersonic Boundary-Layer Transition," AIAA preprint No. 74-134, February 1974.
2. Morkovin, M. V., Lessons from Transition of Shock-Tube Boundary Layers, AFOSR Scientific Report AFOSR-TR-72-0057, November, 1971.
3. Morkovin, M. V., Critical Evaluation of Transition from Laminar to Turbulent Shear Layers with Emphasis on Hypersonically Traveling Bodies, AFFDL-TR-68-149, March 1969.
4. Boison, J. C. Investigation of Test Facility Environmental Factors Affecting Boundary Layer Transition. AFFDL-TR-73-106, September 1973.
5. Reshotko, E., "Transition Reversal and Tollmien-Schlichting Instability," The Physics of Fluids, Vol. 6, No. 1, pp 335-342, March 1963.
6. Mack, L. M., Boundary-Layer Stability Theory. JPL Report No. 900-277, Revision A, November 1969.
7. Ostrach, S. and Thornton, P. R., "Stability of Compressible Boundary Layers Induced by a Moving Wave," Journal of the Aerospace Sciences, Vol. 29, March 1962, pp 289-296.
8. Dunn, D. W. and Lin, C. C., "On the Stability of the Laminar Boundary Layer in a Compressible Fluid," Journal of the Aeronautical Sciences, July 1955, pp 455-477.
9. Mack, L. M., "The Stability of the Compressible Laminar Boundary Layer According to a Direct Numerical Solution," in Recent Developments in Boundary Layer Research, AGARDograph 97, Part I, pp 329-362, 1965.
10. Mack, L. M., "Progress in Compressible Boundary Layer Stability Computations," in Proceedings of the Boundary Layer Transition Workshop, Vol. 4, Aerospace Corp. Report No. TOR-0172, pp 1-1 to 1-35, December 1971.

11. Boehman, L.I., "Recalculation of Brown's Stability Results." Paper presented at the 1971 Boundary Layer Transition Specialist's Workshop, San Bernadino, California. Published in Proceedings of the 1971 Boundary Layer Transition Workshop, Volume 4, Aerospace Corporation, Report No. TOR-0172 (S 2816-16)-5, December 1971.
12. Boehman, L.I., The Effect of Boundary Layer Growth on the Stability of Supersonic Boundary Layers, AFFDL-TR-73-69, Air Force Flight Dynamics Laboratory, Wright-Patterson Air Force Base, Ohio, September 1973.
13. Mack, L.M., "Computation of the Stability of the Laminar Compressible Boundary Layer," in Methods of Computational Physics: Volume 4, Academic Press, New York, pp 247-299, 1965.
14. Mirels, H., "The Wall Boundary Layer Behind a Moving Shock Wave," Boundary Layer Research, Proceedings of Int. Union of Theor. and Appl. Mech., H. Gortler, ed., Springer Verlag (Berlin), 1958, pp 283-293.
15. Golobic, R.A., Measurements of Boundary Layer Transition on a Shock Tube Wall for Wall Cooling Ratios Between 0.39 and 0.255, Frank J. Seiler Research Laboratory Report, SRL-TR-75-0022, USAF Academy, Colorado, December 1975.
16. Boehman, L.I., "Compressible Boundary Layer Stability Equations Without the Parallel Flow Assumption," Developments in Mechanics, Vol. 6, pp 193-206, Proceedings of the 12th Midwestern Mechanics Conference, University of Notre Dame Press, August 1971.
17. Betchov, R. and Criminale, W.O., Stability of Parallel Flows, Academic Press, New York, 1967.
18. Bellman, R.E. and Kalaba, R.E., Quasilinearization and Nonlinear Boundary - Value Problems, American Elsevier, New York, 1965.
19. Roberts, S.M. and Shipman, J.S., Two-Point Boundary Value Problems: Shooting Methods, American Elsevier, New York, 1972.